

**Contract No. and Disclaimer:**

**This manuscript has been authored by Savannah River Nuclear Solutions, LLC under Contract No. DE-AC09-08SR22470 with the U.S. Department of Energy. The United States Government retains and the publisher, by accepting this article for publication, acknowledges that the United States Government retains a non-exclusive, paid-up, irrevocable, worldwide license to publish or reproduce the published form of this work, or allow others to do so, for United States Government purposes.**

## Development of Glass Matrices for HLW Radioactive Wastes

Carol M. Jantzen  
Savannah River National Laboratory  
Aiken, South Carolina, 29808, USA  
carol.jantzen@srnl.doe.gov

### Abstract

Vitrification is currently the most widely used technology for the treatment of high level radioactive wastes (HLW) throughout the world. Most of the nations that have generated HLW are immobilizing in either borosilicate glass or phosphate glass. One of the primary reasons that glass has become the most widely used immobilization media is the relative simplicity of the vitrification process, e.g. melt waste plus glass forming frit additives and cast. A second reason that glass has become widely used for HLW is that the short range order (SRO) and medium range order (MRO) found in glass atomistically bonds the radionuclides and governs the melt properties such as viscosity, resistivity, sulphate solubility. The molecular structure of glass controls contaminant/radionuclide release by establishing the distribution of ion exchange sites, hydrolysis sites, and the access of water to those sites. The molecular structure is flexible and hence accounts for the flexibility of glass formulations to waste variability. Nuclear waste glasses melt between 1050-1150°C which minimizes the volatility of radioactive components such as Tc<sup>99</sup>, Cs<sup>137</sup>, and I<sup>129</sup>. Nuclear waste glasses have good long term stability including irradiation resistance. Process control models based on the molecular structure of glass have been mechanistically derived and have been demonstrated to be accurate enough to control the world’s largest HLW Joule heated ceramic melter in the US since 1996 at 95% confidence.

**Key Words: High level waste, glass, vitrification**

### 1.0 Introduction

Vitrification is currently the most widely used technology for the treatment of high level radioactive wastes (HLW) throughout the world. Most of the nations that have generated HLW are immobilizing in either borosilicate glass or phosphate glass. One of the primary reasons that glass has become the most widely used immobilization media is the relative simplicity of the vitrification process, e.g. melt waste plus glass forming frit additives and cast. Melting homogenizes the mixture and so this process is easier to perform remotely than a ceramic waste form process that requires powder handling, e.g. mechanical mixing of waste and ceramic additives and grinding for particle size control, followed by cold pressing and sintering or hot pressing at elevated temperatures. A second reason that glass has become widely used for HLW is that the amorphous and less

rigid structure of glasses compared to ceramics enables the incorporation of a very large range of elements that are atomically bonded in the flexible glass structure. Thus glasses can accommodate larger waste composition fluctuations than ceramics.

Moreover, HLW glasses melt at lower temperatures (1050-1150°C) compared to higher ceramic waste form processing temperatures which minimizes the volatility of radioactive components such as Tc<sup>99</sup>, Cs<sup>137</sup>, and I<sup>129</sup>. Often in ceramics made by cold pressing and sintering or hot isostatic pressing, an intergranular glassy phase is produced on the ceramic grain boundaries and the radionuclides preferentially migrate to the glassy phase(s) [1,2,3,4,5,6,7]. While ceramics are often credited with having higher chemical durability than glasses, if the radionuclides are incorporated in the intergranular glassy phases, they leach at the same rates as those from glassy waste forms.[8]

Lastly, nuclear waste glasses have good long term stability including irradiation resistance and excellent chemical durability. In addition, the ease of modelling the durability of a homogeneous rather than a heterogeneous material in terms of having only one radionuclide source term is also an advantage. There is >40 years processing experience<sup>§</sup> with commercial borosilicate glasses and borosilicate glasses have favourable systems evaluations in terms of both melting and product behaviour. These attributes of borosilicate HLW glasses are discussed in more details in the sections below.

### 1.1 High Level Waste (HLW) Glass Composition Tolerance

Most nuclear nations have generated high level radioactive wastes from nuclear weapons programs and/or commercial nuclear power generation and most store waste materials from a variety of reprocessing flowsheets. The Plutonium and URanium EXtraction (PUREX) process<sup>†</sup> is the baseline for spent fuel reprocessing for most countries with active fuel cycle programs (see Chapter 1). France and the UK reprocess spent fuel for electric utilities from other countries using the PUREX process to recover uranium (U) and plutonium (Pu). Slight modifications to the PUREX process can be made to recover U, Pu, Np, and Tc (if desired) and a number of countries (e.g., France, Japan, China, etc.) are developing solvent extraction processes to recover the minor actinides (Am and Cm) from spent fuel. Elimination of these actinides and fission products from the HLW reduces the long-term radiotoxicity and heat generation from an immobilized waste form once it is entombed in a geologic repository.

In the US, a moratorium was placed on reprocessing of commercial spent nuclear fuel in 1977. A 2005 energy bill has revived the potential for reprocessing but currently spent fuel rods (once through) are in storage pools across the US and destined for direct disposal in a deep geological repository. Hence, HLW in the US is primarily defense

---

<sup>§</sup> Phosphate glasses (aluminophosphates and iron-phosphates) are not used commercially as frequently as the borosilicates and hence are not as well studied for applications to HLW stabilization.

<sup>†</sup> The PUREX process was developed in the United States in 1950 and the world's first operational full-scale PUREX separation plant, began radioactive operations at the Savannah River Plant in 1954. The process has run continuously at SRP since start-up for defense materials only.

wastes of which 36 million US gallons (136,275 m<sup>3</sup>) are stored at the Savannah River Site (SRS) in South Carolina and 50 million US gallons (189,270 m<sup>3</sup>) are stored at the Hanford site in Richland, Washington (Figure 1). While Hanford has more waste volume, Savannah River Site waste contains higher curie contents. Prior to the 1977 moratorium, a reprocessing facility had been built and initiated operation in West Valley, New York. The West Valley Demonstration Project (WVDP) created ~ 0.66 million US gallons (2,500 m<sup>3</sup>) of HLW from commercial nuclear fuel reprocessing using the PUREX and THOREX processes [9] (Figure 1).

The nuclear nations HLW streams are stored either as a neutralized nitric acid streams in mild steel tanks (U.S. and Russia) or as nitric acid streams in stainless steel tanks (France, UK, Japan, Russia). Although borosilicate glasses have become the preferred waste form for the immobilization of HLW solutions in the majority of the nuclear nations, the chemical variability of the wastes from the different reactor and reprocessing flowsheets coupled with the additional variability imposed by neutralization vs. direct storage of acidic wastes has led to a diverse HLW chemistry, e.g. HLW contains about three fourths of the elements in the periodic table (Figure 2).

Some of these extreme differences in HLW waste chemistry from different facilities operating different flowsheets are shown in Table I. When the HLW wastes are expressed as calcine oxides instead of on a liquid basis [10,11] this wide variability is readily apparent (Table I). To accommodate the differences in heat loads of the different HLW wastes (those produced by different reactor designs and those wastes processed immediately vs. those processed after neutralization and aging) different waste loadings are used (Table I).

## **1.2 High Level Waste (HLW) Glass Adaptive Structure**

Glass has been found to be very flexible and bond many of the HLW constituents (both radioactive and non-radioactive components) atomistically. Borosilicate waste glasses and melts possess short-range order (SRO; radius of influence ~1.6-3Å) around a central atom, e.g. polyhedra such as tetrahedral and octahedral structural units (Figure 3a) and medium range order (MRO) [12] which encompasses second- and third-neighbour environments around a central atom (radius of influence ~3-6 Å; Figure 3a). The polymerization of the SRO and MRO allows glasses to be more flexible in atomically bonding waste species than crystalline (ceramic or mineral) waste forms in which one must more rigorously know what crystalline structure each HLW waste component will reside in.

In glass, the central cation in the SRO tetrahedra is bonded covalently to the four surrounding oxygen atoms (Figure 3a). The central cation in the SRO octahedra is bonded ionically to six surrounding oxygen atoms and is often a HLW waste constituent. The tetrahedra are linked to each other or to an octahedral SRO via a bridging oxygen bond (BO) (Figure 3a; inset). The non-bridging (NBO) atoms carry a negative charge

and, in turn, bonds positively charged cations like  $\text{Cs}^+$ ,  $\text{Sr}^{+2}$ ,  $\text{Ca}^{+2}$  and positively charged contaminants (hazardous and radioactive species) ionically (Figure 3a; inset).

The linkage of the SRO structural units create the MRO structural groups such as  $(\text{Cs,K,Na,Li})\text{AlO}_2$ ,  $(\text{Cs,K,Na,Li})\text{FeO}_2$ ,  $(\text{Cs,K,Na,Li})\text{BO}_2$ , and  $(\text{Cs,K,Na,Li})\text{SiO}_4$  [13] or  $(\text{Cs,K,Na})\text{AlSiO}_4$  [14] which form chains and rings in the glass structure (Figure 3b). Experimentation has confirmed that glasses contain framework units, sheet-like units, chain-like units, and monomers [15] made up of tetrahedra of  $(\text{SiO}_4)^{-4}$ , boron as  $(\text{BO}_4)^{-5}$ †,  $(\text{PO}_4)^{-3}$ ,  $(\text{AlO}_4)^{-5}$ , or  $(\text{BO}_3)^{-3}$  trigonal units‡ which are the same SRO structures found in crystalline minerals. The existence of MRO in melts and glasses led to a redefinition [16] of the widely accepted Zachariasen-Warren random-network structure model of glass [17,18,19] and its predecessor the crystallite structure model of glass [20]. The “modified crystallite model” of glass structure treats the degree of medium-range order as spatial fluctuations in the glass network [16]. Similarly, Greaves [21] proposed a “modified random network (MRN)” model which involves two interlacing “sublattices.” One sublattice is more highly ordered (network regions) while the other is not (inter-network regions made up of large concentrations of network modifiers). The MRN model is able to describe the existence of large cation rich clusters in glass, e.g. clusters of Ca in  $\text{CaSiO}_3$  glasses [21] and  $\text{Na}_2\text{MoO}_4$  (Figure 3b). In the MRN, the tetrahedral SRO non-bridging oxygen atoms define the network regions, while the NBO-cation regions represent percolation channels that can act as ion-exchange paths for elements that are ionically bonded to the NBO (Figure 3c). Such percolation channels are also found in rare-earth aluminoborosilicate glasses [22] Thus, the molecular structure of glass controls contaminant release by establishing the distribution of ion exchange sites, hydrolysis sites, and the access of water to those sites.

In glass, the more highly ordered regions of MRO, referred to as clusters or quasicrystals, often have atomic arrangements that approach those of crystals [12,23]. These clusters or quasicrystals, in conjunction with the octahedral site preference energies [24,25], govern what waste constituents have poor solubility in borosilicate glass [26,27,28,29] and what crystalline species may form at the liquidus or during cooling of the vitrified waste form [24,25]. The same type of SRO and MRO bonding that occurs in glass occurs in mineral waste forms. The primary difference with crystalline waste forms (ceramics/minerals) is that the SRO and MRO are more ordered and the crystallographic polyhedra have higher symmetry and so the mineral structures possess crystallographic long range order (LRO), while the SRO and MRO in glasses have MRO distributions exhibiting polymerization into rings and chains and allow glass structures to accommodate the wide range of species existing in HLW wastes.

Vitreous waste forms can include silicate based glasses, borosilicate glasses, phosphate glasses, etc. Vitreous waste forms are amorphous and leach congruently.<sup>f</sup> Vitreous

† where B is surrounded by four oxygen atoms or IV coordinated

‡ where B is surrounded by three oxygen atoms or III coordinated

<sup>f</sup> Congruent dissolution of a waste form is the dissolving of species in their stoichiometric amounts. For congruent dissolution, the rate of release of a radionuclide from the waste form is proportional to

waste forms can crystallize during cooling and thus can become glass ceramics or glass ceramic composites (GCM's) which leach incongruently. Vitreous waste forms can be made by a variety of melting technologies that include Joule heated melters (this chapter) and Cold Crucible Induction Melters (CCIM; see Chapter 8).

### 1.3 High Level Waste (HLW) Glass Durability: A Single Source Term

Glasses are homogeneous (one phase) and provide a single source term when testing glass and developing durability/leaching models. A basic assumption in all glass dissolution models, as well as in all mineral dissolution models, is that the solid being modeled is comprised of a single phase and so the durability response has only one source term. Therefore, phase separated glasses (with two source terms) cannot be easily modelled in this fashion. The approach to durability prediction for phase separated glasses is often referred to as mixed mechanism modeling, e.g., the separated phase for borosilicate glass is often boron rich and has a poorer durability than the bulk and/or the matrix phase. Having a poorly soluble second phase is not desirable for HLW glasses where the distribution of the radionuclides in the two glassy phases would have to be known for every waste glass fabricated.

Additional mixed mechanism leaching can occur if crystals are present in a glass because crystals create grain boundaries that can (1) selectively undergo accelerated dissolution while the crystals themselves may have a different dissolution response [30] or (2) have compositions not representative of the bulk glass.[31]

Glass formulations with only 1-2 wt% crystals are targeted for HLW in the US. Crystals such as iron spinels are “inert” as they have little impact on glass durability, e.g. they are themselves very durable and cause minimal grain boundary dissolution since the spinels and the glass are both isotropic [30,32]. However, for other phases such as nepheline, acmite, and lithium silicates which are less durable than iron spinels and are not isotropic, the impact on glass durability from the crystal and the grain boundary can be pronounced. This is especially true if the crystal sequesters radionuclides as this gives a secondary source term for radionuclide release. Therefore, durability testing must be performed to confirm that any crystallization that might occur during canister cooling or during GCM formation has minimal impact. [33,34,35,36] This ensures that the last 3 terms in Equation 1 approximate zero and that the dissolution response does not represent mixed mechanisms.

---

both the dissolution rate of the waste form and the relative abundance of the radionuclide in the waste form. Thus for borosilicate glass <sup>99</sup>Tc is released at the same rate, congruently, as Na, Li, and B.

Equation 1

$$\sum Durability = \underbrace{durability}_{1st\ term} (homogeneous) + \underbrace{durability}_{2nd\ term} (amorphous\ phase\ separation) + \underbrace{durability}_{3rd\ term} (crystallization) + \underbrace{durability}_{4th\ term} (accelerated\ grain\ boundary)$$

## 2.0 HLW Glass Processing

### 2.1 Pre-Processing of HLW Acidic and Neutralized HLW

The differences in HLW waste chemistry (Section 1.1 and Table I) and storage methodologies (acidic vs. neutralized) have led to differences in waste pre-processing prior to and during vitrification. In acidic HLW wastes, the HLW contains free nitric acid and nitrate salts (Figure 4a). In HLW neutralized with NaOH, the HLW contains primarily nitrate salts as a supernatant liquid that is less dense than the metal hydroxides formed during the neutralization (Figure 4b). Thus in neutralized HLW, the excess neutralizing agent (NaOH) and nitrated salts must be treated separately from the sludge so that these non-radioactive constituents do not become part of the HLW vitrified product and take up valuable repository space (estimated at one million dollars burial costs per canister in the US).

### 2.2 Removal of Neutralizing Agents from HLW: Sludge Washing

In neutralized HLW, the supernatant liquid is 92% of the waste volume and contains 45% of the radioactivity (primarily Cs<sup>137</sup> and actinides). The hydroxide sludge formed after neutralization is only 8% of the waste volume and contains 55% of the radioactivity. Thus, the supernate is decanted and decontaminated (salt processing in Figure 4b). After the supernatant is decanted from the top of the sludge, the sludge still contains residual supernatant in the interstitial regions. By mobilizing the sludge with water followed by a settling period, the resulting “wash water” can be decanted and processed along with the supernates or evaporated [37] and returned to the tank farm for future processing. This minimizes the amount of soluble salts (NaNO<sub>3</sub>, NaNO<sub>2</sub>, NaOH, Na<sub>2</sub>SO<sub>4</sub>, NaAlO<sub>2</sub> and others) remaining with the HLW sludge and is known as “sludge washing” [38,39]

“Sludge washing” requires additional processing steps and the number of washing stages may be reduced or eliminated altogether. Typical “sludge washing” scenarios are 2-5 wash cycles and remove soluble sodium salts including sodium sulfate. If the washing process is not as efficient as anticipated or fewer washing cycles are performed, additional sodium salts will become part of the sludge waste feed to the melter. In the following section the impact that this has on the calculation of the waste loading (WL) factors will be discussed. Sludge washing, was performed at West Valley [40], is being

performed routinely at the SRS, and will be performed at Hanford Waste Treatment Plant (WTP) in the US.

The radioactivity is usually removed from the supernates by the use of various combinations of ion exchange, selective precipitation, or solvent extraction and the radioactivity removed from the supernatant along with any spent ion exchange media is recombined with the sludge (Figure 4b) to be vitrified as HLW. The low level waste filtrate, often referred to as the Low Activity Waste (LAW) fraction of HLW, is either cemented (SRS or West Valley) or vitrified<sup>f</sup> (Hanford) and buried as low level waste at the individual sites. Alternate mineral waste forms being made by Fluidized Bed Steam Reforming (FBSR) are being examined for the LAW fraction of HLW at Hanford and the mineral waste form is being implemented at Idaho National Laboratory for their sodium bearing waste (SBW).

### 2.3 Removal of Cladding Elements from HLW: Al Dissolution

Defense wastes are high in aluminium (see Table I) as aluminium clad fuel assemblies and targets were dissolved in order to recover the uranium, plutonium and other radioactive isotopes of interest for defense purposes. Because the waste has been neutralized the aluminium is present as gibbsite/bayerite ( $\text{Al}(\text{OH})_3$ ) or has aged to boehmite/diaspore ( $\text{AlOOH}$ ) [41]. Both gibbsite and boehmite are soluble in 19M NaOH at 55-85°C as the sodium hydroxide drives the pH into the stability field of soluble  $\text{NaAlO}_2$ . The NaOH is consumed in the conversion of the aluminium hydroxides to  $\text{NaAlO}_2$  and water [37] and  $\text{NaAlO}_2$  is one of the soluble salts that can be removed by sludge washing (see Section 2.1). A full scale active demonstration of “Al Dissolution” was performed in 1982 [37,42] in waste tank 51. This demonstration, which allowed NaOH to dissolve Al out of the sludge for 5 days, showed that up to 80% of the aluminium in the high alumina defense wastes created in H-Area and M-Area (HM) at SRS could be removed. The alumina dissolution is performed before sludge washing for the high alumina containing sludges and then the excess  $\text{NaAlO}_2$  created becomes part of the low level waste filtrate that is sent to shallow land burial on site (Figure 4b). This reduces the 8% HLW sludge volume at SRS by ~1% which translates to a savings of  $1.56 \times 10^6$  kgs of glass (900 canisters) out of  $1.38 \times 10^7$  kgs of glass (8000 canisters) [37] or 11.25% fewer HLW glass canisters to be buried in a deep geological repository.

### 2.4 Thermal Denitration vs. Chemical Denitration

Both acid and neutralized HLW waste (after sludge washing and Al dissolution) must be denitrated before vitrification (Section 2.2). Denitration can be performed either

---

<sup>f</sup> At the Hanford Site, due to the Hanford Federal Facility Agreement and Consent Order (Tri-Party Agreement between Department of Energy-Richland, the Washington State Department of Ecology, and the Environmental Protection Agency) signed in 1989, the low level filtrate will be vitrified (either Joule heated or bulk vitrification) instead of cemented and buried as done at SRS.

thermally or by the use of chemical additives [43]. Prior to thermal denitration the acidic wastes are concentrated by evaporation or evaporation and denitration can be achieved simultaneously in a rotary kiln (Figure 4a). Thermal denitration via calcination can increase the volatility of certain species such as  $\text{Ru}^{101}$ ,  $\text{Ru}^{102}$ , and  $\text{Ru}^{104}$  and  $\text{Tc}^{99}$  depending on the temperature of the calcinations [43].

The use of various organic reductants (formic acid, formaldehyde and sugar) has been successful for denitration of HLW as well as electrolytic denitration. The use of chemical additives for denitration reduces the acid content of the waste (waste that has not been neutralized) and/or the nitrated salts in the waste (in the case of neutralized wastes). At AVM (Atelier de Vitrification de Marcoule)/AVH (Atelier de Vitrification de La Hague) thermal denitration via a rotary calciner is used in conjunction with chemical additives such as sugar that are co-processed in the rotary calciner which allows the denitration to be performed at temperatures as low as 500°C (Figure 4a).

At the Savannah River Site vitrification facility, the Defense Waste Processing Facility (DWPF), denitration occurs in the Sludge Receipt Adjustment Tank (SRAT) via formic acid additions (Figure 4b). Since this is a neutralized HLW sludge, the formic acid also improves the rheology of the hydroxide sludge, decomposes any carbonates which could create  $\text{CO}_2$  foam during melting, reduces manganese from  $\text{Mn}^{+4}$  to  $\text{Mn}^{+2}$  to prevent oxygen foaming during melting, and reduces mercury to the metallic state so it can be steam stripped before it is volatilized in the vitrification process [44,45,46].

At West Valley sugar was used for denitration and added to the feed preparation tank [9] along with the glass forming additives. At Myack in Russia molasses was added to form a “cold cap” and limit volatility.[47] At the Hanford WTP sugar is being used for denitration.[48] The sugar is added with the feed and the melter is bubbled to enhance reactions, release evolved gases, and improve melt convection and melt rate.

## 2.5 The Evolution of Melter Designs [49]

Commercial glass melters are extremely large and generally built in place, e.g. where they are operated. HLW glass melters are generally smaller and constructed as integrated systems and moved to the operating facilities. At the facilities they are installed and removed using remotely operated cranes. Once installed, the maintenance of the HLW melters is limited to changing out of auxiliary devices and/or complete melter replacement (Figure 8). This type of operating environment requires melters of limited size that produce glass of consistent quality at predictable rates.

Figure 5 shows the types of HLW melter systems that have been developed over the last 40-45 years: batch melters, continuous pot melters, and Joule-heated ceramic-lined melters (JHCM). The first waste glass melters were designed for batch operations. These were unsuitable due to slow heat transfer from external heaters through the canister into the reacting batch. The batch melters also suffered from lack of agitation and non-

uniform temperature distribution which inhibited the glass from melting homogeneously. Calcination of the feed before introduction into the batch melter increased the melt rate but also increased the tendency for crystals to form in the glass. Solids entrainment of the batch materials (caline and glass formers) was also problematic and the small size of the batch melters required that several be operated simultaneously to meet the production rates needed to immobilize the HLW inventories.

Continuous pot melters made of nickel-chrome alloy were tested in the US, Germany, and France. The diameter of the pot was larger than in batch melters and the pot was directly heated by radio frequency induction heating which increased the melt rate over batch melters. Continuous feeding of the raw materials was employed and gas bubblers were used to agitate the melt. The French AVH system is the largest melter of this type ever operated (Figure 6). Melt temperature was limited to 1150°C due to the alloy used for the pot.

Joule-heated ceramic-lined melters (JHCM's) were tested in the US, Europe, Japan, and Russia (Table III). These melters can be calcine fed or slurry fed and vitrification is continuous. The melter is lined with refractory and the glass is Joule heated by electricity transferred through the melt between nickel-chromium alloy electrodes. JHCM's have been selected for all the production melter systems in the US, Germany and Japan because of the high production rate and high glass quality. The size of these systems is limited only by the replacement crane capacity since all the structural support is provided by a stainless steel shell which contains the refractory. The nominal melt temperature is 1150°C which is only 200°C lower than the electrode melting point (electrodes are usually made from Inconel alloys). The DWPF at SRS is the largest production melter of this type ever operated (Figure 7) with a glass surface area of 226 ft<sup>2</sup> (20.996 m<sup>2</sup>). Advanced Joule Heated Ceramic Melters (AJHCM's) with larger surface areas will be discussed in Section 7.2)

Details about the melter designs in use by different countries can be found in recent compendiums by Ojovan and Lee [50,51], Caurant, et.al. [22], and Jain [52]. There is additional information and historical detail in Appendix A.

## **3.0 Glass Formulation and Waste Loading**

### **3.1 Structural Similarity of Glass Formulations**

While borosilicate glasses have been used in the US and in Europe to immobilize radioactive HLW for ultimate geologic disposal, aluminophosphate glasses are used in Russia for permanent disposal and/or long-term storage. Iron phosphate glasses have been proposed for HLW in the US but no wide scale usage of this glass has yet to be implemented. It is believed this is due to the lack of commercial melting experience with this type of glass.

Waste glasses must be formulated to maximize the amount of waste to be vitrified so that waste glass volumes and the associated storage and disposal costs are reduced. The wastes generated by different reactor flowsheets were discussed above and are given in Table I. For borosilicate glasses and phosphate glasses different frit additives and different waste loadings are used to accommodate the waste variability (Table II).

It is significant that the highly variable sludges (Table I) when mixed with the highly variable frits (Table II) at the highly variable waste loadings given in Table I and Table II, fall in a narrow glass forming region in the borosilicate glass forming system (Figure 8a). In other words, successful HLW glass formulations contain 60 wt% or more of glass forming oxides ( $\text{SiO}_2$ ,  $\text{B}_2\text{O}_3$ ,  $\text{ZrO}_2$ ,  $\text{Al}_2\text{O}_3$ ,  $\text{P}_2\text{O}_5$  and fission products), >15 wt% glass modifier oxides ( $\text{Na}_2\text{O}$ ,  $\text{K}_2\text{O}$ ,  $\text{Li}_2\text{O}$ ,  $\text{CaO}$ ,  $\text{MgO}$ ,  $\text{SrO}$ , and  $\text{ZnO}$ ) and from 0-25 wt% glass intermediate oxides ( $\text{Cr}_2\text{O}_3$ ,  $\text{Fe}_2\text{O}_3$ ,  $\text{CuO}$ ,  $\text{NiO}$ ,  $\text{MnO}$ ,  $\text{PbO}$ ,  $\text{TiO}_2$  and actinides). While Figure 8a includes the radioactive glasses given in Tables I and II at the reference waste loadings given, this same glass forming region was defined for simulated HLW glasses over an even broader range of glass compositions [53,54] as shown in Figure 8b.

### 3.2 HLW Glass Waste Loadings

Waste loadings are generally expressed on a calcine waste oxide basis. In other words, if the nitrated or hydroxide wastes were heated to  $1000^\circ\text{C}$  and  $\text{NO}_x$  and  $\text{H}_2\text{O}$  or  $\text{OH}^-$  vaporized, then only calcine oxides would remain. The grams of calcine oxide waste per 100 grams of glass is referred to as the waste loading and expressed in weight percent. High heat wastes and acidic wastes that have not been neutralized have lower waste loadings, e.g. in the 10-25 wt% (Table I) as only the fission products and actinides are included in the waste loadings, e.g. the corrosion products such as  $\text{Fe}_2\text{O}_3$ ,  $\text{Cr}_2\text{O}_3$ , and  $\text{NiO}$  and any small amounts of alkali are not included in the waste loading. For the neutralized US defense wastes the corrosion products and  $\text{Fe}_2\text{O}_3$  from the use of ferrous sulfamate during processing, and some of the alkali used for neutralization that cannot be washed out of the HLW sludge is included in the waste loading calculations. Therefore, waste loadings up to 38-40 wt% on an oxide basis are achieved (Table III). Therefore, Table III demonstrates that the waste loading for the US wastes are higher than those of the European and Russian wastes but the radionuclide content, expressed in Tera-bequerels is lower for the US wastes than the European and Russian wastes.

### 3.3 Systems Approach to Glass Formulation: Basis for Formulation Similarities

The HLW glass formulations are driven by the need to simultaneously optimize [55,56, 57] multiple product/ process (P/P) constraints such as waste component solubility, melt viscosity, melt corrosivity, melt volatility, liquidus and glass product durability (Table IV). A given HLW glass must simultaneously optimize all of the P/P constraints and not just have superior chemical durability while having poor thermal or mechanical stability or while being corrosive to all known melter materials of construction. In other words,

one must look at the entire system, a “systems approach,” e.g. how does this waste form react during processing and how will the product produced react with the disposal environment and meet the regulatory requirements of the disposal system? Most P/P properties, other than melt temperature, cannot be measured directly. The waste streams are often highly variable and difficult to characterize. Therefore, often P/P models are used to relate glass composition to a given property, e.g. durability, viscosity, liquidus. The “systems approach” ensures that the final product safeguards the public, and that the production process used is safe to operate.

It is this inherent need to optimize the multiple P/P constraints that drives the diverse wastes types and frits into a common region of glass formulation (see Section 3.1). For example, the discussion in Section 2.1 of the role that MRO in glass has on glass durability demonstrates that ion exchange occurs along percolation channels that exist in glass. The work of Greaves [21] demonstrated that the percolation channels in glass are defined by the NBO atoms, which ionically bond to the alkali, alkaline earth or contaminant species in a glass (Figure 3c). As the cation species are preferentially leached out of the channels, the leachant can then preferentially attack the Si–O NBO bond. This is in agreement with the calculations of El-Shamey [58], which indicate that a silica content of ~67 mol% silica in alkali alkaline-earth silicate glasses corresponds to a composition at which every silicon atom in the glass becomes associated with a basic ion as a second neighbor. Thus, in glasses with < 67 mol% silica, there is always an interconnected path of nonbridging +Si–O<sup>-</sup> sites that allows exchange of species between leachate solution and the glass. At >67 mol% silica, these sites are isolated from each other by the silica network +Si–O–Si+ groups in the glass that suppress the movement of ions involved in leaching. Therefore, to remain durable most waste glasses contain between >67 wt% glass formers (Figure 8) and thus minimize the interconnected paths by which non-matrix forming elements can leach.

## 4.0 Glass Quality: Feed Forward Process Control

When processing HLW glass, a production facility cannot wait until the melt or waste glass has been made to assess its acceptability, since by then no further changes to the glass composition and acceptability are possible. Therefore, the acceptability decision is made on the upstream process, rather than on the downstream *melt* or glass product. That is, it is based on “feed forward” statistical *process* control (SPC)<sup>†</sup> rather than statistical *quality* control (SQC).<sup>††</sup> In SPC, the feed composition to the melter is controlled *prior* to vitrification. In SQC, the glass product is sampled *after* it is vitrified. In addition, in the US, the P/P constraints must be satisfied to a very high degree of certainty (>95%) as the canister geometry (Table III) makes rework (remelting) of the product impossible. With feed forward process control, individual property models are used to transform constraints on the melt and product properties into constraints on the feed composition,

---

<sup>†</sup> This controls the Slurry Feed to the Melter *prior* to vitrification.

<sup>††</sup> Which would adjudicate product release by sampling the glass *after* it's been made.

e.g. the melter is treated as a “black box” and the glass quality in the canister is controlled at 95% confidence from the incoming feed composition.

The successful “systems approach” used at the Savannah River Sites HLW Defense Waste Processing Facility (DWPF) since 1996 is based on “feed forward statistical process control.” The feed composition to the melter is controlled *prior* to vitrification and a confirmatory glass sample is taken only when the feed tank composition changes, e.g. once every 1-3 years. The feed composition is used to calculate the P/P properties of a melter feed from mechanistic P/P models that relate the melt composition to the P/P properties [55,56]. The P/P models depend on known relationships between glass bonding, thermodynamics, and glass structure. These models are the foundation of the SPC system used to monitor and control glass composition for HLW (Product Composition Control System) [59]. Since 1996, over 5000 metric tons (Table III) of HLW glass has been successfully processed to stringent constraints (95% confidence) without any rework.

The mechanistic models can be extrapolated well outside the glass composition range for which they were developed [60] because they are based on known mechanisms. Therefore, mechanistic models allow more flexibility for process control than empirical models, e.g. empirical models are restricted to the compositional region over which they were developed. The P/P models presented below can, therefore, be directly applied to other types of HLW wastes and borosilicate waste glasses.

## 4.1 ***Property/Process Models for Borosilicate Waste Glasses***

### 4.1.1 **Glass Durability**

The most important glass product property is the glass durability. The durability of a waste glass is the single most important variable controlling release of radionuclides and/or hazardous constituents. The intrusion of groundwater into, and passage through, a waste form burial site in which the waste forms are emplaced is the most likely mechanism by which constituents of concern may be removed from the waste glass and carried to the biosphere. Thus it is important that waste glasses be stable in the presence of groundwater.

For homogeneous borosilicate HLW glasses, acceptable performance is defined as an acceptably low dissolution rate, which is controlled by maintaining the glass composition within an acceptable range. The approach can be represented in terms of linking several relationships:

**process control ↔ composition control ↔ dissolution rate control ↔ performance control ↔ acceptable performance**

This linkage is appropriate for HLW waste glasses because the radionuclides are incorporated within the glass structure and are released congruently as the glass dissolves. In general, for any waste form it must be established that control of performance in a laboratory test predicts acceptable control of performance in a disposal system based on performance tests and modeling.

In the United States the durability and phase stability of vitrified HLW must be assessed during production [61] while the repository is interested in the “maximum radionuclide release.” These are tied together by the linking relationships shown above that process and/or composition control translates into acceptable performance. The “product quality constraint” on the HLW glass requires that the waste form producer demonstrate control of the waste form production by comparing production samples or process control information, separately or in combination to the Environmental Assessment benchmark glass [62,63] using the Product Consistency Test (ASTM C1285-08) [64] or equivalent. For acceptance, the mean concentrations of lithium, sodium, and boron in the leachate, after normalization for the concentrations in the glass, shall be less than those of the benchmark glass. For congruent dissolution, the rate of release of a radionuclide from the waste form is proportional to both the dissolution rate of the waste form and the relative abundance of the radionuclide in the waste form.[65] Thus for borosilicate glass  $Tc^{99}$  is the radionuclide released at the fastest rate ( $Cs^{137}$  is released at a somewhat slower rate). However, extensive testing [66,67,68, 69, 70, 71, 72, 73, 74, 75, 76] demonstrated that  $Tc^{99}$  is released at the same rate, congruently, as Na, Li and B. This enables the Na, Li, and B to be measured in a glass durability test and be equated to the “maximum radionuclide release.” These elements are not sequestered in precipitates that participate in surface alteration reactions, and are also not solubility limited. In the case of a multi-phase glass ceramic waste form it may be important to analyze for elements from each significant phase present.

In vitreous and mineral waste forms, the molecular structure controls dissolution (contaminant release) by establishing the distribution of ion exchange sites, hydrolysis sites, and the access of water to those sites.[77] Thus the DWPF durability model, known as the Thermodynamic Hydration Energy Reaction Model (THERMO™), [78,79] THERMO™ estimates the relative durability of silicate and borosilicate glasses based on their compositions. THERMO™ calculates the thermodynamic driving force of each glass component to hydrate based on the mechanistic role of that component during dissolution, e.g. ion exchange, matrix dissolution, accelerated matrix dissolution, surface layer formation, and/or oxidative dissolution. The overall tendency of a given glass to hydrate is expressed as a preliminary glass dissolution estimator, e.g. the change in the free energy of hydration of a glass ( $\Delta G_p$ ) based solely on its composition. The  $\Delta G_p$  is correlated to the response of a 7 day ASTM C1285 (Product Consistency Test). For glasses that undergo accelerated matrix dissolution, an accelerated hydration free energy,  $\Delta G_a$ , can be calculated from known strong base [SB] weak acid [WA] equilibrium. The  $\Delta G_a$  term is additive to  $\Delta G_p$  such that the overall durability of the glass, expressed as the final hydration free energy ( $\Delta G_f$ ), can be predicted, e.g.  $\Delta G_f = \Delta G_p + \Delta G_a$ . The more negative the  $\Delta G_f$  the more readily the hydration reaction will occur and the less durable

the glass. Improvements to the THERMO™ approach have been suggested by Conradt [80,81,82] in the form of a calculation that accounts for the free energy of formation of the crystalline reference state (c.r.s.) of a glassy material. This calculation improves the model fit between the  $\Delta G_p$  parameter and the leachate response.

Recently, Jantzen and Pareizs [83] have proposed an Activated Complex Theory (ACT) durability model based on the early work of Helgeson [84] and the more recent work of Oelkers [85] on basalt glass dissolution. This approach attempts to define the activated complexes that participate in the irreversible formation of the glass gel layer based on the c.r.s. The formation of the hydrated gel layer is the irreversible step. The leached layer exhibits acid/base properties which are manifested as the pH dependence of the thickness and nature of the gel layer. The gel layer has been found to age into either clay mineral assemblages or zeolite mineral assemblages. The formation of one phase preferentially over the other has been experimentally related to changes in the pH of the leachant and related to the relative amounts of  $Al^{+3}$  and  $Fe^{+3}$  in a glass. The formation of ferrite clay mineral assemblages on the leached glass surface layers (lower pH and  $Fe^{+3}$  rich glasses) causes the dissolution rate to slow to a long-term “steady state” rate. The formation of zeolite mineral assemblages such as analcime (higher pH and  $Al^{+3}$  rich glasses) on leached glass surface layers causes the dissolution rate to increase and return to the initial high forward rate. The return to the forward dissolution rate is undesirable for long-term performance of glass in a disposal environment.

The ACT approach [83] models the role of glass stoichiometry, in terms of the quasi-crystalline mineral species (mineral moieties) in a glass. The stoichiometry of the mineral moieties in the parent glass appears to control the activated surface complexes that form in the leached layers, and these “mineral” quasi-crystals (some  $Fe^{+3}$  rich and some  $Al^{+3}$  rich) play a role in whether or not clays or zeolites are the dominant species formed on the leached glass surface. The chemistry and structure, in terms of Q distributions of the parent glass, are well represented by the atomic ratios of the glass forming components. Thus, glass dissolution modeling using simple atomic ratios and/or the c.r.s. are shown to represent the structural effects of the glass on the dissolution and the formation of activated complexes in the glass leached layer: both are related to the activated complexes on the surface by the law of mass action.

The geochemical code EQ3/EQ6 was used to model the leachate compositions from short and long term ASTM C1285 (PCT) tests to determine what phases could precipitate from the leachate, e.g. what phase was each leachate supersaturated with respect to. The EQ3/EQ6 predictions were coupled with the glass composition data in ACT and this provided a link between the atomic ratios of the glasses and the leachate super saturation with respect to either analcime or ferrite phases [83]. Thus glass composition, in terms of quasi-crystalline structural ratios could be used to determine if a glass would form analcime and return to the forward rate or not. Since the pH of a static leachate is also driven by the glass composition and is a parameter entered into the EQ3/EQ6 model, it was not considered as a separate parameter during modeling. The use of the glass atomic ratios determined in this manner correctly predicted the well studied [86] PAMELA

glasses SM58 and SAN60 glasses. The former did not return to the forward rate and the latter glass did [87,88].

The ACT durability model covers a wider composition range than both the THERMO™ durability model data and the THERMO™ validation data [see reference 60]. This allows either the ACT model or the THERMO™ model to be applied to broader composition ranges of LLW, TRU, and mixed waste glasses than either was developed for since both models are based on known dissolution mechanisms for borosilicate glass.

### 4.1.2 Glass Homogeneity

To ensure that borosilicate HLW glasses do not exhibit glass-in-glass phase separation, a minimum  $\text{Al}_2\text{O}_3$  limit (wt% in the glass) is applied in the US.<sup>ξ</sup> The effect of insufficient  $\text{Al}_2\text{O}_3$  was first hypothesized by French researchers [89] who determined that many glass durability models were non-linear, e.g., glasses had release rates far in excess of those predicted by most models, in regions corresponding to low  $\text{Al}_2\text{O}_3$  and in excess of 15 wt%  $\text{B}_2\text{O}_3$  and this was later confirmed independently by Jantzen, et.al. [78,79,90] The low  $\text{Al}_2\text{O}_3$  was also shown to a cause of glass-in-glass phase separation in  $\text{Al}_2\text{O}_3$ - $\text{Fe}_2\text{O}_3$ - $\text{FeO}$ - $\text{Na}_2\text{O}$ - $\text{SiO}_2$  natural basalt systems. [90]

### 4.1.3 Melt Viscosity

The viscosity of a waste glass melt as a function of temperature is the single most important variable affecting the melt rate and pourability of the glass. The viscosity determines the rate of melting of the raw feed, the rate of glass bubble release (foaming and fining), the rate of homogenization, and thus, the quality of the final glass product. If the viscosity is too low, excessive convection currents can occur, increasing corrosion/erosion of the melter materials (refractories and electrodes) and making control of the waste glass melter more difficult. Waste glasses are usually poured continuously into steel canisters or cans for ultimate storage. Glasses with viscosities >500 poise do not readily pour. Moreover, too high a viscosity can reduce product quality by causing voids in the final glass. Therefore, a range of viscosities between 20 and 110 poise at  $T_{\text{melt}}$ , are currently being used for Joule heated waste glass melters.

The approach taken in the development of the viscosity and resistivity process models [56,91,92] was based on glass structural considerations, expressed as a calculated non-bridging oxygen (NBO) term. This NBO parameter represents the amount of structural depolymerization in the glass (Equation 2). Oxide species were expressed in mole fraction and related to the viscosity-temperature dependence of the Fulcher equation

---

<sup>ξ</sup> In glasses the competition for dominant tetrahedral role can cause one or more of the  $(\text{SiO}_4)^{-4}$ ,  $(\text{BO}_4)^{-5}$ ,  $(\text{PO}_4)^{-3}$  SRO tetrahedral units to phase separate and contaminants/radionuclides can partition to the more soluble of the two or more glassy phases created. However, the presence of  $(\text{AlO}_4)^{-5}$  tetrahedra in glass contract the glass structure and inhibit phase separation.

[93,94], also known as the Vogel-Fulcher-Tammann (VFT)<sup>‡</sup> equation. The VFT relates the viscosity ( $\eta$ ) of a glass to temperature (Equation 3) for Newtonian fluids.

$$\text{Equation 2} \quad \text{NBO} \equiv \frac{2 (\text{Na}_2\text{O} + \text{K}_2\text{O} + \text{Cs}_2\text{O} + \text{Li}_2\text{O} + \text{Fe}_2\text{O}_3 - \text{Al}_2\text{O}_3) + \text{B}_2\text{O}_3}{\text{SiO}_2}$$

$$\text{Equation 3} \quad \log_{10} \eta = A + \frac{B}{T - T_o}$$

In Equation 3,  $\eta$  is viscosity (poise or  $\text{d}\cdot\text{Pa}^*$ ),  $T$  is temperature in  $^\circ\text{C}$ , and  $A$ ,  $B$ , and  $T_o$  are fitted constants. It is well documented that the overall fit of the Fulcher equation is excellent for glasses but that it also overestimates viscosity at lower temperatures in the range of viscosities  $>10^{10}$  Pa.s [95].

Calculation of the NBO term from molar composition was combined with quantitative statistical analyses of response surfaces to express glass viscosity and resistivity as a function of melt temperature and glass composition (see the spline fit in Figure 9a). The DWPF glass viscosity model is given by

$$\text{Equation 4} \quad \log \eta(\text{poise}) = -0.61 + \left( \frac{4472.45}{T(^{\circ}\text{C})} \right) - (1.534 * \text{NBO}).$$

with an  $R^2 = 0.976$ .

The DWPF viscosity model assumes that a pure  $\text{SiO}_2$  glass is fully polymerized; i.e. there are no NBO and 4 BO bonds. Addition of other species known as network modifiers depolymerizes the glass while network formers polymerize the glass. This approach was a simplification of an NBO term developed by White and Minser [96] to describe the structural features observed in Raman spectroscopy data of complex natural glasses (obsidians and tektites) which had no  $\text{B}_2\text{O}_3$  and almost all FeO instead of  $\text{Fe}_2\text{O}_3$ ,

$$\text{i.e. } \frac{\text{NBO}}{T} = \frac{2\{[\text{Na}_2\text{O}] + [\text{K}_2\text{O}] + [\text{CaO}] + [\text{MgO}] + [\text{FeO}] - [\text{Al}_2\text{O}_3] - [\text{Fe}_2\text{O}_3]\}}{[\text{SiO}_2] + 2[\text{Al}_2\text{O}_3] + [\text{Fe}_2\text{O}_3]}.$$

<sup>‡</sup> Fulcher derived this expression to model viscosity of inorganic glasses in 1925. In 1921 Vogel (Phys. Zeit., 22, 645-646) derived a similar expression for the viscosity of water, mercury, and oils and Tammann and Hesse generated a similar equation for organic liquids in 1926 (Z. Anorg. Allg. Chem. 156, 245-257). So all three are credited with the derivation of the mathematical expression and it is often referred to as the VFT equation.

\* The unit of viscosity is the dyne second per square centimeter which is called the poise. The SI unit for viscosity is the Newton second per square meter, or pascal second; one of these units equals 10 poise.

Equation 1 is also consistent with the usage of a viscosity ratio ( $V_r$ ) to model the viscosity of slags [97]. The  $V_r$  is defined as the sum of the  $Z/r$  (charge/radius) of the network formers times the atomic % of the network formers divided by the sum of the  $Z/r$  (charge/radius) of the network modifiers times the atomic % of the network modifiers.

In the DWPF viscosity model it is assumed that each mole of alkali oxide added creates two non-bridging oxygen bonds by forming metasilicate ( $\text{Na}_2\text{SiO}_3$ ) structural units, thus depolymerizing the glass. While the exact number of non-bridging oxygen atoms depends on the molar ratio of all of the species in a waste glass to  $\text{SiO}_2$ , most DWPF glasses have a  $\text{O}^{2-}/\text{Si}^{4+}$  ratio of 2.6 to 3.3 which implies that disilicate and metasilicate structural units predominate for the alkali species in the waste glasses. Calculation of the  $\text{O}^{2-}/\text{Si}^{4+}$  ratio for DWPF glasses included contributions from Na, K, Li, and Cs alkali species and a  $\text{Si}^{4+}$  concentration that was depleted by the amount associated with  $\text{B}_2\text{O}_3$  structural units.

The DWPF viscosity model further assumes that each mole of  $\text{Al}_2\text{O}_3$  creates two bridging oxygen bonds (polymerizes the glass structure) by creating tetrahedral alumina groups that bond as  $\text{NaAlO}_2$  structural groups. In  $\text{Al}_2\text{O}_3$  and/or  $\text{SiO}_2$  deficient glasses,  $\text{Fe}_2\text{O}_3$  can take on a tetrahedral coordination and polymerize a glass by forming  $\text{NaFeO}_2$  structural groups. However, if sufficient  $\text{Al}_2\text{O}_3$  and  $\text{SiO}_2$  are present in a glass such as DWPF waste glasses that typically contain  $>3$  wt%  $\text{Al}_2\text{O}_3$  and  $>40$  wt%  $\text{SiO}_2$ , then  $\text{Fe}_2\text{O}_3$  is octahedral and creates two non-bridging oxygen bonds, i.e. it depolymerizes the glass matrix as assumed in the DWPF viscosity model (Equation 1). This is consistent with the work of Mysen [98] who demonstrated that high iron magmas (iron silicate glasses) that contained levels of 10 wt%  $\text{Fe}_2\text{O}_3$  decreased the melt viscosity. He concluded that  $\text{NaFeO}_2$  structural groups were not incorporated into the silicate network to the same degree as  $\text{NaAlO}_2$  structural groups [98]. Therefore,  $\text{Fe}_2\text{O}_3$  is considered a network modifier and depolymerizer in the DWPF viscosity model. Since FeO is also known to act as a glass network depolymerizer, there is no need for a separate FeO term and all the iron in a given glass is calculated as if it were  $\text{Fe}_2\text{O}_3$ .

Lastly, the DWPF viscosity model assumes that each mole of  $\text{B}_2\text{O}_3$  creates one non-bridging oxygen bond. This is based on data by Smets and Krol [99], and Konijnendijk [100] who demonstrated that for sodium silicate glasses with low  $\text{B}_2\text{O}_3$  content the  $\text{B}_2\text{O}_3$  enters the glass network as  $\text{BO}_4^-$  tetrahedral. At higher  $\text{B}_2\text{O}_3$  concentrations these tetrahedra are converted into planar  $\text{BO}_3^-$  groups. Tetrahedral  $\text{BO}_4^-$  contributes no NBO while planar  $\text{BO}_3^-$  groups contribute one non-bridging oxygen atom [101].

In 1991 the model was developed on as made compositions and revised [92] based on analyses of the same non-radioactive glasses and frits (220 viscosity-temperature measurements). During revision the model was validated [92] on an additional 200 glasses (radioactive and non-radioactive and 1004 viscosity-temperature pairs) (Figure 9a). Uranium was shown to have no impact on glass viscosity and  $\text{ThO}_2$  at  $<1$  wt% had no impact on glass viscosity.

The viscosity model has been validated over composition and temperature regions (800-1500°C) well outside of the regions for which it was developed (Figure 9a) because it is based on known glass structural mechanisms. This affords the ability to use the viscosity model for the broader composition ranges of LLW, TRU, and mixed wastes.

#### 4.1.4 Melt Resistivity

The electrical resistivity of a waste glass melt as a function of temperature is the single most important variable affecting the establishment of Joule heating for electrically heated melters. The electrical resistivity controls the rate of melting after the establishment of Joule heating. At low temperatures, glasses are good insulators, while at high temperatures they conduct electric current relatively well. The current is transferred by ion migration: the modifying ions mobility is much higher than that of network formers at all temperatures. The concentration of alkali ions contributes the most to the electrical conductivity. During passage of direct current through a glass melt, the alkali ions migrate to the cathode while the glass close to the anode is enriched with SiO<sub>2</sub> and the resistivity locally increases. These polarization effects are eliminated by the use of alternating current as used in JHM's. However, the chemical composition of a melt thus has a significant effect on the electrical properties [102] and the melt rate at the melt temperature.

The same melt polymerization model was used for glass resistivity as was used for glass viscosity and a relationship derived between the resistivity, the inverse of the melt temperature, and the NBO (Figure 9b).

Equation 5 
$$\log \varphi(\Omega cm) = -2.48 + \left( \frac{4399.57}{T(^{\circ}C)} \right) - (0.45 * NBO)$$

with an  $R^2 = 0.92$ .

The measured viscosities and electrical resistivities are well correlated (Figure 9c), i.e. if the viscosity is known, then the resistivity can be accurately calculated.

Equation 6 
$$\log \eta(\text{poise}) = 1.82 - (0.67 * NBO) + 2.42 \log \varphi(\Omega cm)$$

With an  $R^2 = 0.95$ .

This phenomena had been noted previously in the commercial glass industry [102] where generally

Equation 7 
$$\log \eta \cong 3 \log \varphi$$

#### 4.1.5 Melt REDOX

Control of the REDuction/OXidation (REDOX) equilibrium in the DWPF melter is critical for processing high level liquid wastes. Foaming, cold cap roll-overs, and off-gas surges all have an impact on pouring and melt rate during processing of waste glass. All of these phenomena can impact waste throughput and attainment. These phenomena are caused by gas-glass disequilibrium when components in the melter feeds convert to glass and liberate gases such as steam, CO<sub>2</sub>, O<sub>2</sub>, H<sub>2</sub>, NO<sub>x</sub>, and/or N<sub>2</sub>. In order to minimize gas-glass disequilibrium a REDOX strategy is used to balance feed reductants and feed oxidants while controlling the REDOX between  $0.09 \leq Fe^{2+}/\Sigma Fe \leq 0.33$ . A  $Fe^{2+}/\Sigma Fe$  ratio  $\leq 0.33$  prevents metallic and sulfide rich species from forming nodules that can accumulate on the floor of the melter. Control of foaming, due to deoxygenation of manganic species, is achieved by converting oxidized MnO<sub>2</sub> or Mn<sub>2</sub>O<sub>3</sub> species to MnO during melter preprocessing. At the lower REDOX ratio of  $Fe^{2+}/\Sigma Fe \sim 0.09$  about 99% of the Mn<sup>+4</sup>/Mn<sup>+3</sup> is converted to Mn<sup>+2</sup> and foaming does not occur. Nominally a  $Fe^{2+}/\Sigma Fe$  of  $\sim 0.2$  in the mid-range of 0.09-0.33 is targeted in the melt pool.

The REDOX model relates the  $Fe^{2+}/\Sigma Fe$  ratio of the final glass to the molar concentrations of the oxidants and reductants in the melter feed. The REDOX model is based on Electron Equivalents (EE) that are exchanged during chemical reduction (making an atom or molecule less positive by electron transfer) and oxidation (making an atom or molecule more positive by electron transfer). Therefore, the number of electrons transferred for each REDOX reaction can be summed and an Electron Equivalents term for each organic and oxidant species defined [103,104,105]. The model accounts for reoxidation of the manganese by nitrate salts in the cold cap and takes the form

$$\text{Equation 8} \quad \frac{Fe^{2+}}{\Sigma Fe} = f \left[ (2[F] + 4[C] + 4[O_T] - 5[N] - 5[Mn]) \frac{45}{T} \right] = f[\xi]$$

where

$f$	=	indicates a function
$[F]$	=	formate (mol/kg feed)
$[C]$	=	coal (carbon) (mol/kg feed)
$[O_T]$	=	oxalate <sub>Total</sub> (soluble and insoluble) (mol/kg feed)
$[N]$	=	nitrate + nitrite (mol/kg feed)
$[Mn]$	=	manganese (mol/kg feed)
$T$	=	total solids (wt%)

$$\xi = (2[F] + 4[C] + 4[O_T] - 5[N] - 5[Mn]) \frac{45}{T}$$

and

$$\frac{Fe^{2+}}{\Sigma Fe} = 0.2358 + 0.1999\xi$$

A model that includes sugar as a reductant can be found in reference 104.

#### 4.1.6 Melt Liquidus

A liquidus temperature model prevents melt pool or volume crystallization during operation. Volume crystallization needs to be avoided because it can involve almost simultaneous nucleation of the entire melt pool as volume crystallization can occur very rapidly. Furthermore, once iron spinel crystals are formed (the most ubiquitous liquidus phase occurring in US defense HLW), these crystals are refractory and cannot be redissolved into the melt pool. The presence of either the spinel or nepheline liquidus phases may cause the melt viscosity and resistivity to increase which may cause difficulty in discharging glass from the melter as well as difficulty in melting via Joule heating. Once a significant amount of volume crystallization has occurred and the resulting crystalline material has settled to the melter floor, melting may be inhibited and the pour spout may become partially or completely blocked making pouring difficult.

The crystal-melt equilibria were modeled based on quasicrystalline concepts [24,25]. A pseudobinary phase diagram between a ferrite spinel (an incongruent melt product of transition metal iron rich acmite) and nepheline was defined. The pseudobinary lies within the  $\text{Al}_2\text{O}_3\text{-Fe}_2\text{O}_3\text{-Na}_2\text{O-SiO}_2$  quaternary system that defines the crystallization of basalt glass melts (note that the basalt glass system is used as an analogue for waste glass durability, liquidus, and the prevention of phase separation). The liquidus model developed based on these concepts has been used to prevent unwanted crystallization in the DWPF HLW melter for the past six years while allowing >10 wt% higher waste loadings to be processed. The liquidus model (Equation 9) and the pseudobinary (Figure 11) are shown [24,25] to be consistent with all of the thermal stability data generated on DWPF HLW glasses. The model ranges developed on 105 different glass compositions and validated over wider ranges (161 glasses). [60]

Equation 9

$$\frac{1}{T_L(K)_{\text{spinel}}} = -0.000260 \ln(M_2) - 0.000566 \ln(M_1) - 0.000153 \ln(M_T) - 0.00144$$

$$= \ln \left\{ (M_2)^{-0.000260} (M_1)^{-0.000566} (M_T)^{-0.000153} \right\} - 0.00144$$

where

$$\begin{aligned} \Sigma_{\text{MT}} &\equiv \phi_{\text{T,SiO}_2} Z_{\text{SiO}_2} + \phi_{\text{T,Al}_2\text{O}_3} Z_{\text{Al}_2\text{O}_3} + \phi_{\text{T,Fe}_2\text{O}_3} Z_{\text{Fe}_2\text{O}_3} \\ \Sigma_{\text{M1}} &\equiv \phi_{\text{M1,Al}_2\text{O}_3} Z_{\text{Al}_2\text{O}_3} + \phi_{\text{M1,Fe}_2\text{O}_3} Z_{\text{Fe}_2\text{O}_3} + \phi_{\text{M1,TiO}_2} Z_{\text{TiO}_2} + \phi_{\text{M1,Cr}_2\text{O}_3} Z_{\text{Cr}_2\text{O}_3} + \phi_{\text{M1,ZrO}_2} Z_{\text{ZrO}_2} \\ &\quad + \phi_{\text{M1,NiO}} Z_{\text{NiO}} + \phi_{\text{M1,MgO}} Z_{\text{MgO}} + \phi_{\text{M1,MnO}} Z_{\text{MnO}} \\ \Sigma_{\text{M2}} &\equiv \phi_{\text{M2,NiO}} Z_{\text{NiO}} + \phi_{\text{M2,MgO}} Z_{\text{MgO}} + \phi_{\text{M2,MnO}} Z_{\text{MnO}} + \phi_{\text{M2,CaO}} Z_{\text{CaO}} \\ &\quad + \phi_{\text{M2,K}_2\text{O}} Z_{\text{K}_2\text{O}} + \phi_{\text{M2,Li}_2\text{O}} Z_{\text{Li}_2\text{O}} + \phi_{\text{M2,Na}_2\text{O}} Z_{\text{Na}_2\text{O}} \\ \Sigma_{\text{T1}} &\equiv \phi_{\text{T1,SiO}_2} Z_{\text{SiO}_2} + \phi_{\text{T1,Al}_2\text{O}_3} Z_{\text{Al}_2\text{O}_3} + \phi_{\text{T1,Fe}_2\text{O}_3} Z_{\text{Fe}_2\text{O}_3} + \phi_{\text{T1,TiO}_2} Z_{\text{TiO}_2} \\ \Sigma_{\text{N1}} &\equiv \phi_{\text{N1,K}_2\text{O}} Z_{\text{K}_2\text{O}} + \phi_{\text{N1,Li}_2\text{O}} Z_{\text{Li}_2\text{O}} + \phi_{\text{N1,Na}_2\text{O}} Z_{\text{Na}_2\text{O}} \end{aligned}$$

and

$$M_2 \equiv \frac{\Sigma_{\text{M2}}}{\Sigma}, M_1 \equiv \frac{\Sigma_{\text{M1}}}{\Sigma}, M_T \equiv \frac{\Sigma_{\text{MT}}}{\Sigma}, \text{ and } \Sigma \equiv \Sigma_{\text{M2}} + \Sigma_{\text{M1}} + \Sigma_{\text{MT}} + \Sigma_{\text{T1}} + \Sigma_{\text{N1}}.$$

and  $R^2 = 0.89$ . The details of the modeling are given elsewhere [106].

### 4.1.7 Melt Sulfate Solubility

Sulfate and sulfate salts are not very soluble in borosilicate waste glass. When the glass is cooled, inclusions and/or phase separation of a sulfate rich phase are often visible in the glass and often a layer of water soluble sulfate is visible on the glass surface. When the glass is molten, the molten salt layer known as gall can float on the melt pool surface (Figure 12a). Soluble sulfate salts are often enriched in cesium and strontium, which can impact radionuclide release from the cooled glass if the salts are present as inclusions or a frozen gall layer. The alkali and alkaline earth sulfate salts, in conjunction with alkali chlorides, collect on the melt surface as a low melting (600-800°C), low density, low viscosity melt phase. At moderate concentrations, the salts have a beneficial effect on melting rates. If a melter is slurry fed as done in the US, steam can get trapped under the layer of gall and cause steam explosions which is undesirable. At excessively high feed concentrations, molten alkali sulfates float on the surface of the melt pool or become trapped as inclusions in the glass.

The results of sulfate solubility measurements from both dynamic melter tests and static crucible tests performed with HLW wastes were compared. This data was also compared to Slurry-Fed Melt Rate Furnace (SMRF) data generated on HLW melts. In addition, a survey was made of both dynamic and crucible tests for Low Activity Wastes (LAW) and crucible tests performed with commercial soda-lime-silica glasses. Phenomenological observations in the various studies, e.g. completeness or lack of gall and secondary sulfate phases, were categorized into melt conditions representing “at saturation, over saturation, and super saturation.” This enabled modeling of the most desirable “at saturation” conditions, e.g. no appearance of a sulfate layer on the melt pool, in relation to undesirable conditions of over saturation (partial melt pool coverage) and super saturation (almost complete melt pool coverage). Sulfate solubility is related to melt polymerization and temperature and so to the HLW viscosity model given in Section 4.1.3. Using the viscosity model given in Equation 4 allows models to be defined for sulfate solubility for the various degrees of sulfate saturation [107,108] as shown in Figure 12b.

Modeling of the sulfate solubility as a function of calculated viscosity (Equation 4) was performed. The glasses were grouped by sulfate saturation which provided a series of three parallel models, one at saturation, one at over saturation, and one at supersaturation:

Equation 10  $\text{SO}_4^{=}$  solubility (at saturation) =  $1.2360 - 0.5408 \log \text{viscosity}_{\text{calc}}$  (poise)

Equation 11  $\text{SO}_4^{=}$  solubility (supersaturation) =  $1.9605 - 0.5229 \log \text{viscosity}_{\text{calc}}$  (poise)

Equation 12  $\text{SO}_4^{=}$  solubility (over saturation) =  $1.7539 - 0.5729 \log \text{viscosity}_{\text{calc}}$  (poise)

with an  $R^2$  values of 0.87, 0.96, and 0.86 respectively.

#### 4.1.8 Product Composition Control System (PCCS) and Process Limits [57,59]

While the individual P/P models are based on glass structural concepts of SRO, MRO and quasicrystalline theory, the process limits are set for a given melter type and geometry by experience with non-radioactive pilot scale melters. Multivariate statistical theory is used in conjunction with the P/P models to control within multi-dimensional composition space.

The regression lines for the individual properties, e.g. durability, liquidus temperature, and viscosity, can be back-solved to determine composition values,  $c_i$ , corresponding to the respective property limits.<sup>†</sup> This transforms the constraints on properties into equivalent constraints,  $c_i^*$ , on composition. In turn,  $c_i^*$  transforms into a constraint on concentrations of individual constituent oxides. Describing all predicted oxide values for a given property that are acceptable defines the Expected<sup>†</sup> Property Acceptable Region (EPAR) for that property (Figure 13). To incorporate modeling error, the appropriate 95% confidence band can also be back-solved to obtain a new limit on the property that includes the modelling error. This is defined as the Property Acceptable Region (PAR) (Figure 13).

Errors in measurement must also be accounted for. During operation, the feed compositions from which the properties must be predicted will not be known, but will be measured. There will be appreciable errors in composition arising from the DWPF sampling and measurement systems; therefore, these errors must be accounted for in order to achieve 95% confidence in the property predictions. In DWPF, a composition measurement is a vector of measurements taken for several constituents simultaneously.<sup>†</sup> Thus the description of compositional uncertainty requires multivariate statistical techniques. The concentrations of the individual constituents in the DWPF composition

---

<sup>†</sup> No such solution is necessary for the homogeneity (including the limit on  $\text{Al}_2\text{O}_3$ ), conservation, frit loading, or waste solubility constraints since again they were originally formulated as limits on composition.

<sup>†</sup> It is denoted "Expected" since it derives from the fitted line, which is the locus of the conditional *expectation* of the property given the composition.

<sup>†</sup> At least, these measurements are taken very close together in time and by consequence may be considered simultaneous.

measurements are assumed to be multivariate Gaussian with a covariance matrix  $\Sigma_{\text{m}}$  and the solution can be solved with a student's t-test for all product and processing constraints incorporating all relevant constituent elements measured in the glass. The confluence of the regions described by the t-tests for all property constraints forms the Measurement Acceptable Region (MAR) (Figure 13) which includes all measurement errors including tank transfer errors.

Glasses inside the MAR are durable and processable within 95% confidence. The ternary representation of the PCCS system demonstrates the flexibility to blend two different types of waste. In this case, the radionuclide rich stream that comes from the removal of these components from the salt supernates (waste I) and the sludge (waste II). This allows the waste glass formulations on lower boundary of the MAR (Figure 13) which maximizes waste sludge component loadings instead of waste glass formulations in the middle of the qualified MAR region. At the same time, it provides the basis for knowing, to within 95% confidence, that a given melter feed will be pourable, will not crystallize inside the melter, and will be durable and acceptable to the geologic repository.

## 5.0 Other Glasses

Borosilicate waste glasses that contain  $(\text{SiO}_4)^{-4}$ ,  $(\text{BO}_4)^{-5}$ ,  $(\text{BO}_3)^{-3}$  and some  $(\text{AlO}_4)^{-5}$  SRO structures that are bound together in MRO configurations. Glasses that contain only  $(\text{SiO}_4)^{-4}$  and  $(\text{AlO}_4)^{-5}$  SRO are aluminosilicate glasses while glasses that contain  $(\text{BO}_4)^{-5}$ ,  $(\text{BO}_3)^{-3}$ , and some  $(\text{AlO}_4)^{-5}$  are aluminoborate glasses. Phosphate glasses contain no  $(\text{SiO}_4)^{-4}$ ,  $(\text{BO}_4)^{-5}$  or  $(\text{BO}_3)^{-3}$  but contain  $(\text{PO}_4)^{-3}$  and  $(\text{AlO}_4)^{-5}$  (aluminophosphate glasses) or  $(\text{PO}_4)^{-3}$  and  $(\text{FeO}_4)^{-5}$  (iron phosphate glasses) instead.

### 5.1 Rare Earth and Lanthanum Borosilicates

As melting technology improves (Section 6) both the melting temperature and the waste loading of waste in nuclear glasses will increase. The waste loading increase will translate into higher glass activity and heat loading and a higher canister temperature. Therefore, new nuclear glass compositions are being developed that will be able to immobilize higher waste concentrations than current glasses. Such glasses must exhibit excellent chemical durability and glass transformation temperatures that are higher than the current alkali borosilicate nuclear glasses in order to avoid crystallization risks (volume increase) during storage. As the concentration of actinide and rare earth elements will be greater in these wastes, researchers have begun to investigate rare earth (RE)-rich glassy matrices such as lanthanide aluminoborosilicate glasses ~LaBS and lanthanide aluminosilicate ~(RESiAlO) glasses. [22,109] These glasses show very good performance, but the high melting temperature will likely increase the volatility of some fission products during melting. Therefore, glasses that melt around 1300°C have initially been investigated with compositions of approximately 51.0 SiO<sub>2</sub>–8.5 B<sub>2</sub>O<sub>3</sub>–12.2 Na<sub>2</sub>O–4.3 Al<sub>2</sub>O<sub>3</sub>–4.8 CaO–3.2 ZrO<sub>2</sub>–16.0 RE<sub>2</sub>O<sub>3</sub>, where each RE was tested individually as was a mixture of La, Ce, Pr, and Nd.

LaBS glasses have also been used to immobilize  $\text{PuO}_2$  and associated neutron absorbers such as Gd (Table V, Frit A). Second generation LaBS glasses for  $\text{PuO}_2$  immobilization incorporated hafnium for improved criticality performance (Table V, Frit B).[110] Actinide solubility testing with the Frit B composition was primarily performed with combinations of plutonium and uranium to more accurately reflect the expected excess weapons useable plutonium feed streams. The solubility of combinations of plutonium and uranium was shown to be even higher than for Pu only. For example, a homogeneous glass containing 9 wt %  $\text{PuO}_2$  and 6 wt %  $\text{UO}_3$  was fabricated for a total actinide loading of 15 wt % [111] was shown to be very durable [112,113]

The commercial lanthanide (rare earth) borosilicate glass upon which the  $\text{PuO}_2$  LaBs glasses were based was first proposed by Loffler [114,115] for use in technical applications where dichroic glasses were needed or for use as decorative highly colored glasses.[114] The lanthanide glasses are known to accommodate Cs, Y, La-Hf (e.g. the lanthanide elements La, Ce, Pr, Nd, Pm, Sm, Eu, Gd, Tb, Dy, Ho, Er, Tm, Yb, and Lu) and the actinides in relatively high concentrations.[115] This family of high lanthanide glasses has been used extensively in nuclear applications for protective purposes since many of the lanthanide elements have large thermal neutron cross-sections.[115] Therefore, several  $\text{La}_2\text{O}_3$ - $\text{B}_2\text{O}_3$ - $\text{SiO}_2$  (LaBS) glasses based on the Loffler formulation were investigated.

The high lanthanide glasses were chosen for investigation rather than conventional borosilicate waste glasses that have inherently low solubilities for  $\text{PuO}_2$  because of the ability of the lanthanide glasses to solubilize actinides. Loffler's glass is unique in that it combines lanthanide oxides as fluxes in an aluminosilicate type glass in place of the usual alkali metal oxides.[115] The glasses melt at conventional melting temperatures ( $\geq 1350^\circ\text{C}$ ) but have an extraordinarily low viscosity. The Loffler glasses typically contain 10-70 wt% of some lanthanide oxides, 9-20 wt%  $\text{Al}_2\text{O}_3$  and the remainder is  $\text{SiO}_2$  (21.5-46 wt %).

The first Loffler glass formulations for  $\text{PuO}_2$  stabilization were tested by Ramsey et. al.[116] and were very similar to the Loffler composition given in Table V. The Ramsey Loffler variants were able to stabilize anywhere from 1.85-17.62 wt%  $\text{ThO}_2$  (a simulant for  $\text{PuO}_2$ ).  $\text{Ce}_2\text{O}_3$  was used in place of the  $\text{La}_2\text{O}_3$  and  $\text{Pr}_2\text{O}_3$  in the Loffler formulation although a mixture of three lanthanide oxides was retained during all testing. Additional testing[117,118] substituted a variety of different rare earth elements (always a minimum of three) with little impact on the solubility of  $\text{ThO}_2$ . This was consistent with the finding of the commercial glass industry that the substitution of various rare earths in the lanthanide borosilicate glasses had little effect on any measured physical properties.[115]

The Loffler and early LaBS glasses contained hazardous metal oxides such as  $\text{PbO}$  and  $\text{BaO}$ . Subsequent formulations [119,120] substituted  $\text{Al}_2\text{O}_3$  and  $\text{SrO}$  for  $\text{PbO}$  and  $\text{BaO}$  and began to examine what combinations of lanthanide oxides ( $\text{Gd}_2\text{O}_3$ ,  $\text{La}_2\text{O}_3$ , and  $\text{Nd}_2\text{O}_3$ ) could be optimized with the actinides ( $\text{ThO}_2$ ). The lanthanide Gd was chosen as

a neutron absorber and samarium and europium oxides were also investigated. A maximum  $\text{ThO}_2$  loading of 25 wt% was achieved with one of the  $\text{Al}_2\text{O}_3/\text{SrO}$  formulations. [120] Further testing of Frit A glass at Pacific Northwest National Laboratory (PNNL) and Savannah River National Laboratory (SRNL) (Table V) with  $\text{PuO}_2$  revealed that the maximum  $\text{PuO}_2$  concentration that could be accommodated in Frit A was 13.4 wt% and a concentration of 9.5 wt% was deemed acceptable for criticality concerns.

The change from the  $\text{PbO}/\text{BaO}$  bearing Loffler glasses to the  $\text{SrO}/\text{Al}_2\text{O}_3$  Frit A glasses caused the total  $\text{Ln}_2\text{O}_3$  content of the glasses to decrease while the  $\text{Al}_2\text{O}_3+\text{SiO}_2$  content increased (Table V). The additional modification to Frit B which added  $\text{HfO}_2$  in place of  $\text{Ln}_2\text{O}_3$  caused a further decrease in the total  $\text{Ln}_2\text{O}_3$  content (Table V). At concentrations of lanthanide oxides,  $\text{Ln}_2\text{O}_3$ , in the range of 15 wt% the SRNL LaBS glass crystallized to lanthanum silicate phases and amorphous phase separation (APS) known as glass-in-glass phase separation was observed.[120] In addition, the liquidus temperature of some of the LaBS formulations were shown to be too low, i.e. the glass easily crystallized lanthanum silicates and oxides during pouring.[121] Therefore, a glass formulation approach was needed that could be used to avoid regions of rare-earth silicate formation and regions of glass-in-glass phase separation.

None of the ternary oxide phase relations are known in the  $\text{Ln}_2\text{O}_3\text{-B}_2\text{O}_3\text{-SiO}_2$  system. However, each of the binary oxide systems which comprise the binary sides of the ternary system are known, e.g.  $\text{Ln}_2\text{O}_3\text{-SiO}_2$  and  $\text{Sm}_2\text{O}_3\text{-SiO}_2$ ,  $\text{La}_2\text{O}_3\text{-B}_2\text{O}_3$ , and  $\text{B}_2\text{O}_3\text{-SiO}_2$ . The phase diagrams for all the  $\text{Ln}_2\text{O}_3\text{-SiO}_2$  systems are similar: each system has three stoichiometric compounds, 1:1, 2:3 and 1:2  $\text{Ln}_2\text{O}_3\text{:SiO}_2$ . Each  $\text{Ln}_2\text{O}_3\text{-SiO}_2$  system has a region of glass-in-glass phase separation at  $>1:2$   $\text{Ln}_2\text{O}_3\text{:SiO}_2$  with lower stability temperatures of  $\sim 1700^\circ\text{C}$ . Each  $\text{Ln}_2\text{O}_3\text{-SiO}_2$  system has one high temperature congruent melting lanthanide silicate compound at 1:1  $\text{Ln}_2\text{O}_3\text{:SiO}_2$  and one incongruent melting lanthanide silicate compound at 1:2  $\text{Ln}_2\text{O}_3\text{:SiO}_2$ . Likewise, all the  $\text{Ln}_2\text{O}_3\text{-B}_2\text{O}_3$  binary phase diagrams are similar. The phase relations and regions of low melting eutectics in the  $\text{Ln}_2\text{O}_3\text{-B}_2\text{O}_3\text{-SiO}_2$  system, the  $\text{Ln}_2\text{O}_3\text{-B}_2\text{O}_3\text{-SiO}_2$  system were inferred from the projections of the pertinent binary oxide systems (using  $\text{La}_2\text{O}_3\text{-SiO}_2$  and the  $\text{B}_2\text{O}_3\text{-SiO}_2$  systems as the prime example). In this manner the ternary phase relations regarding crystallization and phase separation were related to the composition of the fluid melts observed by Loffler.[122]

Since the known binary oxide systems are in mole % oxide, the compositions from Table V have been converted from oxide wt% to oxide mole%. All of the  $\text{Ln}_2\text{O}_3$  have been grouped together and the phase equilibria analyzed with  $\text{SiO}_2$  as the only glass former and with  $(\text{SiO}_2 + \text{Al}_2\text{O}_3)$  grouped with  $\text{SiO}_2$  due to their similar structural role as glass formers. For the Loffler glass, this simplification of the glass chemistry (including the contribution of the  $\text{Al}_2\text{O}_3$ ) accounts for 89.5 wt% of the glass components.

The potential ternary phase relations in the  $\text{La}_2\text{O}_3\text{-B}_2\text{O}_3\text{-(SiO}_2+\text{Al}_2\text{O}_3)$  system are shown in Figure 15. The 1:1  $\text{La}_2\text{O}_3\text{:SiO}_2$  stoichiometric compound which melts at  $1975^\circ\text{C}$  more

than likely forms a high melting temperature ridge in the ternary system with the 1:1  $\text{La}_2\text{O}_3$ :  $\text{B}_2\text{O}_3$  stoichiometric compound which melts at  $1660^\circ\text{C}$ . In the  $\text{La}_2\text{O}_3$ - $\text{B}_2\text{O}_3$ - $(\text{SiO}_2+\text{Al}_2\text{O}_3)$  system (Figure 14) compositions in the proximity of this 1:1 stoichiometric  $(\text{La}_2\text{O}_3\text{-B}_2\text{O}_3)$ : $(\text{La}_2\text{O}_3\text{-SiO}_2)$  ridge will likely have high liquidus temperatures. The lowest melting temperature glasses can be formed in the  $\text{La}_2\text{O}_3$ - $\text{B}_2\text{O}_3$ - $(\text{SiO}_2+\text{Al}_2\text{O}_3)$  system (Figure 15) along a trough defined by a line joining the eutectic compositions at 1:3  $\text{La}_2\text{O}_3$ : $\text{SiO}_2$  and  $\sim 1:3$   $\text{La}_2\text{O}_3$ : $3\text{B}_2\text{O}_3$ . These eutectics melt at temperatures of  $1625^\circ\text{C}$  and  $\sim 1132\text{-}36^\circ\text{C}$ , respectively. Therefore, along the  $\sim 1:3$  stoichiometric axis shown in Figure 14 compositions higher in  $\text{B}_2\text{O}_3$  will melt at a lower temperature than compositions enriched in  $(\text{SiO}_2 + \text{Al}_2\text{O}_3)$ .

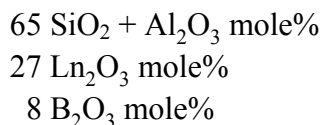
At compositions with less molar  $\text{La}_2\text{O}_3$  than 22-25 mole% on Figure 14, the regions of glass-in-glass (2-liquid) phase separation more than likely form a continual dome as indicated by the shaded region in Figure 15. The lower stability temperature of the 2 liquid regions in the  $\text{La}_2\text{O}_3$ - $\text{SiO}_2$  system is  $\sim 1700^\circ\text{C}$  while the lower stability temperature of the 2-liquid region in the  $\text{La}_2\text{O}_3$ - $\text{B}_2\text{O}_3$  system is  $1136^\circ\text{C}$ . This is a region of potential phase separation and should be avoided during glass formulation in this system. Even if a homogeneous glass of this composition can be made by rapid pouring and/or quenching, it will be metastable and tend to phase separate and/or crystallize when subjected to annealing and/or subsequent heat treatment.

Based on this phase equilibrium approach the following composition modifications to the LaBS formulations for  $\text{PuO}_2$  were recommended [122]:

- $\text{Ln}_2\text{O}_3$  needs to be added and  $\text{Al}_2\text{O}_3$  and  $\text{SiO}_2$  content reduced to modify the glass composition so that it is no longer in the range of potential phase separation
- Sufficient  $\text{Ln}_2\text{O}_3$  should be added and  $\text{Al}_2\text{O}_3$  and  $\text{SiO}_2$  content reduced so that the final glass composition falls on or near the low melting eutectic trough delineated in Figure 14 at  $\sim 1:3$  stoichiometric axis in the  $\text{Ln}_2\text{O}_3$ - $\text{B}_2\text{O}_3$ - $(\text{SiO}_2+\text{Al}_2\text{O}_3)$  system
- Compositions lying along the 1:3 stoichiometric axis in the in the  $\text{Ln}_2\text{O}_3$ - $\text{B}_2\text{O}_3$ - $(\text{SiO}_2 + \text{Al}_2\text{O}_3)$  system (such as the composition shown below) should melt at lower temperatures than the current LaBS formulation and have lower liquidus temperatures:

50  $\text{SiO}_2 + \text{Al}_2\text{O}_3$  mole%  
25-30  $\text{Ln}_2\text{O}_3$  mole%  
20-25  $\text{B}_2\text{O}_3$  mole%

- Mixed  $\text{Ln}_2\text{O}_3$  should continue to be used instead of just  $\text{La}_2\text{O}_3$  since the heat of mixing of the rare earth oxides will effectively lower the melt temperature
- If 20-25%  $\text{B}_2\text{O}_3$  is shown to be ineffective then compositions in the range of the original Loffler glass should be formulated as indicated below



## 5.2 Phosphate Glasses

Phosphate glasses have been studied in several countries (mainly Russia and the US) as potential waste forms to immobilize HLW solutions [11, 51, 123]. In general, the phosphate glasses have not been as well studied as the borosilicate glasses and hence processing knowledge, in terms of process models, are not available to accommodate the wide range of HLW wastes.

Phosphate glasses melt at lower temperatures and can incorporate high concentrations of actinides, rare-earth oxides, molybdates, and sulfates as discussed in 51. However, phosphate melts are generally more corrosive and are less durable in aqueous environments than borosilicate systems. [22,55] Phosphate glasses have lower thermal stability and a tendency to crystallize.

### 5.2.1 Aluminophosphates [124]

The delay in the development of phosphate glasses for use in waste disposal has been attributed to the lack of industrial usage of these types of glasses and hence the lack of commercial experience and technology such as exists for the silicate glasses. Aluminophosphate HLW glasses have been vitrified in Russia since 1987 in a JHCM, the EP-500 Mayak facility in the Ural Region of Russia. [22,125, 126,127,128] These glasses are primarily sodium phosphate glasses to which additions of  $\text{Al}_2\text{O}_3$  have been shown to improve durability.[129] For HLW wastes with high  $\text{Al}_2\text{O}_3$  content from dissolution of Al-cladding, these make good candidate waste forms as they can accept 17-25 wt%  $\text{Al}_2\text{O}_3$  (Table VI). The first melter was put into operation in 1987 and operated for 1.5 years. The composition of the glass-formers (in mass%) was reported as: 22 to 26%  $\text{Na}_2\text{O}$ , 21 to 25%  $\text{Al}_2\text{O}_3$ , 47 to 53%  $\text{P}_2\text{O}_5$ , and up to 1.5%  $\text{Fe}_2\text{O}_3$ . [130] After design changes, a second unit was constructed and placed into operation in 1991 and operated until 1997. A new JHCM melter was constructed and began operation in 2001 and operated until 2006. The JHCM is lined with  $\text{ZrO}_2\text{-Al}_2\text{O}_3$  refractory. Orthophosphate acid is mixed with the aqueous HLW and melted at a maximum temperature of  $1200^\circ\text{C}$  [51]. The EP-500 melters have produced 4000 metric tons of glass in 8800 canisters (Table III).

### 5.2.2 Lead Iron phosphates

Research continued in the area of other phosphate glass compositions, specifically lead-iron phosphate (LIP) glasses. Lead was added to decrease melt temperature and viscosity, and iron was added to increase durability and suppress the tendency towards crystallization. However, the low waste loading (typically < 20 mass%), low corrosion resistance of crystallized glasses, and limited experience in melting LIP glasses resulted in this glass type not being used or considered as a viable waste form matrix for immobilization of HLW. [131]

Jantzen [132,133] found that there was a limited solubility for alumina, silica, and uranium in the LIP glasses. Also, there is limited solubility for zirconia, which forms a zirconium-rich crystalline phase in the glass. With respect to defense HLW waste streams, the LIP glasses were not compatible with the silica rich zeolite found in the waste (the zeolite did not dissolve in the melt and remained in the crucible after pouring). There were also issues with the melting-temperature range, flexibility of the LIP glasses to handle all of the components found in the waste, the durability of the glasses processed at lower temperatures or in a reducing atmosphere, and the inhomogeneity of the waste form. It was also determined that the LIP glasses would be incompatible with the Joule-heated melter because the interactions with the Inconel 690 electrodes and with the refractories would cause inhomogeneous melts.

Concurrent research at PNNL showed that the glass crystallized when poured into canisters and that the Cs leach rate from the crystallized material was orders of magnitude greater than those from borosilicate glass. [134] This would have required special rapid cooling for the LIP glasses to prevent significant devitrification in the tall narrow stainless steel canisters proposed for HLW disposal. (Table III)

Testing performed in Germany on the corrosion (e.g., durability or resistance to aqueous attack) testing of the LIP glasses indicated that these glasses performed well in solutions of distilled water and groundwaters with pH levels between 5 and 9 and temperatures less than 150°C. Corrosion rates were significantly higher in saturated sodium-chloride solutions (representing a salt repository brine) when compared to the same glass in distilled water. [135] Another fundamental issue with the LIP glasses is the fact that lead is a hazardous oxide constituent and as such, the waste form must meet the TCLP, or it would be unacceptable for repository storage. [136]

### 5.2.3 Iron phosphates

Within the last 15 years, numerous studies [137, 138, 139, 140, 141, 142, 143, 144,145] have focused on the use of iron phosphate (FeP) glasses as a viable waste form host for HLW. In contrast to the lead-iron phosphate glasses, FeP glasses have been produced (at laboratory scale) that contain in excess of 40 mass% of certain HLW components. [139]. The atomic structure, specific structure-property relationships, REDOX equilibria, and crystallization characteristics of

binary FeP glasses and those containing a single common waste component, such as Na<sub>2</sub>O, UO<sub>2</sub>, Cs<sub>2</sub>O, SrO, or Bi<sub>2</sub>O<sub>3</sub>, have been reported [146, 147, 148]. Iron phosphate waste forms containing about nine different simulated nuclear wastes of complex composition have also been investigated [140]. Five of these simulated wastes are based on wastes at Hanford; that are high in P<sub>2</sub>O<sub>5</sub>, Bi<sub>2</sub>O<sub>3</sub>, UO<sub>2</sub>, etc. and/or compositions that were considered poorly suited for vitrification in borosilicate glass. Other simulated wastes vitrified to date in FeP glasses include aluminum-clad spent nuclear fuel (SNF), gunite waste from the Oak Ridge Reservation (ORR), a zirconia-rich calcine waste from the Idaho National Engineering and Environmental Laboratory (INEEL), and simulated plutonium wastes. Thus, an extensive body of data exists for FeP waste forms at this time. This section briefly describes some of the major differences of FeP glasses relative to other phosphate-based glass systems, as well as those properties that make them attractive candidates for vitrifying nuclear waste (at least some waste compositions). Some of the characteristics of FeP glasses that are important to waste vitrification are

- their outstanding chemical durability [139, 140, 149, 150, 151]
- their tendency to buffer the pH of solutions in which they may come into contact, thereby preventing the accelerated chemical corrosion that usually occurs when an alkali-containing glass is in contact with a solution whose pH typically increases with time
- their inherently high solubility [144, 151, 152] for many heavy metals (uranium, chromium, zirconium, cesium, molybdenum, etc.); noble metals; and rare earths commonly present in nuclear waste
- their low melting temperatures (950°C to 1100°C), rapid melting rates (few hours), capability of tolerating a wide range in furnace atmospheres (oxidizing to reducing), and high melt fluidity (viscosity typically below one poise), which means that small furnaces can have reasonable throughput
- their unexpectedly low corrosion of oxide refractories [141] commonly used in glass melting furnaces, such as high alumina, zircon, and mullite
- their unexpectedly low corrosion of Inconel alloys [153] commonly used in glass melting furnaces
- their high waste loading, typically between 25 to 50 mass%, depending on the waste, and higher density, typically 3.0 to 3.4 g/cm<sup>3</sup> compared to borosilicate glasses of 2.75-2.80 g/cm<sup>3</sup> at 28-40 wt% waste loading which combines to slightly minimize the volume of vitrified waste
- the influence of PO<sub>4</sub> on solubility of actinides in repository-like environments.

## 6.0 Future Trends

### 6.1 Joule Heated Melters (JHM's) vs. Advanced Joule Heated Melters (AJHM)

Joule heated melters have production rates that are approximately proportional to the surface area of the melt, but convection caused by the Joule heating is enhanced as the size of the melter is increased.[49] So larger melters have proportionately higher melt rates. The melt temperature is limited by the materials of construction of the electrodes, generally Inconel™ 690. However, melt rate can be improved by (1) the addition of lid

heaters (Figure 15) to increase the temperature of the melter plenum and enhance melting of the cold cap, (2) adjusting the proportions of frit and cold chemical additions, (3) increased use of reducing agents (formic acid/sugar) to control oxygen foaming (see Section 4.1.5), (4) use of surface-active species such as sulfates and halides, (5) increased melter convection by melting lower viscosity glasses, power skewing the bottom electrodes, or mechanical agitation (stirrer/bubblers/airlift pumps), and (6) dry feeding instead of slurry feeding [49]. In addition higher melt temperatures improve melt rate.

Round or oval melters avoid having cold corners and enhance natural convection while square or oblong melters need agitation with bubblers or stirrers to enhance convection in the corners (Figure 15). For example, the DWPF is outfitted with an airlift bubbler [154] which increases the glass circulation while transferring additional energy from within the melt pool to the pool surface (cold cap) to better utilize electrode power.

The Hanford HLW melter will be outfitted with eight twin orifice melt bubblers that bubble air and thus improve melt rate and convection.[155] The use of multiple bubblers with fairly frequent bubbler replacements is considered an advanced JHM design. While it has been well tested at the pilot scale such a AJHM has yet to be demonstrated with actual radioactive waste.

It should be noted that the Hanford HLW melter shown in Figure 14 is the largest JHM/AJHM in terms of melt pool surface area, 3.75 m<sup>2</sup>. The DWPF melter is 1.5X smaller (2.6 m<sup>2</sup>) and currently the largest HLW melter in operation. The DWPF but could be lifted by a crane (Figure 7) for replacement as could the West Valley Demonstration Project melter which had a melt pool surface area of 2.2 m<sup>2</sup>. Therefore, replacement melters for Hanford must enter and be disposed of via a rail system which is visible in Figure 15.

JHM's can be designed with sloped bottoms and bottom drains with or without mixing to facilitate periodic draining of noble metals that may precipitate as done with the Tokai JHM. JHM's can be operated at ~1200°C before different materials of construction are necessitated. However, increased melt pool volatility, refractory corrosion, and electrode corrosion are to be expected at higher operating temperatures. The increasing production capability is offset by increasing complexity of the melter system (Figure 16).

Joule heated melters are intolerant of crystal growth in the melt which causes slag formation. [156] Recently, Sellafield has shown the ability to go to 38 wt% waste loading [157] from 25 wt% waste loading [158] by allowing spinel formation in the melt but the Sellafield melter is induction heated not a JHM design. However, 1-2% crystallization of spinels is planned for Hanford's HLW AJHM and it is anticipated that the spinel crystals will stay buoyant from the melt pool agitation afforded by the bubblers.[159, 160] This strategy will likely work unless during long maintenance outages, the crystals grow larger than the size that the agitation can sustain or the melt pool will have to be diluted with components that dilute the spinel forming tendencies

because JHM’s and AJHM’s cannot be drained without causing damage to the electrodes.

## 6.2 Advanced Melter Designs and GCM’s

The cold crucible induction-heated melter (CCIM) is being pursued in Russia, France, and the US as an alternative to JHM and AJHM melter technology. The major advantages of CCIM over JHM/AJHM are higher productivity, higher temperatures, longer lifetime, smaller dimensions, and higher waste loadings while maintaining the same product quality. The CCIM is also capable of producing GCM’s and mineral waste forms by a melt and controlled crystallization route.[50,51]

The melter is composed of water-cooled tubes that are arranged to form a crucible that is heated by induction-heating. A slag forms along the crucible wall to form a barrier and container, and the inductor couples directly with the glass to provide melting. Presently, two different pour designs are being pursued for the CCIM technology, which are side pouring and a bottom drain. The side pouring method is similar to the overflow design used in the DWPF. The bottom drain configuration uses a plunger type arrangement. It is water-cooled and unseated when ready to pour. It can also be used to clear the drain when plugging occurs. The CCIM technology targets a low viscosity glass (i.e., ~20 poise) to ensure pourability. Limited testing has also been performed with a stirrer in the CCIM, and preliminary data indicated increased productivity by ~15 to 20%.[51] While testing has been performed with the CCIM technology, the melter has not been installed for high level waste application. This technology has the potential to increase waste throughput and capacity at minimal complexity (Figure 16). Additional discussion of this technology can be found in Chapter 8.

## 7.0 Sources of further information

Text books such as those indicated in references 22, 50, 51, and the 1989 textbook given in reference 123 were especially helpful and many of the US DOE references can be obtained at [www.osti.gov/bridge](http://www.osti.gov/bridge). Another excellent compendium about melter technology pre-2001 is available in reference 124. An excellent compendium on glass durability not cited in the references below is J.K. Bates, C.R. Bradley, E.C. Buck, J.C. Cunnane, W.L. Ebert, X. Feng, J.J. Mazer, and D.J. Wronkiewicz, “High-Level Waste Borosilicate Glass A Compendium of Corrosion Characteristics, Vol. 1,2,3, U.S. DOE Office of Waste Management Report DOE-EM-0177, (March 1994).

## 8.0 References

1. D.R. Clarke, “Preferential Dissolution of an Intergranular Amorphous Phase in a Nuclear Waste Ceramic,” J. Am. Ceram. Soc., 64, C89-90 (1981).

2. J.A. Cooper, D.R. Cousens, J.A. Hanna, R.A. Lewis, S. Myhra, R.L. Segall, R.St.C. Smart, P.S. Turner, and T.J. White, “**Intergranular Films and Pore Surfaces in Synroc C: Structure, Composition, and Dissolution characteristics**,” J. Am. Ceram. Soc, 69 [4] (1986).
3. W.J. Buykx, K. Hawkins, D.M. Levins, H. Mitamura, R.St. C. Smart, G.T. Stevens, K.G. Watson, D. Weedon, and T.J. White, “**Titanate Ceramics for the Immobilization of Sodium-Bearing High-Level Nuclear Waste**,” J. Am. Ceram. Soc. 71 [8], 768-88 (1988).
4. F.J. Dickson, H. Mitamura, and T.J. White, “**Radiophase Development in Hot-Pressed Alkoxide-Derived Titanate Ceramics for Nuclear Waste Stabilization**,” J. Am. Ceram. Soc., 72 [6] 1055-1059 (1989).
5. W.J. Buykx, D.M. Levins, Roger St.C. Smart, K.L. Smith, G.T. Stevens, K.G. Watson, D. Weedon and T.J. White, “**Interdependence of Phase Chemistry, Microstructure, and Oxygen Fugacity in Titanate Nuclear Waste Ceramics**,” J. Am. Ceram. Soc. 73 [5], 1201-1207 (1990).
6. W.J. Buykx, D.M. Levins, Roger St.C. Smart, IK.L. Smith, G.T. Stevens, K.G. Watson, and T.J. White, “**Processing Impurities as Phase Assemblage Modifiers in Titanate Nuclear Waste Ceramics**,” J. Am. Ceram. Soc. 73, 217-225 (1990).
7. H. Mitamura, S. Matsumoto, K.P. Hart, T. Miyazaki, E.R. Vance, Y. Tamura, Y. Togashi, and T.J. White, “**Aging Effects on Curium-Dopped Titanate Ceramics Containing Sodium-Bearing High-Level Nuclear Waste**,” J. Am. Ceram. Soc., 75[2], 392-400 (1992).
8. C.M. Jantzen, D.R. Clarke, P.E.D. Morgan, and A.B. Harker, “**Leaching of Polyphase Nuclear Waste Ceramics: Microstructural and Phase Characterization**,” J. Am. Ceram. Soc., 65 [6], 292-300 (1982)
9. V.Jain and S.M. Barnes, “**Radioactive Waste Solidification at the West Valley Demonstration Project (WVDP)**,” Ceramic Transactions, v. 29, 545-552 (1993).
10. IAEA, “**Design and Operation of High Level Waste Vitrification and Storage Facilities**,” IAEA Technical Reports Series No. 339(1992).
11. I.W. Donald, B.L. Metcalfe, and R.N.J. Taylor, “**The Immobilization of High Level Radioactive Wastes Using Ceramics and Glasses**,” J. Materials Science, V. 32, 5851-5887 (1997).
12. G.E. Brown, Jr., F. Farges, and G. Calas, “**X-Ray Scattering and X-Ray Spectroscopy Studies of Silicate Melts**,” Structure, Dynamics and Properties of

- 
- Silicate Melts, J.F. Stebbins, P.F. McMillan, and D.B. Dingwell (Eds.), *Reviews in Mineralogy*, V.32, 317-410 (1995).
13. A.J.G. Ellison and A. Navrotsky, "**Thermochemistry and Structure of Model Waste Glass Compositions**," *Sci. Basis for Nuclear Waste Management, XIII*, V.M. Oversby and P.W. Brown (Eds.) Materials Research Society, Pittsburgh, PA, 193-207 (1990).
  14. H. Li, Y. Su, J.D. Vienna, and P. Hrma, "**Raman Spectroscopic Study - Effects of B<sub>2</sub>O<sub>3</sub>, Na<sub>2</sub>O, and SiO<sub>2</sub> on Nepheline (NaAlSiO<sub>4</sub>) Crystallization in Simulated High Level Waste Glasses**," *Ceramic Trans.* 107, 469-477 (2000).
  15. W.B. White, "**Glass Structure and Glass Durability**," *Materials Stability and Environmental Degradation*, A. Barkatt, E.D. Vernik, and L.R. Smith (Eds.), MRS Symposium Proceedings V. 125 (1988).
  16. E.A. Porai-Koshits, **The Structure of Glass**, p.25, Consultants Bureau, NY (1958).
  17. W.H. Zachariasen, "**The Atomic Arrangement in Glass**," *J. Am. Chem. Soc.*, v.54, 3841-3851 (1932).
  18. W.H. Zachariasen, "**The Vitreous State**," *J. Chem. Phys.* v. 3, 162-163 (1933).
  19. B.E. Warren, "**X-ray Diffraction of Vitreous Silica**," *Zeit. Krist.* v. 86, 349-358 (1933).
  20. A.C. Wright, "**Neutron Scattering from Vitreous Silica, V. The structure of Vitreous Silica: What have we Learned from 60 years of Diffraction Studies?**," *J. Non-Crystalline Solids*, v. 179, 84-115 (1994).
  21. G.N. Greaves, "**EXAFS and the Structure of Glass**," *J. Non-Crystalline Solids*, 71, 203-217 (1985).
  22. D. Caurant, P. Loiseau, and O. Majerus, V. Aubin-Chevaldonnet, I. Bardez, and A. Quintas, "**Glasses, Glass-Ceramics and Ceramics for Immobilization of Highly Radioactive Nuclear Wastes**," Nova Science Publishers, Inc., New York, 359p. (2009).
  23. C.W. Burnham, "**The Nature of Multicomponent Aluminosilicate Melts**," *Phys. Chem. of the Earth*, v13 & 14, 191-227 (1981).
  24. C.M. Jantzen and K.G. Brown, "**Predicting the Spinel-Nepheline Liquidus for Application to Nuclear Waste Glass Processing: Part I. Primary Phase Analysis, Liquidus Measurement, and Quasicrystalline Approach**," *J. Am.*

---

Ceramic Soc., 90 [6], 1866-1879 (2007).

25. C.M. Jantzen and K.G. Brown, “**Predicting the Spinel-Nepheline Liquidus for Application to Nuclear Waste Glass Processing: Part II. Quasicrystalline Freezing Point Depression Model,**” J. Am. Ceramic Soc. 90 [6], 1880-1891 (2007).
26. R. Nyholm and L.O. Werme, “**An ESCA Investigation of Molybdenum Containing Silicate and Phosphate Glasses,**” Sci. Basis of Nucl. Waste Mgt., III, Plenum Press, (1981).
27. G. Calas, M. Le Grand, L. Galoisy, D. Ghale, **Structural Role of Molybdenum in Nuclear Glasses: an EXAFS Study,** Journal of Nuclear Materials 322 (2003) 15–20.
28. D. Cauranta, O. Majérusa, E. Fadela, A. Quintasa, C. Gervaisb, T. Charpentiere, “**Structural Investigations of Borosilicate Glasses Containing MoO<sub>3</sub> by MAS NMR and Raman Spectroscopies,**” J. Nucl. Materials (in press).
29. N.C. Hyatt, R.J. Short, R.J. Hand, W.E. Lee, F. Livens, J.M. Charnock, and R.L. Bilsborrow, “**The Structural Chemistry of Molybdenum in Model High Level Nuclear Waste Glasses, Inventigated by Mo K-Edge X-Ray Absorption Spectroscopy,**” Ceramic Transactions, V. 168, American Ceramic Society, 179-187 (2004).
30. C.M. Jantzen and D.F. Bickford, “**Leaching of Devitrified Glass Containing Simulated SRP Nuclear Waste,**” Sci. Basis for Nuclear Waste Management, VIII, C.M. Jantzen, J.A. Stone and R.C. Ewing (eds.), Materials Research Society, Pittsburgh, PA 135-146 (1985).
31. M.J.D. Rushton, R.W. Grimes, and S.L. Owens, “**Changes to Alkali Ion Content Adjacent to Crystal-Glass Interfaces,**” Sci. Basis for Nucl. Waste Mgt., XXXI, W.E. Lee, J.W. Roberts, N.C. Hyatt, and R.W. Grimes (Eds.), Materials Research Society, Pittsburgh, PA, 207-213 (2008).
32. M.I. Ojovan and W.E. Lee, “**Topologically Disordered Systems at the Glass Transition,**” J. Phys.: Condens. Matter, 18, 11507-11520 (2006).
33. D.K. Peeler, “**Batch 1 Variability Study Using Twice Washed Tank 51 Sludge,**” WSRC-RP-1045, Rev. 1 (January 1995).
34. D.K. Peeler, “**Batch 1 Variability Study Using Twice Washed Tank 51 Sludge and Frit 200,**” WSRC-RP-96-20, Rev. 0 (1996).

- 
35. J.R. Harbour, T.B. Edwards, and R.J. Workman, "**Summary of Results for Macrobatch 3 Variability Study**", WSRC-TR-2000-00351, Rev.0 (2000).
  36. C.C. Herman, T.B. Edwards, and D.M. Marsh, "**Summary of Results for Expanded Macrobatch 3 Variability Study**", WSRC-TR-2001-00511, Rev. 0 (2001).
  37. M.T. Keefer, B.A. Hamm, and J.A. Pike, "**Low Temperature Aluminum Dissolution of Sludge Waste**," WM2008 Conference Paper #8175 (2008).
  38. J.A. Stone, J.A. Kelley, T.S. McMillan, "**Sampling and Analyses of SRP High-Level Waste Sludges**," U.S. DOE Report DP-1399, E.I. DuPont DeNemours & Co., Savannah River Laboratory, Aiken, SC (August 1976).
  39. J.A. Stone, "**Separation of SRP Waste Sludge and Supernate**," U.S. DOE Report DP-1441, E.I. DuPont DeNemours & Co., Savannah River Laboratory, Aiken, SC (November 1976).
  40. C.C. Chapman, "**Design Preferences For a Slurry –Fed Ceramic Melter Suitable for Vitrifying West Valley Wastes**," Adv. In Ceramics V. 8 149-160 (1984).
  41. B.M. Rapko and G.J. Lumetta, "**Status Report on Phase Identification in Hanford Tank Sludges**," PNNL-13394, December (2000)
  42. T. Motyka, "**Technical Data Summary for In-Tank Sludge Processing**," U.S. DOE Report DPSTD-84-100, E.I. DuPont DeNemours & Co., Savannah River Laboratory, Aiken, SC (April 1984).
  43. E.R. Merz, "**Overview on The Application of Dentrination in the Nuclear Field**," p. 1-10 in Denitration of Radioactive Liquid Waste, L. Cecille and S. Halaszovich (Eds.) Graham & Trotman, Ltd. For the Commission of the European Communities, 180pp (1986).
  44. C.M. Jantzen, J.R. Zamecnik, D.C. Koopman, C.C. Herman, and J.B. Pickett, "**Electron Equivalents Model for Controlling REDuction/OXidation (REDOX) Equilibrium During High Level Waste (HLW) Vitrification**," U.S. DOE Report WSRC-TR-2003-00126, Rev.0 (May 9, 2003).
  45. C.M. Jantzen, D.C. Koopman, C.C. Herman, J.B. Pickett, and J.R. Zamecnik, "**Electron Equivalents REDOX Model for High Level Waste Vitrification**," Environmental Issues and Waste Management Technologies IX, J.D. Vienna and D.R. Spearing (Eds), Ceramic Transactions 155, 79-91 (2004).

- 
46. C.M. Jantzen and M.E. Stone, “**Role of Manganese Reduction/Oxidation (REDOX) on Foaming and Melt Rate in High Level Waste (HLW) Melters,**” US DOE Report WSRC-STI-2006-00066 (2007).
  47. D.J. Bradley, “**Behind the Nuclear Curtain: Radioactive Waste Management in the Former Soviet Union,**” Battelle Press, Columbus, OH, 716pp. (1997)
  48. J.M. Perez, S.M. Barnes, S. Kelly, L. Petkus, and E.V. Morrey, “**Vitrification Testing and Demonstration for the Hanford Waste Treatment and Immobilization Plant,**” Ceramic Transactions 168, 3-21 (2005).
  49. D.F. Bickford, P.Hrma, and B.W. Bowan II, “**Control of Radioactive Waste Glass Melters: II. Residence Time and Melt Rate Limitations,**” J. Amer. Ceram. Soc., 73[10], 2903-15 (1990).
  50. M.I. Ojovan and W.E. Lee, “**An Introduction to Nuclear Waste Immobilization,**” Nova Science Publishers, Oxford, 315pp. (2007).
  51. M.I. Ojovan and W.E. Lee, “**New Developments in Glassy Nuclear Wasteforms,**” Elsevier Publishers, Oxford, 315pp. (2005).
  52. V. Jain, “**Survey of Solidification Process Technologies,**” Report CNWRA 98-005, Center for Nuclear Waste Regulatory Analyses, San Antonio, Texas (April 1998).
  53. W. G. Ramsey, “**Durability Study of Simulated Radioactive Waste Glass in Brine Environment,**” Unpublished M.S. Thesis, Clemson University, Clemson, South Carolina, 101pp. (1989).
  54. G.G. Wicks, W.D. Rankin, and S.L. Gore, “**International Waste Glass Study – Composition and Leachability Correlations,**” Scientific Basis for Nuclear Waste Management VIII, C.M. Jantzen, J.A. Stone, and R.C. Ewing (Eds.), Materials Research Society, Pittsburgh, PA, 171-177 (1985).
  55. C.M. Jantzen, “**Systems Approach to Nuclear Waste Glass Development,**” J. Non-Cryst Solids ,84 [1-3], 215-225 (1986).
  56. C.M. Jantzen, “**Relationship of Glass Composition to Glass Viscosity, Resistivity, Liquidus Temperature, and Durability: First Principles Process-Product Models for Vitrification of Nuclear Waste,**” Ceramic Transactions V. 23, American Ceramic Society, Westerville, OH, 37-51 (1991).
  57. C.M. Jantzen, and K.G. Brown, “**Statistical Process Control of Glass Manufactured for the Disposal of Nuclear and Other Wastes,**” Am. Ceramic Society Bulletin, 72, 55-59 (May, 1993).

- 
58. T.M. El-Shamy, “**The Chemical Durability of K<sub>2</sub>O-CaO-MgO-SiO<sub>2</sub> Glasses,**” *Phys. Chem. Glasses*, 14[1], 1-5 (1973).
  59. K.G. Brown and R.L. Postles “**The DWPF Product Composition Control System at Savannah River: Statistical Process Control Algorithm,**” *Ceram. Trans.*, V. 23, 559-568 (1991).
  60. C.M. Jantzen, and J.C. Marra, ‘**High Level Waste (HLW) Vitrification Experience in the US: Application of Glass Product/Process Control to Other HLW and Hazardous Wastes**” *Materials Research Society Symposium Scientific Basis for Nuclear Waste Management XXXI, MRS Symposium Volume 1107*, 183-190 (2008)
  61. Department of Energy, “**Civilian Radioactive Waste Management System Waste Acceptance System Requirements Document, Revision 5,**” U.S. DOE Report DOE/RW-0351 REV. 5 (March 2008).
  62. C.M. Jantzen, N.E. Bibler, D.C. Beam, and M.A. Pickett, “**Characterization of the Defense Waste Processing Facility (DWPF) Environmental Assessment (EA) Glass Standard Reference Material,**” U.S. DOE Report WSRC-TR-92-346, Rev. 1, Westinghouse Savannah River Company, Aiken, SC (1993).
  63. C.M. Jantzen, N.E. Bibler, D.C. Beam, and M.A. Pickett , “**Development and Characterization of the Defense Waste Processing Facility (DWPF) Environmental Assessment (EA) Glass Standard Reference Material,**” *Environmental and Waste Management Issues in the Ceramic Industry*, *Ceramic Transactions*, 39, American Ceramic Society, Westerville, OH (1994) 313-322.
  64. ASTM C1285. “**Standard Test Methods for Determining Chemical Durability of Nuclear, Hazardous, and Mixed Waste Glasses and Multiphase Glass Ceramics: The Product Consistency Test (PCT),**” *Annual Book of ASTM Standards*, Vol. 12.01, (2008).
  65. W.B. White, “**Theory of Corrosion of Glass and Ceramics,**” *Corrosion of Glass, Ceramics, and Ceramic Superconductors*, D.E. Clark and B.K. Zaitos, Noyes Publications, Park Ridge, NJ, 2-28 (1992).
  66. W. Sinkler, T.P. O’Holleran, S.M. Frank, M.K. Richmann, S.G. Johnson, “**Characterization of A Glass-Bonded Ceramic Waste Form Loaded with U and Pu,**” *Scientific Basis for Nuclear Waste Management, XXIII*, R.W. Smith and D.W. Shoesmith (Eds.), *Materials Research Society, Pittsburgh, PA*, 423-429 (2000).

- 
67. T. Moschetti, W. Sinkler, T. Disanto, M.H. Hois, A.R. Warren, D. Cummings, S.G. Johnson, K.M. Goff, K.J. Bateman, S.M. Frank, “**Characterization of a Ceramic Waste Form Encapsulating Radioactive Electrorefiner Salt,**” *Scientific Basis for Nuclear Waste Management*, XXIII, R.W. Smith and D.W. Shoosmith (Eds.), Materials Research Society, Pittsburgh, PA, 577-582 (2000).
  68. N.E. Bibler and J.K. Bates, “**Product Consistency Leach Tests of Savannah River Site Radioactive Waste Glasses,**” *Scientific Basis for Nuclear Waste Management*, XIII, Oversby, V. M. and Brown, P. W., eds., Materials Research Society, Pittsburgh, PA, 1990, pp. 327–338.
  69. J.K. Bates, D.J. Lam, M.J. Steindler, “**Extended Leach Studies of Actinide-Doped SRL 131 Glass,**” *Scientific Basis for Nuclear Waste Management*, VI, D.G. Brookins (Ed.), North-Holland, New York, 183-190 (1983).
  70. N.E. Bibler and A.R. Jurgensen, “**Leaching Tc-99 from SRP Glass in Simulated Tuff and Salt Groundwaters,**” *Scientific Basis for Nuclear Waste Management*, XI, M.J. Apted and R.E. Westerman (Eds.), Materials Research Society, Pittsburgh, PA, 585-593 (1988).
  71. D.J. Bradley, C.O. Harvey, and R.P. Turcotte, “**Leaching of Actinides and Technetium from Simulated High-Level Waste Glass,**” Pacific Northwest Laboratory Report, PNL-3152, Richland, WA (1979).
  72. S. Fillet, J. Nogues, E. Vernaz, and N. Jacquet-Francillon, “**Leaching of Actinides from the French LWR Reference Glass,**” *Scientific Basis for Nuclear Waste Management*, IX, L.O. Werme, Materials Research Society, Pittsburgh, PA, 211-218 (1985).
  73. F. Bazan, J. Rego, and R.D. Aines, “**Leaching of Actinide-doped Nuclear Waste Glass in a Tuff-Dominated System,**” *Scientific Basis for Nuclear Waste Management*, X, J.K. Bates and W.B. Seefeldt (Eds.), Materials Research Society, Pittsburgh, PA, 447-458 (1987).
  74. E.Y. Vernaz and N. Godon, “**Leaching of Actinides from Nuclear Waste Glass: French Experience,**” *Scientific Basis for Nuclear Waste Management*, XV, C.G. Sombret (Ed.), Materials Research Society, Pittsburgh, PA, 37-48 (1992).
  75. W.L. Ebert, S.F. Wolf, and J.K. Bates, “**The Release of Technetium from Defense Waste Processing Facility Glasses,**” *Scientific Basis for Nuclear Waste Management*, XIX, W.M. Murphy and D.A. Knecht (Ed.), Materials Research Society, Pittsburgh, PA, 221-227 (1996).

- 
76. B.P. McGrail, “**Waste Package Component Interactions with Savannah River Defense Waste Glass in a Low-Magnesium Salt Brine,**” Nuclear Technology, 168-186 (1986).
  77. B.C. Bunker, G.W. Arnold, D.E. Day and P.J. Bray, “**The Effect of Molecular Structure on Borosilicate Glass Leaching,**” *J. Non-Cryst. Solids*, **87**, 226-253 (1986).
  78. C.M. Jantzen, K.G. Brown, T.B. Edwards, and J.B. Pickett, “**Method of Determining Glass Durability (THERMO™),**” U.S. Patent #5,846,278, (December 1998).
  79. C.M. Jantzen, J.B. Pickett, K.G. Brown, T.B. Edwards, and D.C. Beam, “**Process/Product Models for the Defense Waste Processing Facility (DWPF): Part I. Predicting Glass Durability from Composition Using a Thermodynamic Hydration Energy Reaction Model (THERMO),**” U.S. DOE Report WSRC-TR-93-0672, Westinghouse Savannah River Co., Savannah River Technology Center, Aiken, SC, 464p. (Sept. 1995).
  80. R. Conradt, “**A Proposition for an Improved Theoretical Treatment of the Corrosion of Multi-component Glasses,**” *Jour. Nucl. Materials.*, 298, 19-26 (2001).
  81. R. Conradt, “**Chemical Structure, Medium Range Order, and Crystalline Reference State of Multicomponent Oxide Liquids and Glasses,**” *J. Non-Cryst. Solids*, 345&346, 16-23 (2004).
  82. R. Conradt, “**Chemical Durability of Oxide Glasses in Aqueous Solutions: A Review,**” *J. Am. Ceram. Soc.*, 91[3], 728-735 (2008).
  83. C.M. Jantzen, and J.M. Pareizs, “**Glass Durability Modeling: The Role of Activated Complexes and Quasicrystalline Structural Ratios,**” (accepted *J. Nucl. Mat.*).
  84. H.C. Helgeson, W.M. Murphy, and P. Aagaard, “**Thermodynamic and Kinetic Constraints on Reaction Rates Among Minerals and Aqueous Solutions, II. Rate Constants, Effective Surface Area, and the Hydrolysis of Feldspar,**” *Geochimica et Cosmochimica Acta*, 48, 2405-2432 (1984).
  85. E.H. Oelkers and S.R. Sislason, “**The Mechanism, Rates, and Consequences of Basaltic Glass Dissolution: I. An Experimental Study of the Dissolution Rates of basaltic Glass as a Function of Aqueous Al, Si, and Oxalic Acid Concentration at 25°C and pH = 3 and 11,**” *Geochim. Cosmochim. Acta*, 65 [21], 3671-3681 (2001).

- 
86. P. Van Iseghem and B. Grambow, “**The Long-Term Corrosion and Modeling of Two Simulated Belgian Reference High-Level Waste Glasses,**”*Sci. Basis for Nuclear Waste Mgt. XI, Mat. Res. Soc.*, Pittsburgh, PA, 631-639 (1987).
  87. C.M. Jantzen, D.I. Kaplan, N.E. Bibler, D.K. Peeler, and M.J. Plodinec, “**Performance of a Radioactive High Level Waste Glass After 24 Years Burial,**” *J. Nucl. Materials*, 378, 244-256 (2008).
  88. C.M. Jantzen, K.G. Brown, and J.B. Pickett “**Durable Glass for Thousands of Years,**” *International Journal of Applied Glass Science*, 1 [1], 38-62 (March 2010).
  89. I. Tovená, T. Advocat, D. Ghaleb, E. Vernaz, and F. Larche, “**Thermodynamic and Structural Models Compared with the Initial Dissolution Rate of SON Glass Samples,**” *Sci. Basis for Nucl. Waste Mgt., XVII*, A. Barkatt and R.A. VanKonynenburg (Eds.), Materials Research Society, Pittsburgh, PA, 595-602 (1994).
  90. C.M. Jantzen and K.G. Brown, “**Impact of Phase Separation on Waste Glass Durability,**” *Environmental Issues and Waste Management Technologies in the Ceramic and Nuclear Industries*, V, G. T. Chandler (Eds.), Ceramic Transactions, V. 107, 289-300 (2000).
  91. C.M. Jantzen, “**Method for Controlling Glass Viscosity**” U.S. Patent #5,102,439, (April, 1992).
  92. C.M. Jantzen, “**The Impacts of Uranium and Thorium on the Defense Waste Processing Facility (DWPF) Viscosity Model,**” U.S. DOE Report WSRC-TR-2004-00311 (February 2005).
  93. G.S. Fulcher, “**Analysis of Recent Measurements of the Viscosity of Glasses,**” *J. Am. Ceram. Soc.* 8, 339-355 (1925).
  94. G.S. Fulcher, “**Analysis of Recent Measurements of the Viscosity of Glasses, II,**” *J. Am. Ceram. Soc.*, 8 [12]789-794 (1925).
  95. G.W. Scherer, “**Editorial Comments on a Paper by Gordon S. Fulcher,**” *J. Am. Ceram. Soc.*, 75 [5], 1060-1062 (1992).
  96. W.B. White and D.G. Minser, “**Raman Spectra and Structure of Natural Glasses,**” *J. Non-Cryst. Solids*, 67, 45-59 (1984).

- 
97. E.T. Turkdogan, “**Physicochemical Properties of Molten Slags and Glasses,**” The Metals Society, London (1983).
  98. B.O. Mysen, D. Virgo, C.M. Scarfe, and D.J. Cronin, “**Viscosity and Structure of Iron- and Aluminum-Bearing Calcium Silicate Melts at 1 Atm.,**” Am. Mineralogist, 70, 487-498 (1985).
  99. B.M.J. Smets and D.M. Krol, “**Group III Ions in Sodium Silicate Glass. Part 1. X-ray Photoelectron Spectroscopy Study,**” Phys. Chem. Glasses, 25 [5], 113-118 (1984).
  100. W.L. Konijnendijk, “**Structural Differences Between Borosilicate and Aluminosilicate Glasses Studied by Raman Scattering,**” Glastechn. Ber. 48 [10], 216-218 (1975).
  101. T. Furukawa and W.B. White, “**Raman Spectroscopic Investigation of Sodium Borosilicate Glass Structure,**” J. Mat. Sci., 16, 2689-2700 (1981).
  102. J. Hlavac, “**The Technology of Glass and Ceramics: An Introduction,**” Elsevier Scientific Publishing Company, Amsterdam (1983).
  103. C.M. Jantzen, J.R. Zamecnik, D.C. Koopman, C.C. Herman, and J.B. Pickett, “**Electron Equivalents Model for Controlling REDuction/OXidation (REDOX) Equilibrium During High Level Waste (HLW) Vitrification,**” U.S. DOE Report WSRC-TR-2003-00126, Rev.0 (May 2003).
  104. C.M. Jantzen, D.C. Koopman, C.C. Herman, J.B. Pickett, and J.R. Zamecnik, “**Electron Equivalents REDOX Model for High Level Waste Vitrification,**” Environmental Issues and Waste Management Technologies IX, J.D. Vienna and D.R. Spearing (Eds), Ceramic Transactions 155, 79-91 (2004).
  105. C.M. Jantzen, and M.E. Stone, “**Role of Manganese Reduction/Oxidation (REDOX) on Foaming and Melt Rate in High Level Waste (HLW) Melters,**” US DOE Report WSRC-STI-2006-00066 (2007).
  106. K.G. Brown, C.M. Jantzen, and G. Ritzhaupt, “**Relating Liquidus Temperature to Composition for Defense Waste Processing Facility (DWPF) Process Control,**” U.S. DOE Report WSRC-TR-2001-00520, Rev. 0, Westinghouse Savannah River Company, Aiken, SC (October 2001).
  107. C.M. Jantzen, and M.E. Smith, “**Revision of the Defense Waste Processing Facility (DWPF) Sulfate Solubility Limit,**” U.S. DOE Report WSRC-TR-2003-00518 (January 2004).

- 
108. C.M. Jantzen, D.K. Peeler, and M.E. Smith, M.E. “**Dependency of Sulfate Solubility on Melt Composition and Melt Polymerization,**” *Ceram. Trans.* 168, 141-151 (2005).
  109. I. Bardez, D. Caurant, J. L. Dussossoy, P. Loiseau, C. Gervais, F. Ribot, D. R. Neuville, N. Baffier, and C. Fillet, “**Development and Characterization of Rare Earth–Rich Glassy Matrices Envisaged for the Immobilization of Concentrated Nuclear Waste Solutions,**” *Nuclear Science and Engineering*, 153, 272–284 (2006).
  110. T.F. Meaker, and N. E. Bibler, “**Characterization and Product Consistency Leach Tests on Lanthanide Borosilicate Glasses Containing Plutonium and Uranium or Impurities,**” contained in Plutonium Immobilization: The Glass Option – A Compendium of Reports and Presentations, WSRC-RP-97-00902, Westinghouse Savannah River Company, Aiken, SC (1997).
  111. T.F. Meaker, and D. K. Peeler, “**Solubility of Independent Plutonium Bearing Feed Streams in a Hf-Based LaBS Frit,**” contained in Plutonium Immobilization: The Glass Option – A Compendium of Reports and Presentations, WSRC-RP-97-00902, Westinghouse Savannah River Company, Aiken, SC (1997).
  112. T.F. Meaker, T. F. and N. E. Bibler, “**Comparison of the Durabilities and Microstructures of an Amorphous and Devitrified Plutonium Bearing Lanthanide Borosilicate Glass,**” contained in Plutonium Immobilization: The Glass Option – A Compendium of Reports and Presentations, WSRC-RP-97-00902, Westinghouse Savannah River Company, Aiken, SC (1997).
  113. T.F. Meaker and N. E. Bibler, “**Characterization and Product Consistency Leach Tests of Lanthanide Borosilicate Glasses Containing Plutonium and Uranium or Impurities,**” contained in Plutonium Immobilization: The Glass Option – A Compendium of Reports and Presentations, WSRC-RP-97-00902, Westinghouse Savannah River Company, Aiken, SC (1997).
  114. J. Von Löffler, “**Chemical Decolorization,**” Glasstechnische Berichte, 10 (1932).
  115. M.B. Volf, “**Chemical Approach to Glass,**” *Glass Science and Technology*, Vol. 7, Elsevier Science Publishing Co. Inc., New York, (1984).
  116. W.G. Ramsey, N.E. Bibler, and T.F. Meaker, “**Compositions and Durabilities of Glasses for Immobilization of Plutonium and Uranium,**” *Waste Management '95*, Record 23828-23907, WM Symposia, Inc., Tucson, AZ (1995).
  117. N.E. Bibler, W. G. Ramsey, T. F. Meaker, and J. M. Pareizs, “**Durabilities and Microstructures of Radioactive Glasses for Immobilization of Excess Actinides**”

- 
- at the Savannah River Site,” Mat. Res. Soc. Symp. Proc., Vol. 412, Materials Research Society, Pittsburgh, PA (1995).
118. T.F. Meaker, W. G. Ramsey, J. M. Pareizs, and D. G. Karraker, “**Composition Development for Vitreous Plutonium Products,**” Ceramic Transactions, Vol. 72, American Ceramic Society, Westerville, OH (1996).
119. T.F. Meaker, “**Compositional Development of a Plutonium Surrogate Glass without Listed RCRA Elements (Lead and Barium),**” WSRC-TR-96-0322, Westinghouse Savannah River Company, Aiken, SC (1996).
120. T.F. Meaker, T.F., “**Homogeneous Glass Processing Region Defined for a Lanthanide Borosilicate Glass Composition for the Immobilization of Plutonium Using Thorium as a Surrogate,**” WSRC-TR-96-0323, Westinghouse Savannah River Company, Aiken, SC (1996).
121. T. Jones, J. C. Marra, D. Immel, and B. Meers, “**Glass Macrocracking Determination in Prototypic Cans Containing Lanthanide Borosilicate Glass,**” WSRC-TR-06-00015, Washington Savannah River Company, Aiken, SC (2006).
122. J.C. Marra, D.K. Peeler, and C.M. Jantzen, C.M., “**Development of an Alternate Glass Formulation for Vitrification of Excess Plutonium,**” U.S. DOE Report WSRC-TR-2006-00031 (January 2006)
123. B.C. Sales and L.A. Boatner, “**Lead-Iron Phosphate Glass,**” Chapter 3 in R.C. Ewing and W.Lutze (Eds.), Radioactive Waste Forms for the Future,” North Holland, Amsterdam, The Netherlands, 193-231 (1988).
124. J.M. Perez, Jr., D.F. Bickford, D.E. Day, D.S. Kim, S.L. Lambert, S.L. Marra, D.K. Peeler, D.M. Strachan, M.B. Triplett, J.D. Vienna, R.S. Wittman, “**High-Level Waste Melter Study Report,**” PNNL-13582 (2001).
125. International Atomic Energy Agency (IAEA). “**Design and Operation of HLW Vitrification and Storage Facilities.**” TRS N339, IAEA, Vienna, Austria (1992).
126. A.S. Aloy, B.Y. Galkin, and B.S. Kuznetsov. “**Fractioning of Liquid High-Radioactive Waste and Incorporation of Long-Lived Radionuclides into Ceramics and Vitreous Compositions,**” in Waste Management’89, Vol. 1, pp. 677-681. University of Arizona, Tucson, AZ (1989).
127. A.S. Aloy, A.V. Trofimenko, and O.A. Iskhakova. “**The Development of a Glass Matrix for the Immobilization of Simulated Strontium and Cesium Concentrate after HLW Separation,**” in International Topical Meeting on Nuclear and Hazardous Waste Management (SPECTRUM '94), Vol. 1, 791- 764. American Nuclear Society, Atlanta, Georgia (1994)

- 
128. Y.A. Revenko, L.N. Lazarev, and V.N. Romanovsky, “**Radioactive Waste Management of the Radiochemical Plant Under Construction near Krasnoyarsk,**” in International Topical Meeting on Nuclear and Hazardous Waste Management (SPECTRUM '94), Vol. 3, 2015-2018. American Nuclear Society, Atlanta, Georgia (1994).
  129. H. Scholze, “**Glass: Nature, Structure, and Properties**”. Springer-Verlag, New York (1990).
  130. A.S. Aloy, V.A. Bel'yukov, A.V. Demin, and Y.A. Revenko, “**Experiences with Vitrification of HLW and Development of New Approaches in Russia,**” In Glass as a Waste Form and Vitrification Technology: Summary of an International Workshop, pp. E.50-E.51. National Academy Press, Washington, DC (1996).
  131. G.K. Marasinghe, M. Karabulut, X. Fang, C.S. Ray, D.E. Day, “**Vitrified Iron Phosphate Nuclear Waste Forms Containing Multiple Waste Components,**” Ceramic Transactions, Vol. 107, pp.115-122. American Ceramic Society, Westerville, Ohio (2000).
  132. C.M. Jantzen, “**Investigation of Lead-Iron-Phosphate Glass for SRP Waste**” DP-1729, Savannah River Site, Aiken, South Carolina (1986).
  133. C.M. Jantzen, “**Investigation of Lead-Iron-Phosphate Glass for SRP Waste,**” Advances in Ceramics, 20, D.E. Clark, W.B. White and A.J. Machiels (Eds.), American Ceramic Society, Westerville, OH, 157-165 (1986)
  134. L.A. Chick, L.R. Bunnell, D.M. Strachan, H.E. Kissinger, and F.N. Hodges, “**Evaluation of Lead-Iron-Phosphate Glass as a High Level Waste Form,**” Advances in Ceramics, 20, D.E. Clark, W.B. White and A.J. Machiels (Eds.), American Ceramic Society, Westerville, OH, 149-156(1986)
  135. L. Kahl, “**Hydrolytic Durability of Lead-Iron-Phosphate Glasses,**” Advances in Ceramics, 20, D.E. Clark, W.B. White and A.J. Machiels (Eds.), American Ceramic Society, Westerville, OH, 141-148 (1986)
  136. Lawrence Livermore National Laboratory (LLNL). “**Fissile Material Disposition Program – Screening of Alternate Immobilization Candidates for Disposition of Surplus Fissile Materials,**” UCRL-ID-118819, L-20790-1, LLNL, Livermore, California (1996).
  137. X. Yu and D.E. Day, “**Effect of Raw Materials on the Redox State of Iron and Properties of Iron Phosphate Glasses,**” In *Proceedings of the 17th International Congress on Glass*, Vol. 2, pp. 45-51. International Academic Publishers, Beijing, The Peoples Republic of China (1995)

- 
138. A. Mogus-Milankovic, M. Fajic, A. Drasner, R. Tojiko, and D.E. Day  
**“Crystallization of Iron Phosphate Glasses,”** *Physics and Chemistry of Glasses*,  
39(2): 70-75 (1998).
139. D.E. Day, Z. Wu, C.S. Ray, and P.R. Hrma, **“Chemically Durable Iron Phosphate  
Glass Wasteforms,”** *Journal of Non-Crystalline Solids* 241(1): 1-12 (1998)
140. M. Mesko, D.E. Day, and B.C. Bunker, **“Immobilization of High-Level  
Radioactive Sludges in Iron Phosphates Glasses,”** In *Science and Technology for  
Disposal of Radioactive Tank Waste*, eds. W.W. Schulz and N.J. Lombardo, pp.  
379-390. Plenum Publishing Corp., New York (1998).
141. F. Chen and D.E. Day, **“Corrosion of Selected Refractories by Iron Phosphate  
Melts”** *Ceramic Transactions*, Vol. 93, pp. 213-220. The American Ceramic  
Society, Westerville, Ohio (1999).
142. C.R. Ray, X. Fang, M. Karabulut, G.K. Marasinghe, and D.E. Day, **“Iron Redox  
and Crystallization of Iron Phosphate Glass,”** *Ceramic Transactions*, Vol. 43,  
pp.187-194. American Ceramic Society, Westerville, Ohio (1999).
143. M. Mesko, and D.E. Day, **“Immobilization of Spent Nuclear Fuel in Iron  
Phosphate Glass,”** *Journal of Nuclear Materials*, 273(1): 27-36 (1999).
144. Y. Badyal, M. Karabulut, G.K. Marasinghe, M.L. Saboungi, D. Haeffner, S. Shastri,  
D.E. Day, and C.S. Ray, **“The Effects of Uranium Oxide High-Level Waste on  
the Structure of Iron Phosphate Glasses,”** *Scientific Basis for Nuclear Waste  
Management XXII*, Vol. 556, pp. 297-303. Materials Research Society, Pittsburgh,  
Pennsylvania (1999).
145. G.K. Marasinghe, M. Karabulut, X. Fang, C.S. Ray, and D.E. Day, **“Iron  
Phosphate Glasses: An Alternative to Borosilicate Glasses for Immobilizing  
Certain Nuclear Wastes,”** *Environmental Issues and Waste Management  
Technologies VI*; *Ceramic Transactions* v. 119, 361-368 (2001).
146. G.K. Marasinghe, M. Karabulut, C.S. Ray, D.E. Day, M.G. Shumsky, W.B. Yelon,  
C.H. Booth, P.G. Allen, and D.K. Shuh, **“Structural Features of Iron Phosphates  
Glasses,”** *J. Non-Crystalline Solids*, 222, 144-152 (1997).
147. G.K. Marasinghe, M. Karabulut, C.S. Ray, D.E. Day, C.H. Booth, P.G. Allen, and  
D.K. Shuh, **“Redox Characteristics and Structural Properties of Iron  
Phosphate Glasses: A Potential Host Matrix for Vitrifying High Level Nuclear  
Waste,”** *Ceramic Transactions*, Vol. 87, pp. 261-270. American Ceramic Society,  
Westerville, Ohio (1998)

- 
148. G.K. Marasinghe, M. Karabulut, C.S. Ray, D.E. Day, P.G. Allen, J.J. Bucher, D.K. Shuh, Y. Bagyal, M.L. Saboungi, M. Grimsditch, S. Shastri, and D. Heaffner, **“Effects of Nuclear Waste Composition on Redox Equilibria, Structural Features, and Crystallization Characteristics of Iron Phosphate Glasses,”** Ceramic Transactions, Vol. 93, pp. 195-202. American Ceramic Society, Westerville, Ohio (1999)
  149. D.E. Day, X. Yu, G.J. Long, and R.K. Brow, **“Properties and Structure of Sodium-Iron Phosphate Glasses,”** J.Non-Crystalline Solids, 215(1): 21-31 (1997)
  150. M. Mesko, D.E. Day, and B.C. Bunker, **“Immobilization of CsCl and SrF<sub>2</sub> in Iron Phosphate Glass,”** *WasteManagement*, 20(4): 271-278 (2000).
  151. G.K. Marasinghe, M. Karabulut, X. Fang, C.S. Ray, D.E. Day, **“Vitrified Iron Phosphate Nuclear Waste Forms Containing Multiple Waste Components,”** Ceramic Transactions, Vol. 107, pp.115-122. American Ceramic Society, Westerville, Ohio (2000).
  152. M. Karabulut, G.K. Marasinghe, C.S. Ray, D.E. Day, O. Ozturk, and G.D. Waddill, **“X-ray Photoelectron and Mossbauer Spectroscopic Studies of Iron Phosphate Glasses Containing U, Cs, and Bi,”** *J. Non-Crystalline Solids*, 249(2-3): 106-116 (1999).
  153. D.E. Day and C.W. Kim, **“Reaction of Inconel 690 and 693 in Iron Phosphate Melts: Alternative Glasses for Waste Vitrification,”** Final Report for Contract DE-FG02-04ER63831 Project 0010255 (2005).
  154. D.C. Witt, T.M. Jones, and D.F. Bickford, **“Airlift Mini-Bubbler Testing in the Slurry Fed Melt Rate Furnace,”** USDOE Report WSRC-TR-2002-00494, Rev. 0 24p. (2002).
  155. B.W. Bowan, R.Meigs, and E.C. Smith, **“Bubbling as a Means to Enhance Joule Heated Ceramic Melter Production Rates for Vitrifying Radioactive Wastes,”** Ceramic Transactions, 168, 21-30 (2005).
  156. C.M. Jantzen, **“Lack of Slag Formation in the Scale Glass Melter,”** US DOE Report DPST-87-373, E.I. DuPont deNemours & Co., Savannah River Laboratory, Aiken, SC (April 1987).
  157. N.R. Gribble, R. Short, E. Turner, and A.D. Riley, **“The Impact of Increased Waste Loading on Vitrified HLW Quality and Durability,”** Sci. Basis for Nuclear Waste Mgt, XXXIII, Materials Research Society, Pittsburgh, PA, 283-289 (2009).

- 
158. A. Riley, S. Walker, N.R. Gribble, “**Composition Changes and Future Challenges for the Sellafield Waste Vitrification Plant,**” Sci. Basis for Nuclear Waste Mgt, XXXIII, Materials Research Society, Pittsburgh, PA, 267-273 (2009).
  159. P. Hrma, P. Schill, and L. Nemeč, “**Settling of Spinel in a High-Level Waste Glass Melter,**” Final Report, US DOE Contract DE-AC06-76RL01830, Project Number: 65422 (2001).
  160. J.D. Vienna, T.B. Edwards, J.V. Crum, D.S. Kim, and D.K. Peeler, “**Liquidus Temperature and One Percent Crystal Content Models for Initial Hanford HLW Glasses,**” Ceramic Transactions, V. 168, 133-140 (2005).

Table I. HLW Waste Compositions in the US on a Calcine Oxide Basis (Wt%)

Oxide Species (wt%)	DWPF High Fe (Purex HAW) <sup>a</sup>	DWPF High Al Waste Sludge (HM HAW) <sup>a</sup> before Al Dissolution	DWPF High Al Waste Sludge (HM HAW) <sup>a</sup> after Al Dissolution	West Valley, NY Reprocessing Plant <sup>c</sup>	Hanford 76-68 <sup>d</sup>	INL HLW Blended <sup>e</sup>	UK Magnox Wastes (MW) <sup>d</sup>	French UOX1 Reprocessed Waste <sup>f</sup>	Belgium SM58 <sup>d</sup>	Russian Myak <sup>g</sup>	Japan Tokai <sup>h</sup>
WASTE LOADING (wt% calcine oxide)	28-38	28-38	28-38	25 <sup>b</sup>	32.5	17.7	25-31	16.5	11.1	~10	18.29
pH	BASIC	BASIC	BASIC	BASIC	BASIC	ACID	ACID	ACID	ACID	ACID	ACID
Fission product oxides <sup>t</sup>	2.71 (0.53 RuO <sub>2</sub> )	0.78 (0.04 RuO <sub>2</sub> )	1.27 (0.08RuO <sub>2</sub> )	3.16 (0.34 RuO <sub>2</sub> )	38.48 (5.60 ZrO <sub>2</sub> )	80.1 (79.1 ZrO <sub>2</sub> )	44.40 3.46 RuO <sub>2</sub> ; 6.39MoO <sub>3</sub> )	72.24 (6.00 RuO <sub>2</sub> )	54.95	37.91	65.01 (7.16 MoO <sub>3</sub> ; 12.14 Gd <sub>2</sub> O <sub>3</sub> ; 4.00 RuO <sub>2</sub> )
Actinides <sup>tt</sup>	7.24 UO <sub>2</sub> >ThO <sub>2</sub>	3.47 UO <sub>2</sub> >ThO <sub>2</sub>	6.65 UO <sub>2</sub> >ThO <sub>2</sub>	18.35 ThO <sub>2</sub> >UO <sub>2</sub>	13.95	0.33	1.60	2.25	---	---	5.41
Al <sub>2</sub> O <sub>3</sub>	5.99	62.78	30.02	2.39	---	8.9	19.60	---	---	---	---
CaO	2.46	1.42	2.73	---	---	0.45	---	---	---	---	---
Cr <sub>2</sub> O <sub>3</sub>	0.71	0.24	0.46	2.92	1.21	---	1.60	3.15	---	0.58	1.69
CuO	0.17	0.06	0.11	---	---	0.36	---	---	---	---	---
Fe <sub>2</sub> O <sub>3</sub>	50.64	10.89	20.82	50.30	29.09	0.26	10.00	18.06	10.81	6.07	9.02
HgO	0.33	4.31	8.26	---	---	---	---	---	---	---	---
K <sub>2</sub> O	0.16	0.15	0.29	0.44	---	6.29	---	---	---	22.00	---
MgO	0.56	0.27	0.51	---	---	---	21.60	---	---	2.07	---
MnO	12.70	3.05	5.83	1.34	---	---	---	---	---	---	---
Na <sub>2</sub> O	6.33	3.48	7.04	6.77	15.15	---	---	---	33.33	27.98	16.46
NiO	6.52	1.17	2.24	2.01	0.60	---	1.20	2.54	0.91	3.39	1.48
PbO	0.68	0.01	0.02	---	---	0.01	---	---	---	---	---
P <sub>2</sub> O <sub>5</sub>	0.28	0.69	0.45	11.09	1.52	2.93	---	1.76	---	---	0.93
SiO <sub>2</sub>	1.35	6.71	12.84	---	---	0.37	---	---	---	---	---
ZnO	0.28	0.06	---	---	---	---	---	---	---	---	---
F	---	0.16	0.30	---	---	---	---	---	---	---	---
Cl	0.18	---	---	0.10	---	---	---	---	---	---	---
SO <sub>4</sub>	0.72	0.31	0.15	1.02	---	---	---	---	---	---	---
SUM	100.00	100.00	100.00	100.00	100.00	100.00	100.00	100.00	100.00	100.00	100.00

t Fission product oxides (ZrO<sub>2</sub>, SrO, Y<sub>2</sub>O<sub>3</sub>, MoO<sub>3</sub>, TcO<sub>2</sub>, Ag<sub>2</sub>O, CdO, SnO<sub>2</sub>, SeO<sub>2</sub>, TeO<sub>2</sub>, Rb<sub>2</sub>O, Cs<sub>2</sub>O, BaO,Ce<sub>2</sub>O<sub>3</sub>, Pr<sub>2</sub>O<sub>3</sub>, Nd<sub>2</sub>O<sub>3</sub>, La<sub>2</sub>O<sub>3</sub>,Sm<sub>2</sub>O<sub>3</sub>, Eu<sub>2</sub>O<sub>3</sub>,Gd<sub>2</sub>O<sub>3</sub>, Pm<sub>2</sub>O<sub>3</sub>,RuO<sub>2</sub>, Rh<sub>2</sub>O<sub>3</sub>, PdO)

tt Actinide Oxides (UO<sub>2</sub>, NpO<sub>2</sub>, PuO<sub>2</sub>, AmO<sub>2</sub>, and CmO<sub>2</sub>, ThO<sub>2</sub>) with oxides of Np, Pu, Am, Cm, Bk, Cf,Es,Fm,Md, No, and Lw being considered transuranic (TRU) in the United States.

a R.E.Eibling and J. R. Fowler, “Updated Waste Composition at the Savannah River Plant,” DPST-83-313 (February 1983).

b. R.A. Palmer, H., Smith, G. Smith, M. Smith, R. Russell, and G. Patello, “Chemical and Physical Characterization of the First West Valley Demonstration Project High-Level Waste Feed Batch,” Ceramic Transactions, V.132, 345-355 (2002) and V.Jain and S.M. Barnes, “Radioactive Waste Solidification at the West Valley Demonstration Project (WVDP), Ceramic Transactions, v. 29, 545-552 (1993).

- c. C.C. Chapman, “Design Preferences For a Slurry –Fed Ceramic Melter Suitable for Vitrifying West Valley Wastes,” Adv. In Ceramics V. 8 149-160 (1984).
- d. J.A.C. Marples, “The preparation, Properties, and Disposal of Vitrified High level Waste From Nuclear Fuel Reprocessing,” Glass Technology, 29[6] (1988).
- e. The “all blend” composition given in this table assumes that the following wastes at INL are blended, e.g. sodium bearing waste (SBW), an Al-calcine, a Zr-calcine, solids, and ion-exchange resins - see D.K. Peeler, I. Reamer, J. Vienna, and J.A. Crum, “Technical Status Report: Preliminary Glass Formulation Report for INEELHAW,” U.S. DOE Report WSRC-TR-98-00132 (March 1998) for details.
- f. D. Caurant, P. Loiseau, O. Majerus, V. Aubin-Chevaldonnet, I. Bardez, and A. Quintas, “Glasses, Glass-Ceramics and Ceramics for Immobilization of high Radioactive Nuclear Waste,” Nova Science Publishers, Inc., New York, 359pp. (2009).
- g. M.I. Ojovan and W.E. Lee, “New Developments in Glassy Nuclear Wasteforms,” Nova Science Publishers, Inc., New York (2007).
- h. personal communication, IHI (2001).

**Table II. Variations in Frit Additives on an Oxide Basis (Wt%)**

Oxide Species (wt%)	DWPF High Fe (Purex HAW) <sup>a</sup>	DWPF High Al Waste Sludge (HM HAW) <sup>a</sup> before Al Dissolution	DWPF High Al Waste Sludge (HM HAW) <sup>a</sup> after Al Dissolution	West Valley, NY Reprocessing Plant <sup>c</sup>	Hanford 76-68 <sup>d</sup>	INL HLW Blended <sup>e</sup>	UK Magnox Wastes (MW) <sup>d</sup>	French UOX1 Reprocessed Waste <sup>f</sup>	Belgium SM58 <sup>d</sup>	Russian Myak <sup>g</sup>	Japan Tokai <sup>h</sup>
WASTE LOADING (wt% calcine oxide)	28-38	28-38	28-38	25 <sup>b</sup>	32.5	17.7	25-31	16.5	11.1	~10	18.29
Al <sub>2</sub> O <sub>3</sub>	---	---	---	---	---	2.99	---	5.89	1.35	21.11	6.13
B <sub>2</sub> O <sub>3</sub>	10.00	10.00	10.00	15.4	14.18	6.08	21.93	16.67	13.82	---	17.38
CaO	---	---	---	---	2.99	---	---	4.80	4.27	---	3.66
K <sub>2</sub> O	---	---	---	5.33	---	---	---	---	---	---	---
Li <sub>2</sub> O	7.00	7.00	7.00	2.36	---	6.11	5.35	2.35	4.16	---	3.66
MgO	1.00	1.00	1.00	1.78	---	---	---	---	2.25	---	---
Na <sub>2</sub> O	13.00	13.00	13.00	14.29	11.19	22.81	11.09	12.05	5.17	21.11	8.54
P <sub>2</sub> O <sub>5</sub>	---	---	---	---	---	---	---	---	---	57.78	---
SiO <sub>2</sub>	68.00	68.00	68.00	59.35	59.7	62.01	61.63	54.04	63.93	---	56.97
TiO <sub>2</sub>	---	---	---	1.49	4.48	---	---	---	5.06	---	---
ZnO	---	---	---	---	7.46	---	---	2.98	---	---	3.66
ZrO <sub>2</sub>	1.00	1.00	1.00	---	---	---	---	1.21	---	---	---
SUM ALKALI	20.00	20.00	20.00	21.98	11.19	28.92	16.44	14.4	9.33	78.89	12.2
SUM	100.00	100.00	100.00	100.00	100.00	100.00	100.00	100.00	100.00	100.00	100.00

- a C.M. Jantzen, “Glass Compositions and Frit Formulations Developed for DWPF” DPST-88-952 (November 1988).  
b L.R. Eisenstatt, “Description of the West Valley Demonstration Project Reference High –Level Waste Form and Canister,” U.S. DOE Report WVDP-056, Rev.0 (1986).  
c C.C. Chapman, “Design Preferences For a Slurry –Fed Ceramic Melter Suitable for Vitriifying West Valley Wastes,” Adv. In Ceramics V. 8 149-160 (1984).  
d J.A.C. Marples, “The preparation, Properties, and Disposal of Vitriified High level Waste From Nuclear Fuel Reprocessing,” Glass Technology, 29[6] (1988).  
e D.K. Peeler, I. Reamer, J. Vienna, and J.A. Crum, “Technical Status Report: Preliminary Glass Formulation Report for INEELHAW,” U.S. DOE Report WSRC-TR-98-00132 (March 1998).  
f D. Caurant, P. Loiseau, O. Majerus, V. Aubin-Chevaldonnet, I. Bardez, and A. Quintas, “Glasses, Glass-Ceramics and Ceramics for Immobilization of high Radioactive Nuclear Waste,” Nova Science Publishers, Inc., New York, 359pp. (2009).  
g M.I. Ojovan and W.E. Lee, “New Developments in Glassy Nuclear Wasteforms,” Nova Science Publishers, Inc., New York (2007).  
h personal communication, IHI (2001)

**Table III. Data on HLW Glass Production**

Vitrification Plant	Location	Melting Process	Waste Glass Produced (metric tons)	Waste Loading Range (wt%)	Size of Canisters (meters)	Number of Canisters	TBq <sup>‡</sup>
Defense Waste Processing Facility (DWPF), Savannah River Site	Aiken, South Carolina, USA	JHCM	5,000*	28-40 <sup>c</sup>	0.6 x 3	2,845	7.7 x 10 <sup>5</sup>
West Valley Demonstration Project (WVDP)	West Valley, New York, USA	JHCM	~500**	~20.4-23.5 <sup>b</sup>	0.6 x 3	275	8.9 x 10 <sup>5</sup>
Waste Vitrification Plant (WVP), BNFL	Sellafield, UK	Induction, hot crucible	~1,800 <sup>†</sup>	~25 <sup>a</sup>	0.43 x 1.34	4319 <sup>††</sup>	1.9 x 10 <sup>7</sup>
Areva NC (R7/T7) <sup>d</sup>	La Hague, France	Induction, hot crucible	5,573 <sup>f</sup>	12-18 <sup>§§</sup>	0.43 x 1	14,045	2.38 x 10 <sup>8</sup>
AVM or Atelier de Vitrification de Marcoule <sup>d</sup>	Marcoule, France	Induction, hot crucible	1,138 <sup>ξ</sup>	12-18 <sup>§§</sup>	0.43 x 1	3,159	1.69 x 10 <sup>6</sup>
Pamela	Mol, Belgium	JHCM	500 <sup>§</sup>	15-25 <sup>§§</sup>	0.30 x 1.2 0.43 x 1.34	2200	4.5 x 10 <sup>5</sup>
Tokai Vitrification Facility <sup>e</sup> (TVF)	Japan	JHCM	>100	20-30 <sup>§§</sup>	0.43 x 1	247 <sup>ff</sup>	1.5 x 10 <sup>4</sup>
Mayak Vitrification Facility <sup>f</sup> (EP-500)	Ural Region, Russia	JHCM	~8000	33 <sup>§§</sup>	0.57 x 1	17,600	3.33 x 10 <sup>7</sup>

<sup>‡</sup> 1 Tera-Becquerel (TBq) = 10<sup>12</sup> atoms decaying per second or transmutations per second

\* 1996-2009

\*\* 1996-2002 – mission complete

<sup>†</sup> 1991-2007 at 150L glass per canister and an assumed glass density of 2.75 g/cc

<sup>††</sup> predicted mission completion is 6582 canisters

<sup>f</sup> 1989-2008

<sup>ξ</sup> 1978-2008

<sup>§</sup> 1985-1991

<sup>ff</sup> 1995-2006

<sup>§§</sup> acidic waste loadings are comprised of fission products and minor actinides – corrosion products and alkali are not included as for neutralized wastes

<sup>a</sup> A. Riley, S. Walker, N.R. Gribble, “Composition Changes and Future Challenges for the Sellafield Waste Vitrification Plant,” Sci. Basis for Nuclear Waste Mgt, XXXIII, Materials Research Society, Pittsburgh, PA, 267-273 (2009).

- b. J.M. Perez, Jr., D.F. Bickford, D.E. Day, D.S. Kim, S.L. Lambert, S.L. Marra, D.K. Peeler, D.M. Strachan, M.B. Triplett, J.D. Vienna, R.S. Wittman, “High-Level Waste Melter Study Report,” PNNL-13582 (2001).
- c. C.M. Jantzen, A.D. Cozzi, and N.E. Bibler, “High Level Waste Processing Experience with Increased Waste Loadings,” Environmental Issues and Waste Management Technologies X, J.D. Vienna, C.C. Herman, and S.L. Marra (Eds), Ceramic Transactions 168, 31-49 (2005).
- d. Caterine Veyer of AREVA, personnel communication (2010).
- e. Seiichiro Mitsui of JAEA, personnel communication (2010).
- f. P.P. Poluektor, private communication (2010).

**Table IV. HLW Waste Glass Product and Process Constraints**

<b>Product Constraints</b>	<b>Process Constraints</b>
chemical durability	melt viscosity
glass homogeneity	liquidus
thermal stability	waste solubility
regulatory compliance	melt temperature/corrosivity
mechanical stability	radionuclide volatility
	REDOX*

\* REDuction/OXidation which controls foaming and melt rate

**Table V. Comparative Oxide Compositions (Wt%) of Lanthanide/Plutonium Borosilicate Glasses [131]**

Oxide	Loffler Glass <sup>‡</sup>	Ramsey Loffler ThO <sub>2</sub> -1	Ramsey Loffler ThO <sub>2</sub> -2	Meaker Loffler ThO <sub>2</sub>	LaBS PNNL PuO <sub>2</sub>	LaBS Frit A PuO <sub>2</sub>	LaBS Frit B PuO <sub>2</sub>	LaBS Frit X PuO <sub>2</sub>	LaBS Frit B ZrO <sub>2</sub>	LaBS Frit B HfO <sub>2</sub>	LaBS Frit X HfO <sub>2</sub>
Al <sub>2</sub> O <sub>3</sub>	9.0	9.08	3.58	16.25	19.04	19.46	19.27	9.05	20.35	19.17	9.00
BaO	2.0	2.02	2.14	-	-	-	-	-	-	-	-
B <sub>2</sub> O <sub>3</sub>	5.0	5.05	7.88	8.85	10.4	10.59	10.50	11.77	11.07	10.44	11.70
Ce <sub>2</sub> O <sub>3</sub> (Pr <sub>2</sub> O <sub>3</sub> )	(3.2)	18.61	-	-	-	-	-	-	-	-	-
Gd <sub>2</sub> O <sub>3</sub>	-	-	-	17.16	7.61	7.78	11.58	12.22	12.23	11.52	12.15
HfO <sub>2</sub> (frit component)	-	-	-	-	-	-	5.97	6.34	6.23	5.94	6.30
HfO <sub>2</sub> (PuO <sub>2</sub> surrogate)	-	-	-	-	-	-	-	-	-	10.00	10.00
La <sub>2</sub> O <sub>3</sub>	18.3	0.91	1.21	3.80	11.01	11.22	7.33	17.20	7.70	7.29	17.10
Nd <sub>2</sub> O <sub>3</sub>	32.5	32.81	34.76	4.05	11.37	11.58	7.42	13.58	7.80	7.38	13.50
PbO	7.9	7.97	8.44	-	-	-	-	-	-	-	-
PuO <sub>2</sub> (Pu <sub>2</sub> O <sub>3</sub> )	-	-	-	-	11.39	9.50†	9.50	9.50	-	-	-
SiO <sub>2</sub>	21.5	21.7	24.36	22.0	25.80	26.43	26.15	18.10	27.52	26.01	18.00
SrO (CaO+ZnO)	-	-	-	1.9	2.22	2.26	2.26	2.26	2.42	2.25	2.25
ThO <sub>2</sub> (PuO <sub>2</sub> surrogate)	-	1.85	17.62	25	11.39	-	-	-	-	-	-
ZrO <sub>2</sub> (frit component)	-	-	-	1	1.15	1.18	-	-	-	-	-
ZrO <sub>2</sub> (PuO <sub>2</sub> surrogate)	-	-	-	-	-	-	-	-	4.56	-	-
Na <sub>2</sub> O and Li <sub>2</sub> O	-	-	-	-	-	-	-	-	-	-	-
Melt Temp (° C)	1350	1400	1425	1475	1450-1500	1500	1500	1500	1500	1500	1500
Total Ln <sub>2</sub> O <sub>3</sub>	54.0	52.33	35.97	25.0	29.99	30.58	26.33	43.00	27.73	26.19	42.75
Ln <sub>2</sub> O <sub>3</sub> +(Th,Zr,Hf)O <sub>2</sub>	54.0	54.18	53.59	51.0	45.16	40.08	41.80	58.84	38.52	42.13	59.05
SiO <sub>2</sub> +Al <sub>2</sub> O <sub>3</sub>	30.5	30.78	27.94	38.25	44.84	45.89	45.42	27.15	47.87	45.18	27.00
SUM	99.4	100	99.99	100.01	99.99	100	99.98	100.02	99.88	100.00	100.00

This glass also has 0.1 wt% As<sub>2</sub>O<sub>5</sub> as a fining agent

† maximum waste loading determined to be 13.4 wt% PuO<sub>2</sub>

<sup>‡</sup> This glass also has 0.1 wt% As<sub>2</sub>O<sub>5</sub> as a fining agent

† maximum waste loading determined to be 13.4 wt% PuO<sub>2</sub>

**Table VI. Compositions of Proposed Phosphate Glasses**

Oxide	Russian Alumino-phosphate*	Russian Alumino-phosphate Glass Tested at SRNL**	Waste Engineering Solidification Prototypes (WSEP) <sup>†</sup>	Lead Iron Phosphate (LIP) <sup>f</sup>	Fe-P Nominal <sup>§</sup>
Al <sub>2</sub> O <sub>3</sub>	19.0	17.0	0-35	1-2	5
Bi <sub>2</sub> O <sub>3</sub>					3-13
CaO		0.64			7-10
CaF <sub>2</sub>					5
Cr <sub>2</sub> O <sub>3</sub>	0.1				3
Fe <sub>2</sub> O <sub>3</sub>	1.5	3.49			20-38
Fe <sub>2</sub> O <sub>3</sub> + NiO+Cr <sub>2</sub> O <sub>3</sub>	1.6	4.81	0-30	6-13	
K <sub>2</sub> O		0.4			5-10
La <sub>2</sub> O <sub>3</sub>					3
MgO		0.01			
MnO		0.09			
Mn <sub>2</sub> O <sub>3</sub>					5
MoO <sub>3</sub>					4-8
Na <sub>2</sub> O	21.2	22.2	5-25	1-2	10
NiO		1.23			6
PbO			0-30	36-53	
P <sub>2</sub> O <sub>5</sub>	52	51.2	30-55	25-42	42-50
SiO <sub>2</sub>		0.07	0-6	0-0.25	10
ZrO <sub>2</sub>		0.18			6
Fission Products (Cs <sub>2</sub> O + SrO)	6		30	0-0.25	20
Actinides (U <sub>3</sub> O <sub>8</sub> )		1.62	1-2.5		12
Melt Temp (° C)	1200	1150-1200	1050-1200	800-1050	950 to 1100

\* M.I. Ojovan and W.E. Lee, “New Developments in Glassy Nuclear Wasteforms,” Elsevier Publishers, Oxford, 315pp. (2005).

\*\* N.E. Bibler, C.M. Jantzen, and W.G. Ramsey, “Characterization of Two Russian Phosphate Waste Glasses – Interim Report,” U.S. DOE Report WSRC-RP-1213 (August 1993).

† J.L. McElroy, K.J. Schneider, J.N. Hartley, J.E. Mendel, G.L. Richardson, R.W. McKee and A.G. Blasewitz, “Waste Solidification Program Summary Report, Vol. 11, Evaluation of WSEP High Level Waste Solidification Processes,” U.S. DOE Report, BNWL-1667, Battelle Northwest Laboratories, Richland, WA 99352.

*f* The ratio  $\text{Fe}_2\text{O}_3/(\text{PbO} \bullet \text{P}_2\text{O}_5) \cong 9$  wt%; B.C. Sales and L.A. Boatner, “Physical and Chemical Characteristics of Lead-Iron-Phosphate Nuclear Waste Glasses,” *J. Non-Crystalline Solids*, 79, 83-116 (1986).

*§* the O/P mole ratio of the final waste form should be in the range 3.4-3.8; the  $\text{P}_2\text{O}_5$  content must be between 42 and 50 wt% and the  $\text{Fe}_2\text{O}_3$  content must be at least 20 wt% although smaller amounts are permissible when  $\text{Al}_2\text{O}_3$ ,  $\text{Bi}_2\text{O}_3$ ,  $\text{La}_2\text{O}_3$ ,  $\text{U}_3\text{O}_8$  and other similar oxides are present. J.M. Perez, Jr., D.F. Bickford, D.E. Day, D.S. Kim, S.L. Lambert, S.L. Marra, D.K. Peeler, D.M. Strachan, M.B. Triplett, J.D. Vienna, R.S. Wittman, “High-Level Waste Melter Study Report,” PNNL-13582 (2001).



Figure 1. Distribution of HLW in the United States.

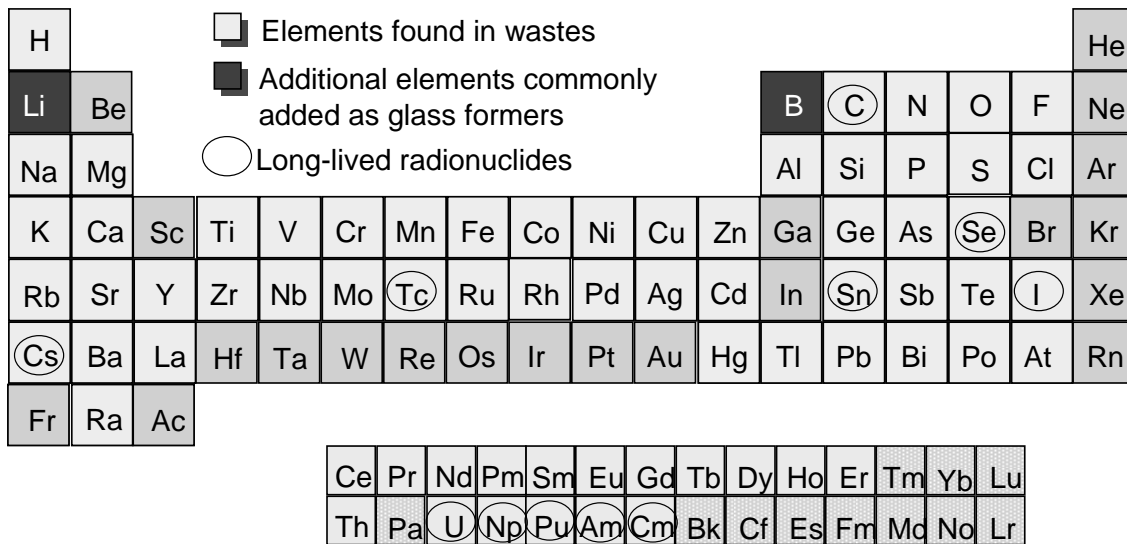


Figure 2. Elements in US defense wastes.

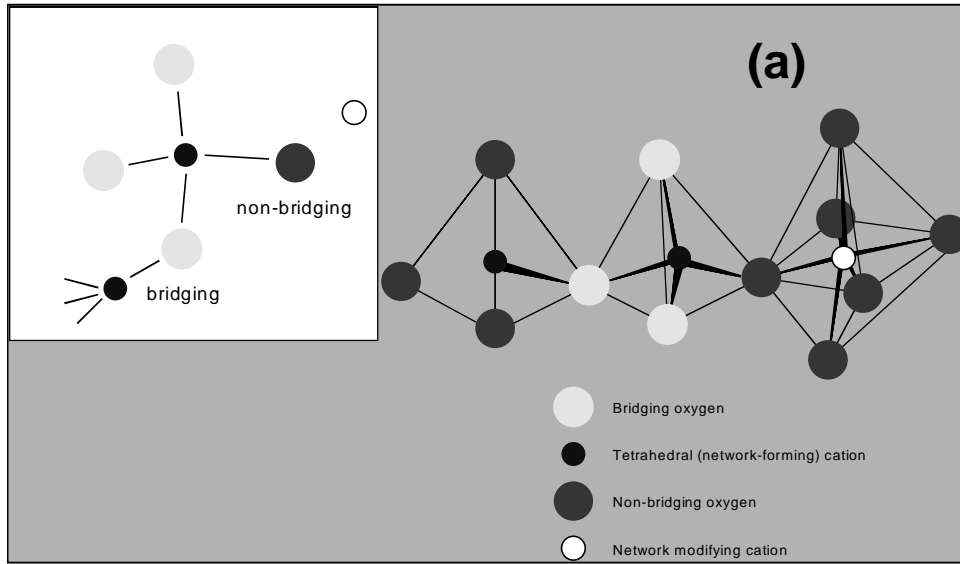


Figure 3a. An example of short range order (SRO; tetrahedra and octahedra) and medium range order (MRO; tetrahedra and octahedra with a network modifying cation attracted to the non-bridging oxygen of the SRO tetrahedra in inset and two tetrahedra linked to an octahedra) structural units in glass and crystalline structures. Glass is a polymerized random structure of  $(\text{SiO}_4)^{-4}$ ,  $(\text{AlO}_4)^{-5}$ ,  $(\text{BO}_4)^{-5}$ ,  $(\text{PO}_4)^{-3}$  tetrahedral and  $(\text{BO}_3)^{-3}$  trigonal structural units.

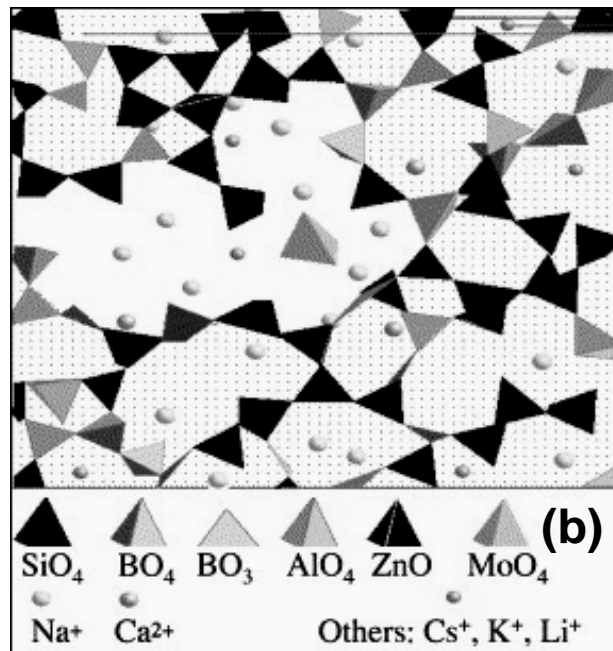


Figure 3b. Polymerization of SRO and MRO in the atomic structure of glass. Unshaded region shows formation of an alkali molybdate cluster (from Calas, et. al. 2003).

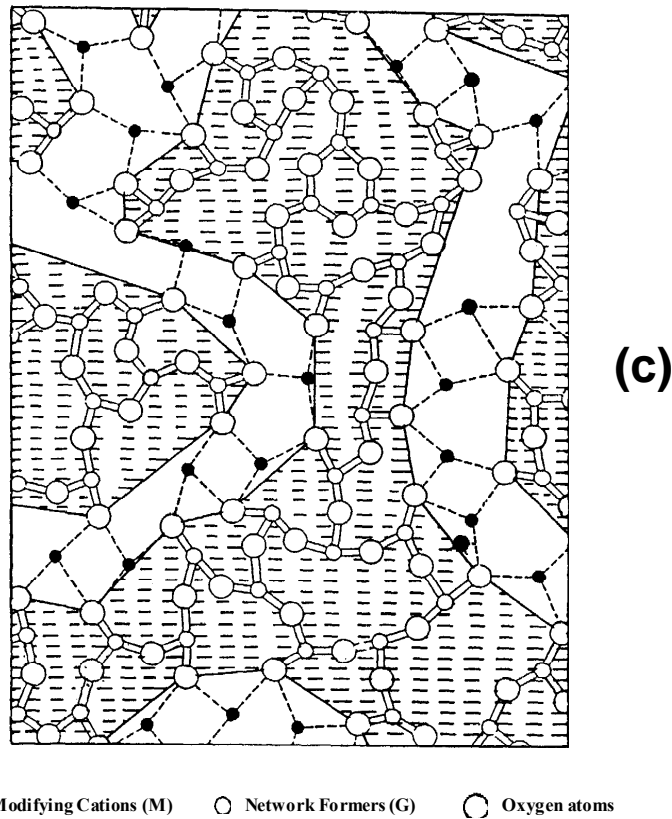


Figure 3c. A modified random network (MRN) for a glass of nominal composition  $M_2O_3(G_2O_3)_2$ , where M represents the modifying cations and G represents the tetrahedral cations. Covalent bonds are shown by the solid lines and the ionic bonds by the dotted lines. The shaded regions are defined by the boundary which runs along the G-O non-bridging bonds. The unshaded regions represent the percolation channels defined by the M-O bonds that run through the glass network (Greaves, 1989).

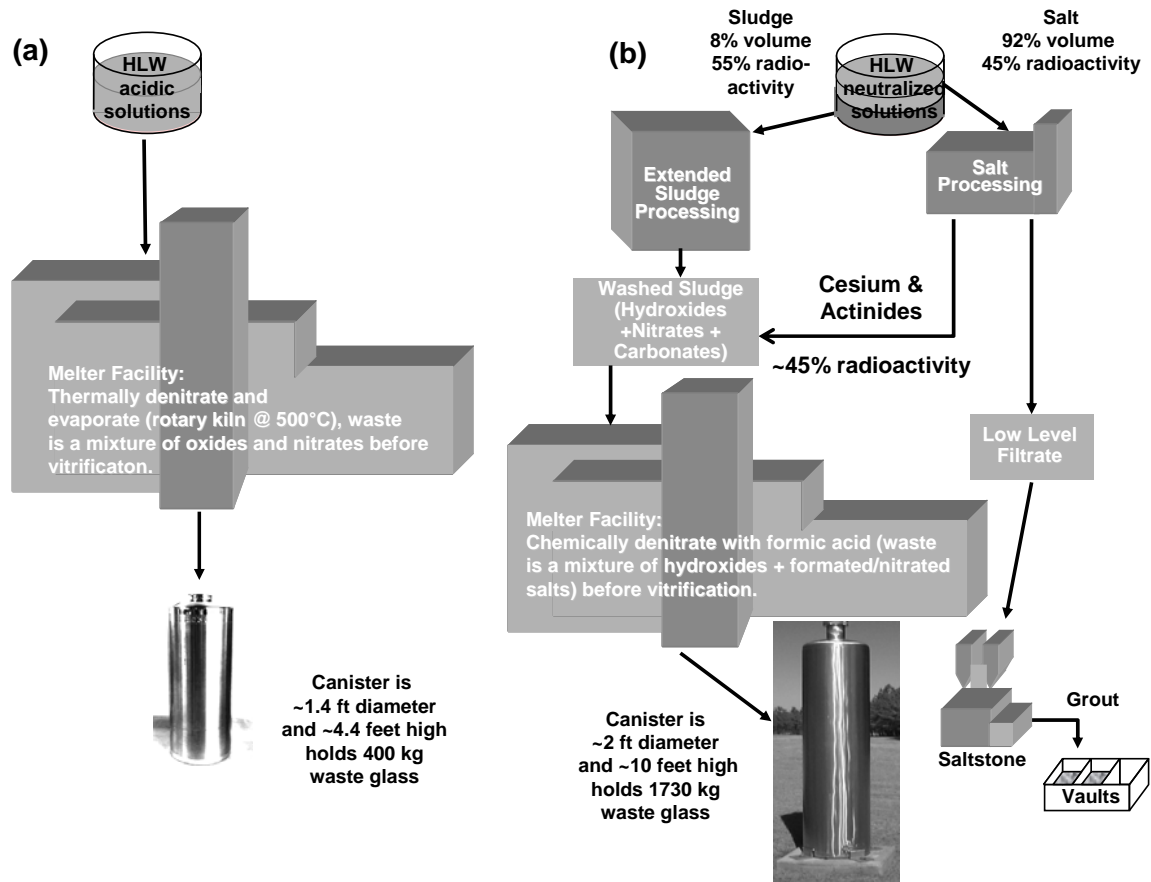


Figure 4. Typical vitrification flowsheets (a) the AVM/AVH vitrification process for acid HLW wastes and (b) the Defense Waste Processing Facility (DWPF) vitrification process for neutralized HLW waste.

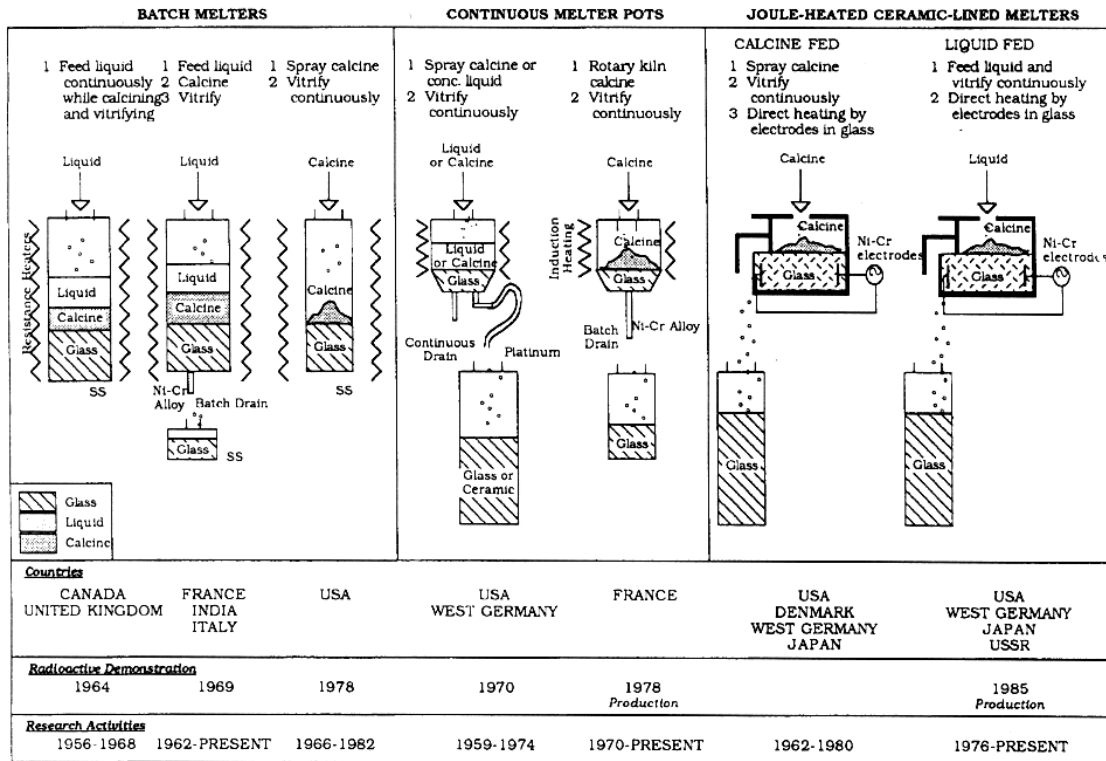


Figure 5. Evolution of HLW glass melter designs over time (from Bickford, Hrma and Bowen, 1990).

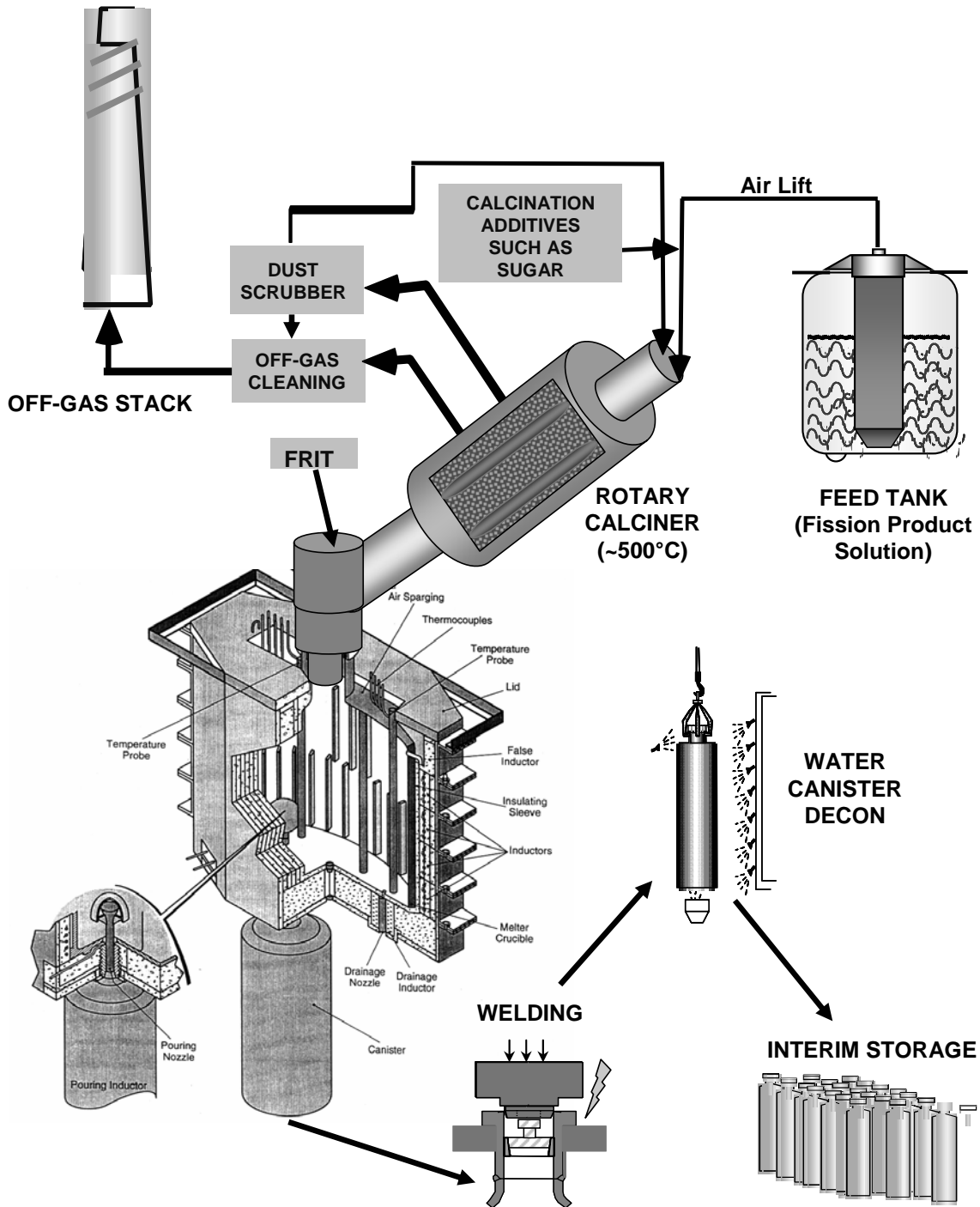


Figure 6a. Melter Facility: Thermally denitrate and evaporate (rotary kiln @ 500°C), waste is a mixture of oxides and nitrates, mix with frit additives, induction heated Inconel Melter (1150°C).

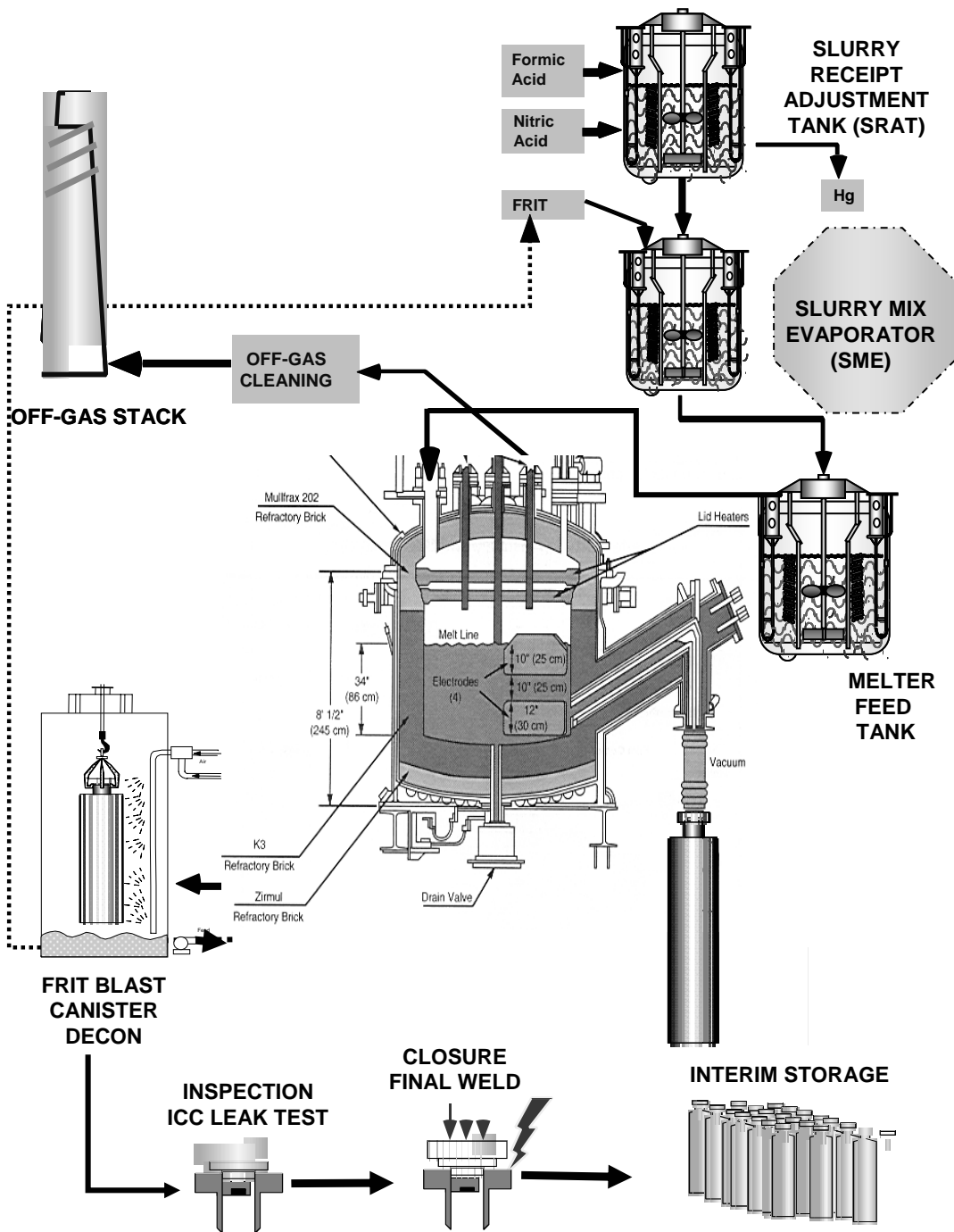


Figure 6b. Melter Facility: Chemically denitrated with formic acid. Waste is a mixture of

hydroxides + formated salts. Mix with frit (or glass formers). Joule heated Melter, Inconel® electrodes, refractory lined (1150°C).

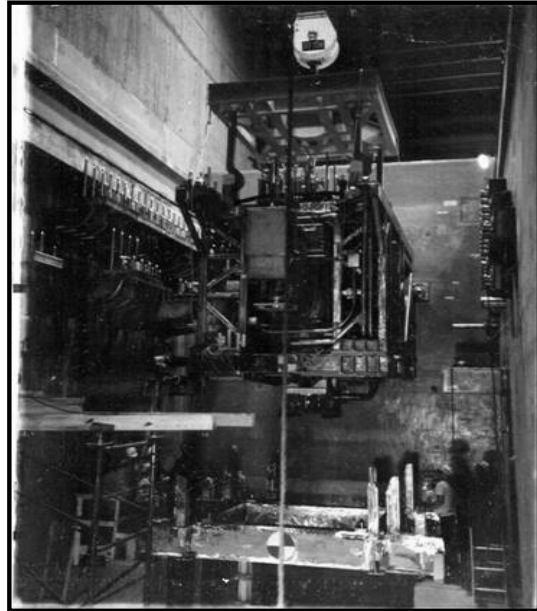
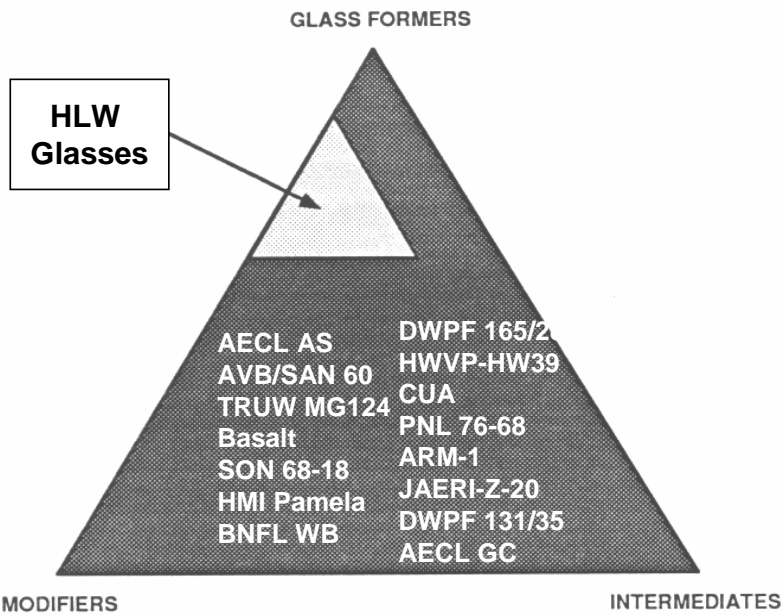
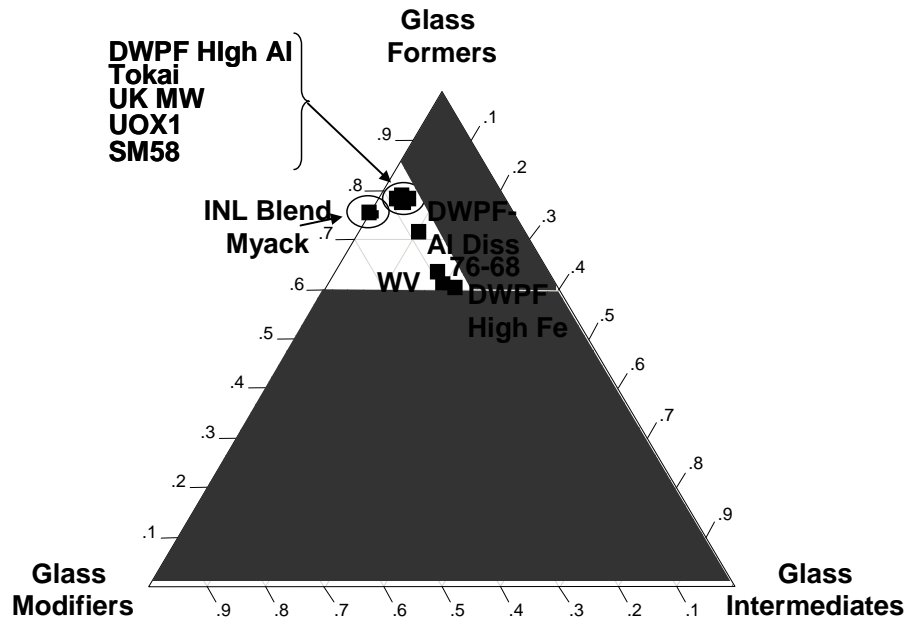


Figure 7. DWPF melter one being disposed of after 9 years of operation. Melter was emptied through emergency bottom drain and lifted out of the melt cell into a waste box for storage and eventual disposal (Courtesy of Savannah River Site).



(b)

Figure 8. Ternary diagram depicting compositional similarities for a variety of HLW glasses expressed in terms of the structural components of the glasses.

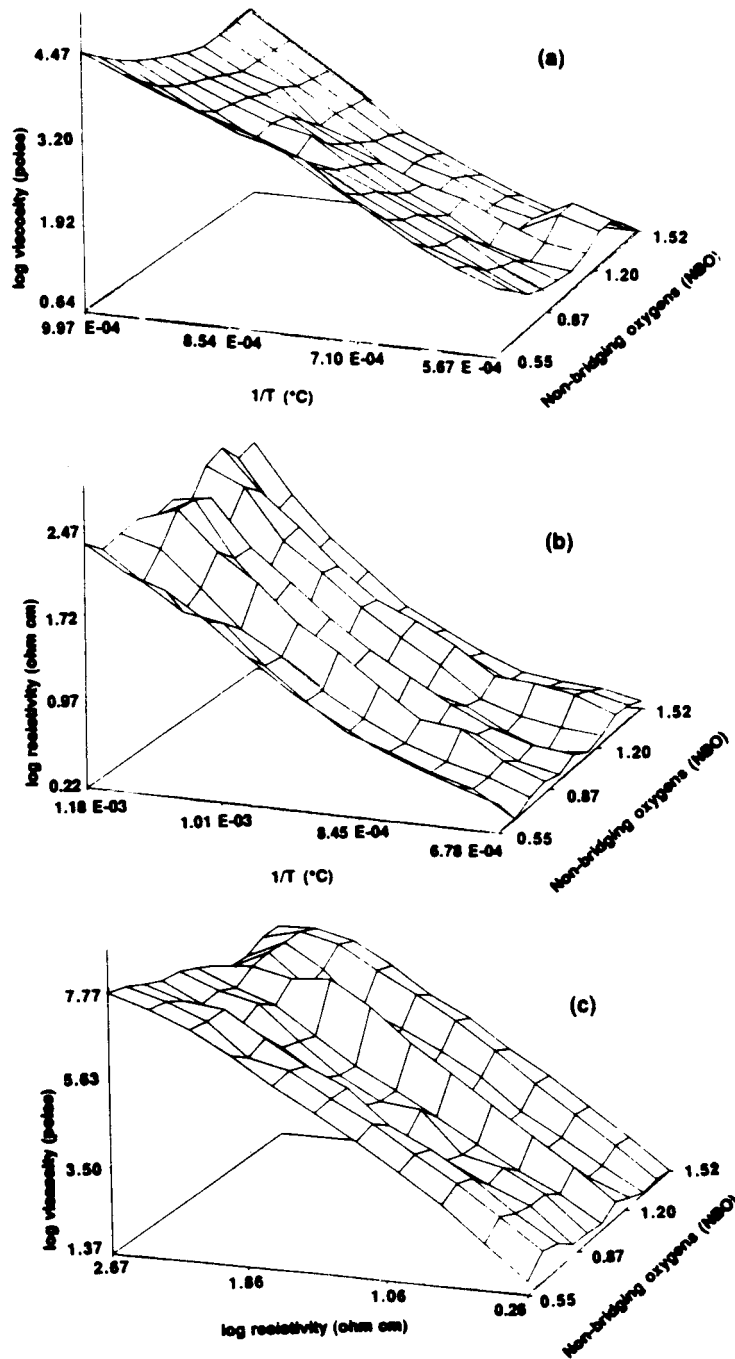


Figure 9a. Relationship between log viscosity (poise), inverse melt temperature, and NBO.

Figure 9b. Relationship between log resistivity (ohm cm), inverse melt temperature, and NBO.

Figure 9c. Relationship between log viscosity (poise), log resistivity (ohm cm), and NBO. From Jantzen (1986 – reference 55).

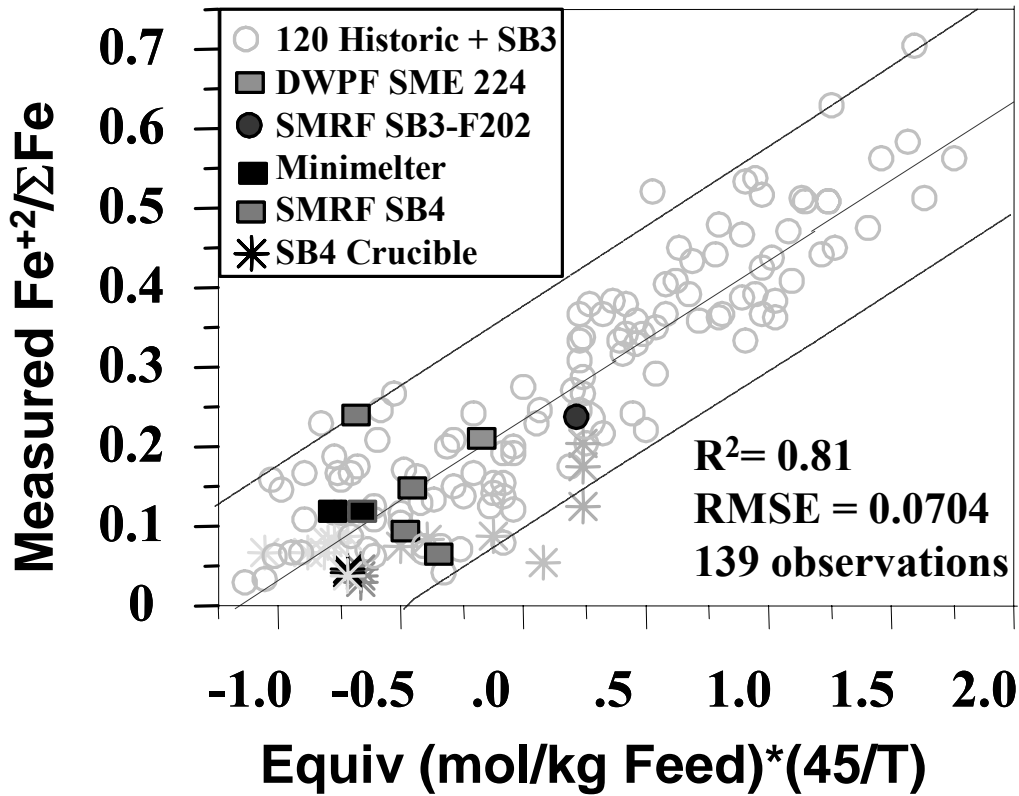


Figure 10. Correlation of glass REDOX expressed as Fe<sup>+2</sup>/ΣFe versus melter feed oxidants and reductants expressed as electron equivalent transfers and weighted by the wt% solids in the slurry feed. Open circles and asterisks represent crucible data used to develop the model and the solid symbols represent melter testing including radioactive testing in the DWPF.

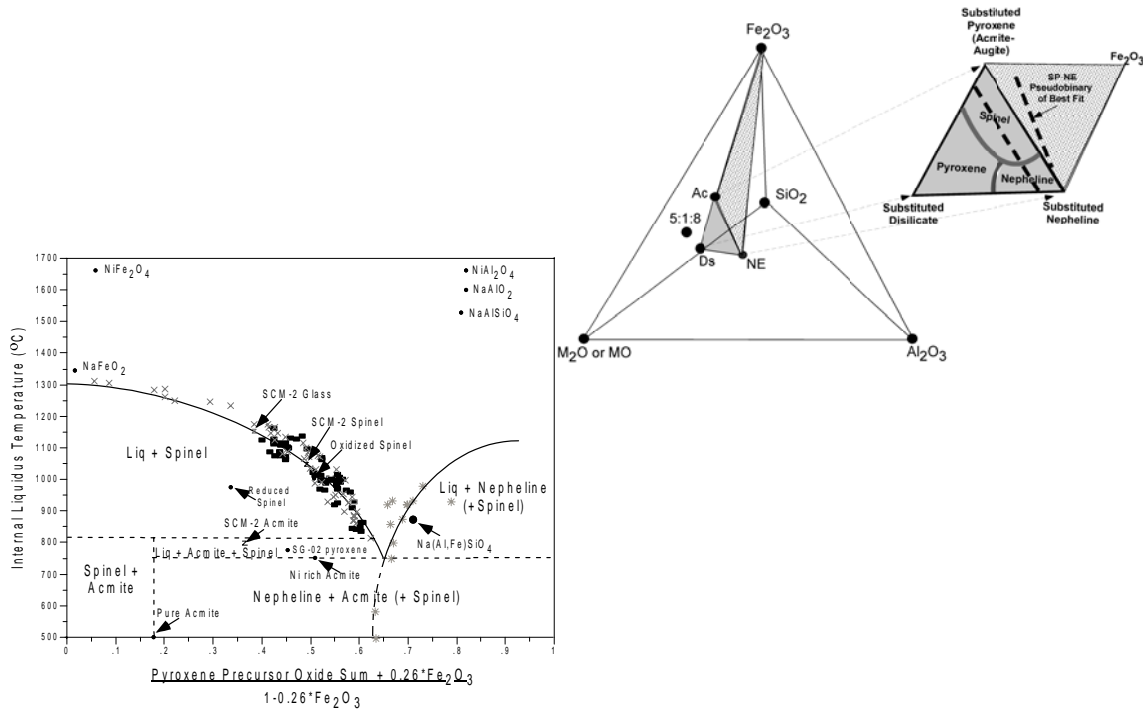


Figure 11. Pseudobinary phase diagram between acmite and nepheline expressed in terms of the pyroxene and nepheline quasi-crystalline precursor compositions (un-normalized mol%) on which the liquidus model is based. Inset shows the position of this pseudobinary in the quaternary ( $B_2O_3$  free) system as  $B_2O_3$  does not participate in the crystallization. From Jantzen and Brown 2007 - reference 25.

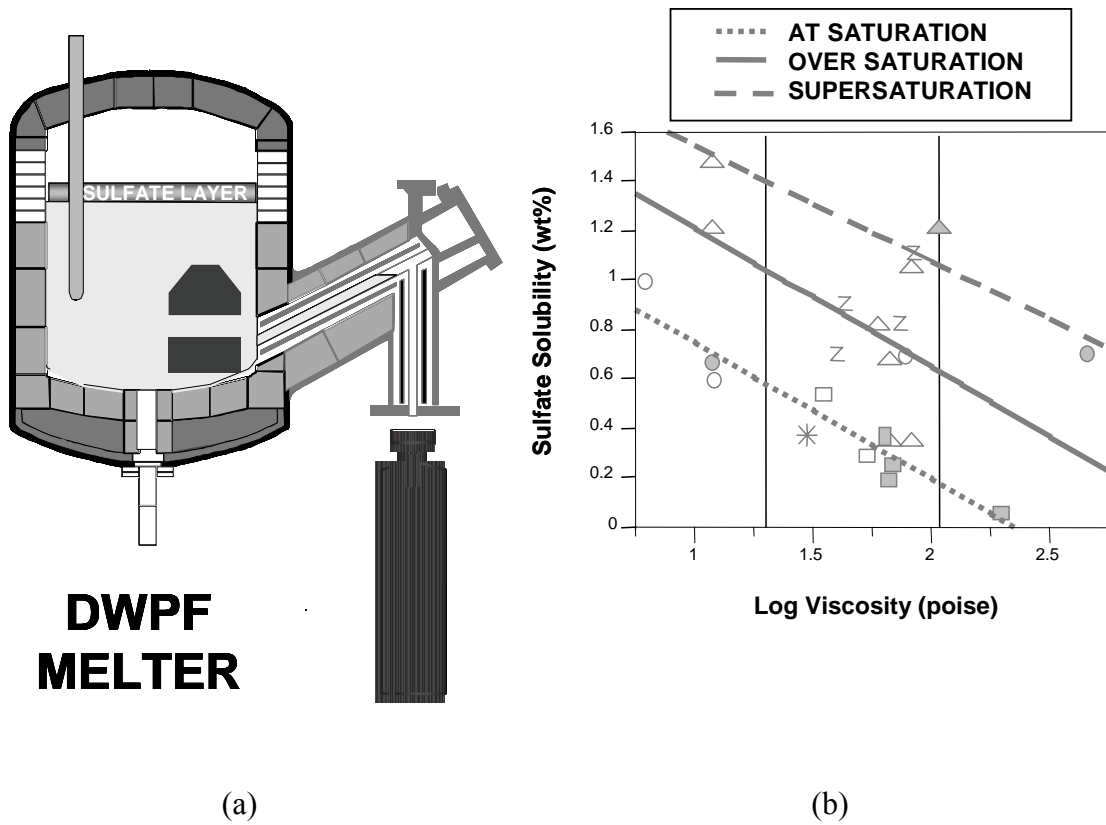


Figure 12a. Flotation of excess sulfate on the melt pool during supersaturation as gall and vespicles in the glass. This can cause operational problems and poor glass Quality.

Figure 12b. Relationships between the calculated melt viscosity at 1150°C and  $SO_4^{=}$  solubility in DWPF HLW glasses as a function of sulfate saturation. From references 109, 110.

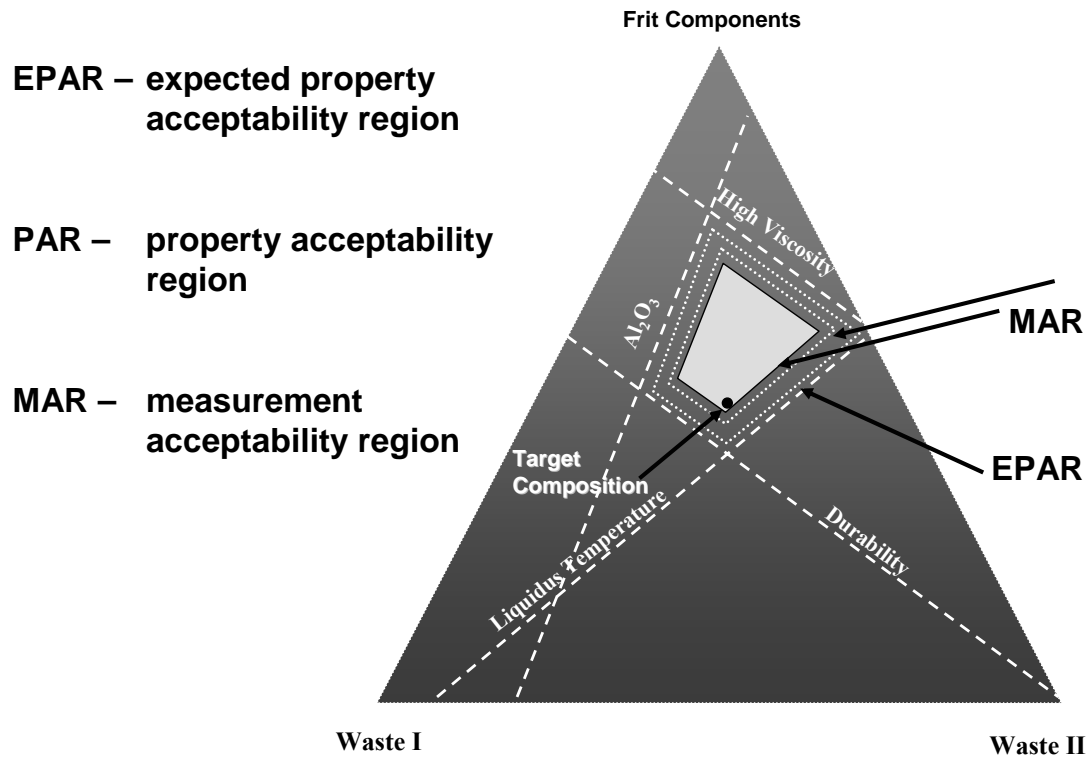


Figure 13. Product Composition Control System (PCCS).

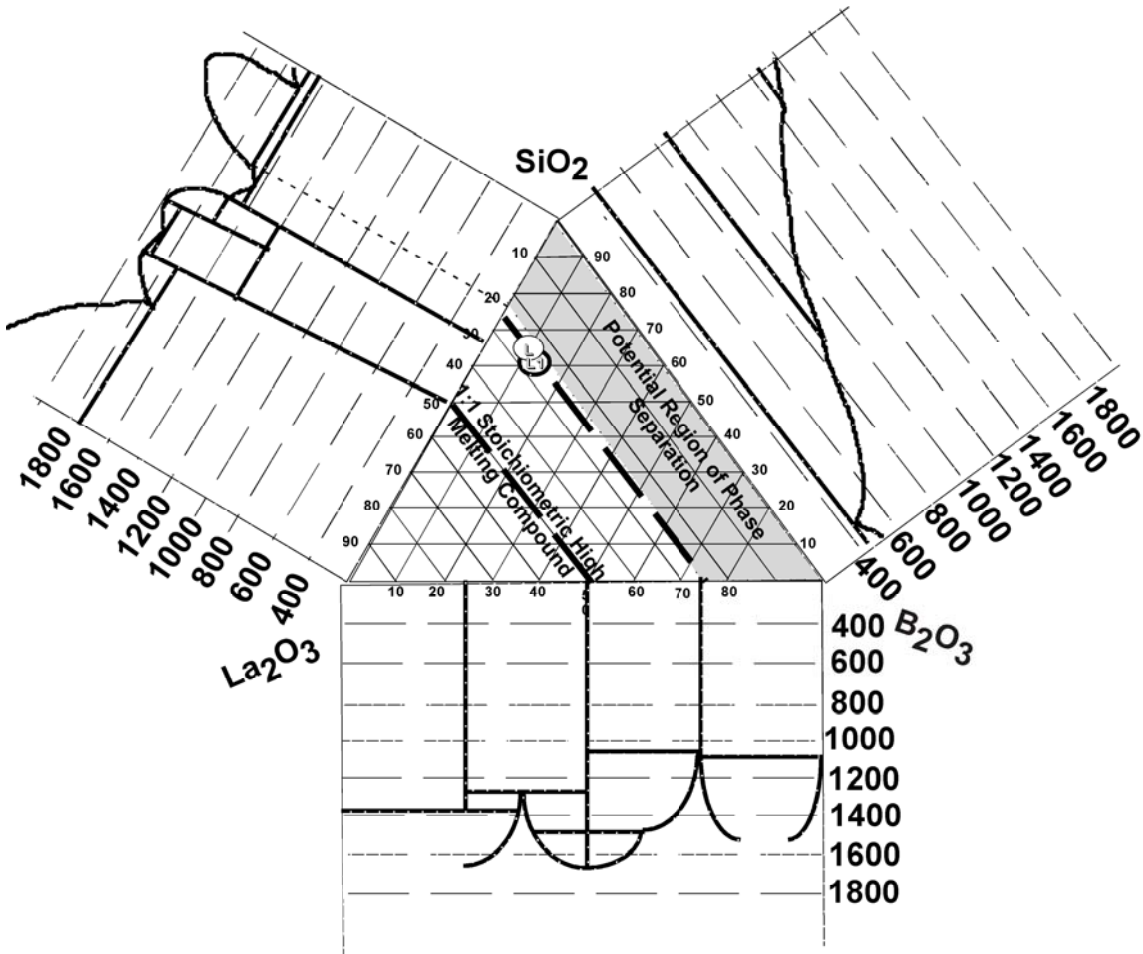


Figure 15. The inferred Ternary Oxide System  $\text{Ln}_2\text{O}_3\text{-B}_2\text{O}_3\text{-SiO}_2$  (mole %) from the known binary oxide systems. Note that the Loffler glass formulation in the  $\text{Ln}_2\text{O}_3\text{-B}_2\text{O}_3\text{-SiO}_2$  system is indicated in the circle with the letter “L1” and that if the ternary is generalized to include  $\text{SiO}_2+\text{Al}_2\text{O}_3$  at the apex then the Loffler glass formulation in the  $\text{Ln}_2\text{O}_3\text{-B}_2\text{O}_3\text{-(SiO}_2+\text{Al}_2\text{O}_3)$  system is indicated as “L”.

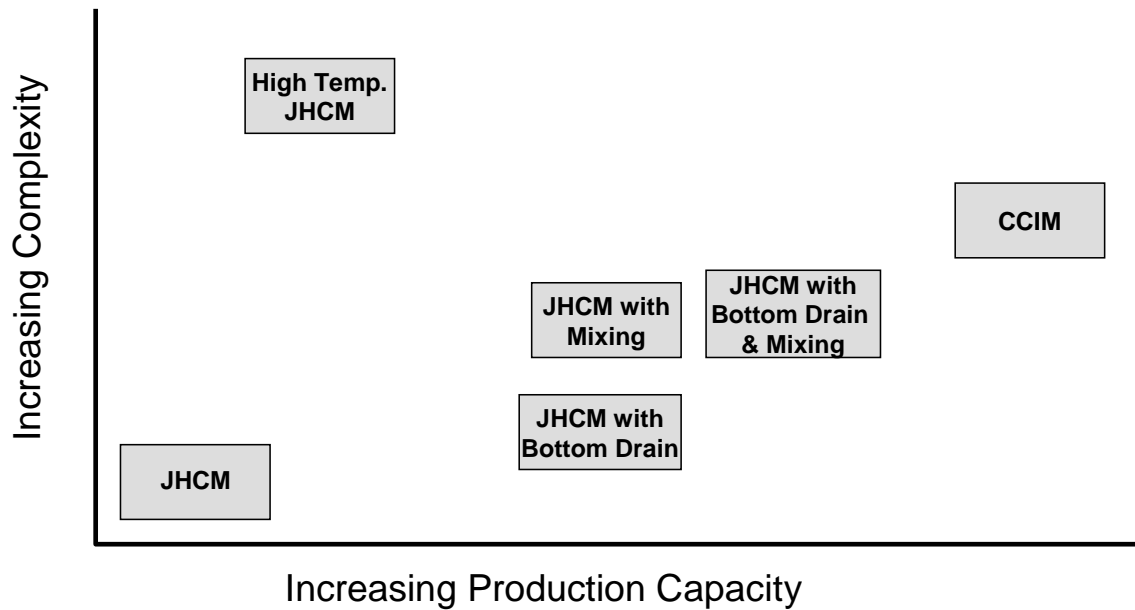


Figure 16. Representation of Advanced Melter Technologies Based on Complexity and Capability (after J.M. Perez, Jr., D.F. Bickford, D.E. Day, D.S. Kim, S.L. Lambert, S.L. Marra, D.K. Peeler, D.M. Strachan, M.B. Triplett, J.D. Vienna, R.S. Wittman, “High-Level Waste Melter Study Report,” PNNL-13582 (2001).

## Appendix A. Historical Development of Glassy Waste Forms

Development of glasses for the solidification of HLW began at different times in the US, Canada, Europe, and the USSR. Different glass formulations (borosilicate, aluminosilicate, and phosphate glasses) and processing strategies were developed as discussed in the body of Chapter 11. The borosilicate glass formulations were developed in the US between 1956 and 1957. The aluminosilicate (nepheline syenite based) glass formulations were simultaneously being developed in Canada in 1957. Phosphate-based glasses were the last to be investigated for solidification of nuclear waste. A systems evaluation of phosphate glasses demonstrated that the positive aspects of processing, e.g. low melting temperatures, were outweighed by other negative processing aspects, e.g. melt corrosivity, and by poor product performance. The aluminosilicate glasses and the ceramic waste forms are still being investigated for certain types of nuclear waste because the systems evaluation for these waste forms is favourable under certain conditions. However, repeated systems evaluations of borosilicate waste glass formulations and the associated processing technology have found this family of glasses to be applicable to a wide range of waste compositions melted by various processing methodologies. The favourable systems evaluations of borosilicate waste glasses have led to their acceptance as the reference nuclear waste form in ten countries including Canada. [161]

Figure A1 is an attempt to unify the development of vitreous waste form by year and country starting in the late 1950's to the present. The historical development of the glass formulations and the importance of a whole systems evaluation (waste form performance vs. processing aspects) will be summarized below with special reference to the development in the US. Figure A1 shows the relative processing temperature of the various glass, glass ceramic, and ceramic waste forms and the time line of development for each. Solid lines mean active development in the US and/or Canada while dotted lines indicate inactive development of a waste form in the US and/or Canada but active development in other countries. Significant development by certain laboratories is indicated as discussed below.

Borosilicate glasses are alkali-aluminosilicate type glasses which are fluxed with boron. The lower alumina content and the presence of boron lowers the melt viscosity and hence the processing temperature ( $\sim 1150^{\circ}\text{C}$ ) relative to that of the aluminosilicate glasses. The boron increases the solubility of many waste constituents in the silica-based glass [162] while maintaining thermal and mechanical stability [163] and decreasing chemical durability only slightly [163,164] relative to the highly durable but more difficult to produce aluminosilicate glasses.

The typical borosilicate waste glasses currently in use for solidification of nuclear waste are quite different from Pyrex or Vycor type borosilicate glasses (Figure A2). Since the borosilicate waste glasses are between 18-25 wt% actinides and fission products, much of the chemistry is still dominated by the chemistry of the  $\text{Na}_2\text{O}-\text{B}_2\text{O}_3-\text{SiO}_2$  system. The

range of compositions for commercial and defense borosilicate waste glasses expressed as a function of  $\text{Na}_2\text{O}-\text{B}_2\text{O}_3-\text{SiO}_2$  are shown on the ternary phase diagram in Figure A2. Note that Pyrex has a higher silica content than the waste glasses and, hence, melts at a higher temperature. The alkali content of the waste glasses is higher than that of Pyrex or Vycor while the boron content overlaps that of some Vycors.

A systems evaluation of the borosilicate waste glasses indicates that these glasses exhibit good chemical durability, thermal stability, mechanical stability and waste solubility while being processed at temperatures of  $1150^\circ\text{C}$  which limits the volatility of the radionuclides and hazardous species. The borosilicate waste melts are generally less corrosive than commercial glass melts, such as Pyrex, due to the lower temperature of fabrication. The technology used for commercial waste glass fabrication can, therefore, easily be adapted. Borosilicate glasses exhibit favourable product performance as well as ease of processability.

### **Borosilicate Glass Development in the United States**

The initial borosilicate glass formulations were developed in the US between 1956 and 1957 by Goldman and others at the Massachusetts Institute of Technology (MIT). [165,166,167] They examined calcium-aluminosilicate porcelain glazes to which  $\text{B}_2\text{O}_3$  had been added to achieve a pourable glass melting at  $1300^\circ\text{C}$ . The quality of these glasses did not suffer from the incorporation of such substances as  $\text{ZrO}_2$  and  $\text{Fe}_2\text{O}_3$  which were present in the nuclear waste solutions. Eliassen and Goldman [166] felt that the most promising vitreous systems for future development were borosilicate based, e.g.  $\text{CaO}-\text{Al}_2\text{O}_3-\text{B}_2\text{O}_3-\text{SiO}_2$  and  $\text{Na}_2\text{O}-\text{CaO}-\text{Al}_2\text{O}_3-\text{B}_2\text{O}_3-\text{SiO}_2$ .

Although the early borosilicate glass formulations were developed in the US, vitrification process development and testing during the early 1960's was carried out primarily in the UK and Europe. [168,169,170] In the mid 1960's the Waste Solidification Engineering Prototypes (WSEP) program demonstrated the overall ease of processability and compositional flexibility of borosilicate type glasses [171] and Pacific Northwest laboratories demonstrated the advantages of ceramic Joule heated melters. [168] Other waste producers in the US such as the Savannah River Site built upon both the European and US experience and chose borosilicate glass as the reference solid waste form as early as 1975. [172] The Savannah Rive Site started up their Joule heated melter, the Defense Waste Processing Facility (DWPF), in April 1994 and ran simulated waste and frit until radioactive operation started in March 1996. West Valley Demonstration Project (WVDP) started up their operations shortly after the DWPF in 1994 and finished their mission in 2002. The Hanford Vitrification Facility is still under construction.

### **Borosilicate Glass Development in France**

Laboratory research on containment matrices for radioactive waste from nuclear energy began in France in 1957. Borosilicate glass quickly proved to be more suitable for incorporating the forty-odd elements created by uranium fission (as well as additives and corrosion products resulting from fuel reprocessing) into a homogeneous matrix.

The first industrial vitrification facility, PIVER (Pilote Verre a batch vitrification process that did not employ a separate calcination step), began operating in 1969. Before it was shut down in 1972, PIVER produced 164 glass blocks, weighing a total of 12 tons, from 24 m<sup>3</sup> of concentrated fission product solutions containing  $6 \times 10^6$  Ci. The facility resumed operation a few years later to vitrify HLW solutions arising from the reprocessing of fast breeder reactor fuel, producing ten glass blocks of 90 kg each with very high specific activity. In 1989, PIVER was named a Nuclear Historic Landmark by the American Nuclear Society.

Faced with increasing demand, research was undertaken in the 1970's to develop a continuous vitrification process to obtain a final glass waste form by first evaporating and calcining the feed solution in a rotary furnace, then melting the calcine with glass frit in an induction-heated metal melter. The Marcoule Vitrification Facility (AVM or Atelier de Vitrification de Marcoule) was commissioned in 1978 to vitrify fission product solutions from the French UP1 reprocessing plant. By the end of 1995, AVM had logged nearly 64,800 hours of operation and vitrified 1,920 m<sup>3</sup> of solution containing 401 million curies, producing 857.5 tons of glass in 2,412 canisters, each containing 360 kg of glass.

The successful operating record and experience gained with AVM allowed the start-up of a commercial-scale high level waste vitrification plant in France. Two similar facilities, R7 and T7, are on line at the La Hague reprocessing plant. R7 was commissioned in 1989 and T7 in 1992. Fission-product oxides are incorporated in quantities ranging from 12 to 18% of the R7T7 glass package (this value ranges from 6% to more than 20% depending on waste composition and type of glass. In the La Hague vitrification facilities, the metal pot is heated to 1,150 °C using a 200-kW power generator operating at a frequency of 4 kHz. The glass inside the metal pot is melted by conduction upon contact with the metal wall. Glass can react with metals at the process temperature, with the result that melting pots corrode and must be periodically replaced. They currently have an average lifetime of 5,000 hours with R7T7 glass. The melter lifetime has been extended considerably since the vitrification unit was commissioned, however, by modifying the composition of the nickel-based alloy from which the pots are made and by optimizing the management of the thermal power dissipated in the glass during the process. The unit also includes equipment for process off-gas treatment, comprising a particle separator, a condenser, and scrubbing columns.

For future use, the CEA has developed a process in which the glass is melted by induction heating inside a water-cooled crucible. The use of this cold crucible induction melter (CCIM) will allow glass or glass ceramic materials (GCM's) to be produced at higher temperatures and higher melt rates with no risk of corrosion, as the melter shell is

made of the same glass and remains at a lower “frozen” temperature. A nonradioactive prototype CCIM melter 55 cm in diameter and 70 cm high has been operating together with a calciner for several years at Marcoule. A unit of this type could advantageously replace the current melter in the future.

### **Borosilicate Glass Development in the United Kingdom**

Borosilicate glass has been under development in the UK over the last 40 years with initial work carried out at Harwell in the 1950's. Process development was temporarily halted in the 1960's due to lack of an economic incentive for treating the HLW and a high degree of confidence in the integrity of the HLW storage tanks. Work on the Harvest vitrification process was restarted in the 1970's. In 1981 it was decided to adopt the continuous French AVM melting process instead of the Harvest batch vitrification (calcination and vitrification took place in the same reaction vessel) process.

From 1983 a Full Scale Inactive Facility (FSIF) was constructed and operated by BNFL at Sellafield to develop the vitrification process for BNFL HLW. A parallel program developed and fine tuned the glass composition(s) required to vitrify the waste. These programs culminated in the construction, commissioning and active operation of the Waste Vitrification Plant (WVP) at Sellafield in 1991.

The WVP plant consists of a high active (HA) liquor storage and distribution cell, two parallel vitrification lines consisting of vitrification and pouring cells and container decontamination and monitoring/control cells and is based on the French AVM procedure. The process incorporates a rotary calciner through which HA liquor is fed and partially denitrated. The calcine is mixed with glass frit (glass beads of 1 to 2 mm in diameter) and fed into a elliptical Inconel melter that is inductively heated. In December 2005 a third vitrification line began operation in parallel with the existing two. This allows two vitrification lines to operate while the third line is under maintenance. The first two lines was retrofitted with “thick wall” melters which have increased throughput.

### **Aluminosilicate Glass Development in Canada**

Aluminosilicate-based glass formulations were investigated from 1955 to 1962 at the Chalk River Nuclear Laboratories (CRNL) funded by the Atomic Energy of Canada, Ltd (AECL).[173,174,175] These glasses were fused from crushed nepheline syenite rock (abundant in Canada) and mixed with waste at temperatures above 1350°C.

The waste being immobilized was a HLW UO<sub>2</sub> fuels recycle waste and the major radionuclides were <sup>242</sup>Pu and <sup>238</sup>U but the activity was primarily generated by <sup>137</sup>Cs and <sup>90</sup>Sr. [176,177,178,179] Two sets of glass blocks based on ground nepheline syenite rock with 15% CaO were buried without secondary containers, one in 1959 and one in 1960. This ended the active stage of research and development on aluminosilicate glasses until the blocks were exhumed in 1978 and the chemistry and glass surfaces examined.

The aluminosilicate or nepheline syenite type glasses have undergone continued development in Canada since the late 1950's into the 1980's when the exhumed blocks were characterized and studied as indicated in Figure A1. The major advantage of aluminosilicate waste glasses is the excellent chemical durability, thermal stability, and mechanical stability due to the high silica and alumina content. The disadvantages were the high melt temperature of 1350°C which caused volatilization of hazardous species and limited waste loading. [162] Melt corrosivity is comparable to commercial Pyrex glass but greater than that of borosilicate glasses due to the higher fabrication temperature of the aluminosilicate glasses. A system evaluation of the aluminosilicate glasses, therefore, indicates that they have superior product characteristics but are difficult to process. [180]

A new HLW glass program was initiated in 1976 [181] and focused on interim storage of spent fuel and its immobilization since no spent fuel reprocessing was being considered. The reference waste form examined from 1976-1981 was a dilute borosilicate glass with  $\leq 3$  wt% fission products to keep the heat of radioactive decay in the canister low. When a new nuclear fuel waste management program was established in 1981 the glass forming systems being investigated were  $\text{Na}_2\text{O}-\text{B}_2\text{O}_3-\text{SiO}_2$  and  $\text{Na}_2\text{O}-\text{Al}_2\text{O}_3-\text{B}_2\text{O}_3-\text{SiO}_2$ . [174,182,183]

### **Phosphate Glass Development in the US, Russia, Germany and Belgium**

The major research into phosphate waste glasses in the US started at Brookhaven National Laboratory around 1967 by Tuthill and others. [184] The delay in the development of phosphate glasses for use in waste disposal has been attributed to the lack of industrial usage of these types of glasses and hence the lack of commercial experience and technology such as exists for the various silica-based glasses. [162] The attractive low melting temperature of the phosphate glasses is offset by the corrosivity of the melt and the ease with which these glasses devitrify. [162] Phosphate glasses were also attractive because molybdenum and sulfate were more soluble than in borosilicate glass. [185] This was particularly applicable to wastes in Germany and hence the Pilot Anlage Mol zur Erzeugung Lagerfähiger Abfälle (PAMELA) process [186] was developed in the early 1960's. In this process, phosphate glass is formed as small beads which are then placed in a metal matrix in a steel canister (see Figure A1). The small size of the beads, plus the high thermal conductivity provided by the metal matrix, assures that the phosphate glass does not devitrify.

Development of the phosphate beads in Germany began in the early 1960's and subsequent solidification in a continuous metallic melter at Erurchemic in Mol, Belgium continued until the late 1970's. About 1976 Karlsruhe and Eurochemic changed to a borosilicate waste glass produced by a Joule-heated ceramic melter, after experience in the glass industry and at PNL [168] had demonstrated that this type of melter had a higher capacity per physical size, produced a more uniform glass, and had fewer problems with volatile losses than other melting techniques. The time interval for

development of phosphate beads in a metal matrix was, therefore, relatively short on Figure A1.

In 1966 the WSEP program was initiated at PNL. WSEP was a pilot plan designed for a radioactive demonstration of three solidification processes, two for borosilicate glass and one for phosphate glass. [171] Eleven canisters of radioactive phosphate waste glass were solidified. The results of the WSEP program showed that phosphate glass has several shortcomings when compared with borosilicate glasses. These shortcomings included the following: (1) high ruthenium volatility during preparation (denitration) of the liquid waste slurry; (2) additions of ferric nitrate and sodium hydroxide required to adjust the melting point and melt viscosity; (3) extreme corrosivity of the phosphate melt which required the use of platinum melters; extreme corrosivity of the phosphate melt which placed limitations on the temperature of the melt poured into the canisters; (5) low solubility of certain waste components including alumina, alkaline earth oxides, sulphates and fission products; (6) segregation of fission products in the glass; (7) rapid thermal devitrification at temperatures above 500°C; (8) a factor of 1000 increase in the leach rate of the glass after devitrification.

At the conclusions of the WSEP program in 1972 phosphate glasses were abandoned for waste solidification in the US as indicated in Figure A1. In 1984 lead-iron-phosphate (LIP) glasses were proposed as a new, very stable and easily prepared medium for the immobilization of all types of high-level liquid waste [183,187,188,189,190]. The developers demonstrated that the corrosion rate of the LIP waste glass was 10<sup>2</sup>-10<sup>3</sup> times lower than the corrosion rate of a comparable borosilicate waste glass. In addition, they determined that (1) melt temperatures could be as low as 800°C since the glasses had low melt viscosities in the 800-1050°C range; (2) the glasses did not devitrify up to temperatures as high as 550°C; and (3) the glasses were not adversely affected by large doses of gamma radiation in water at 135°C. The developers suggested that the improved chemical durability thermal stability of this phosphate glass over previous WSEP formulations was due to the Fe<sub>2</sub>O<sub>3</sub> content of the glass [188,189,190] and the structural role of iron in the glass which strengthens the cross bonding between the polyphosphate chains. [190,191] A highly stable waste form is realized when the iron concentration is adjusted to a content of Fe<sub>2</sub>O<sub>3</sub>/(PbO•P<sub>2</sub>O<sub>5</sub>) ~ 9 wt% and the PbO content is between 45 and 66 wt%. Comparing the LIP glass formulations to WSEP phosphate glasses demonstrate that the LIP glasses have higher PbO content and a lower waste loading. The iron and phosphate levels are, however, comparable. Likewise melt corrosivity [189,190,192,193] and incompatibility with certain canister materials [192,193] were observed. Low waste component solubility even at elevated temperatures (>1150°C) produced non-homogeneous glasses which gave leach rates comparable to those of borosilicate glass. [192,193] Thermal stability was poor as evidenced by rapid thermal devitrification above 550°C [194]

Iron phosphate (Fe-P or IPG) glasses were studied from ~1995 to the present at the bench scale. Most of the research and development was championed at the University of Missouri in Rolla in the US while pilot scale testing has been performed in Russia.

Some of the characteristics of FeP glasses that are improvements over previous phosphate glass formulations are

- excellent chemical durability [195,196,197]
- high solubility [151, 198] for many heavy metals (uranium, chromium, zirconium, cesium, molybdenum, etc.); noble metals; rare earths and sulfate
- their low melting temperatures (950°C to 1100°C), rapid melting rates (few hours), tolerance of a wide range in furnace atmospheres (oxidizing to reducing), and high melt fluidity (viscosity typically below one poise)
- low corrosion of oxide refractories [199] commonly used in glass melting furnaces, such as high alumina, zircon, and mullite
- low corrosion of Inconel alloys [200] commonly used in glass melting furnaces
- high waste loadings, typically between 25 to 50 mass%, depending on the waste.

The only other work continuing on phosphate glasses for waste disposal is in the USSR. Both borosilicate and phosphate glasses were studied from the mid 1950's until the startup of the Mayak facility in 1987. A ceramic melter without precalcination is used. [201] Glass systems including  $\text{Na}_2\text{O}-\text{Al}_2\text{O}_3-\text{P}_2\text{O}_5$ ,  $\text{Na}_2\text{O}-\text{Al}_2\text{O}_3-\text{B}_2\text{O}_3-\text{SiO}_2$ , and  $\text{Na}_2\text{O}-\text{CaO}-\text{Al}_2\text{O}_3-\text{B}_2\text{O}_3-\text{SiO}_2$  glasses were studied [183] but the alumino-phosphate formulations have been pursued since the 1980's and into the present for the incorporation of high sodium-high aluminium type wastes. [202]

### **Ceramic Waste Form Development in Various Countries**

Although ceramics waste forms have also been examined as hosts for the solidification of nuclear waste, these forms were difficult to process and not as flexible toward variations in waste composition as glass. [185,203,204,205,206,207,208,209] The objective of the development of ceramics was to provide a waste form with chemical, thermal, and mechanical stability that was superior to glass. However, during ceramic processing, intergranular glassy phases often formed in the ceramic materials, especially when alkali-containing wastes were processed. This intergranular glass limited the product stability and durability. [210,211,212,213] However, both the historical development and the systems evaluation of glass ceramics and ceramics as solid waste forms parallels that of the vitreous waste forms and will be briefly discussed.

The concept of immobilizing the radioactive elements of nuclear waste in an assemblage of mineral phases was originally introduced by Hatch [214] at Brookhaven National Laboratory in 1953. The feasibility of making a ceramic of natural mineralogically stable phases was demonstrated by McCarthy [203,204] and Roy [215,216] at the Pennsylvania State University between 1973 and 1976. Since that time, a number of other mineralogic-ceramic assemblages have been developed. Among them are the Sandia titanate-based ceramic [205], the Australian titanate-based ceramic “SYNROC” [206,217,218], the

silicate-phosphate supercalcine ceramics [219], the alumina based tailored ceramics [183,220], and the Pu pyrochlores [221]. Silicate glass ceramics were developed in the mid 1970's in Germany.[209] Silicate and phosphate glass ceramics were also developed in the USSR [222], silicate glass ceramics were developed in Japan, [223] and titanium aluminosilicate glass ceramics were developed in Canada.[224]

At the turn of the 21<sup>st</sup> century, the public's interest in sources of clean energy has led to increased interest in advanced nuclear power production, often referred to as the “nuclear renaissance.” The development of advanced waste forms is a necessary component of this new strategy. Therefore, advanced nuclear waste forms can be designed for robust disposal strategies. This renaissance has led to renewed interest in forming Glass Composite Materials (GCM's) [225, 226] by JHM, AJHM, CCIM or HIPing which allow crystals to form in a glassy matrix. Implicit in the ceramics and glass ceramic waste form development is the idea of using additives to “tailor” the waste chemically so that the desired host radionuclide phases are produced after consolidation.

## Appendix References

- 
- 161 F. L. Parker, R. E. Broshears, Janos Pasztor, “**The Disposal of High-Level Radioactive Waste**,” Vol. I. Beijer Institute, Stockholm. Sweden (October 1984).
  - 162 J. E. Mendel, “**The Storage and Disposal of Radioactive Waste as Glass in Canisters**,” U.S. DOE Report PNL 3946, Battelle Pacific Northwest Laboratories. Richland, WA (December 1978).
  - 163 M. J. Plodinec, G. G. Wicks, N. E. Bibler, “**Borosilicate Glass as a Matrix for the Immobilization of Savannah River Plant Waste**”; pp. 336–45 in *The Technology of High-Level Nuclear Waste Disposal*, Vol. 2. P. L. Hofmann. U.S. Department of Energy, Washington, DC (1982).
  - 164 C.M. Jantzen and M.J. Plodinec, “**Thermodynamic Model of Natural, Medieval, and Nuclear Waste Glass Durability**,” *J. Non-Cryst Solids* 67, 207-233 (1984).
  - 165 M.I. Goldman, J.A. Servizi, R.S. Daniels, T.H.Y. Tebbutt, R.T. Burns and R.A. Lauderdale, “**Retention of Fission Products in Ceramic-Glaze-Type Fusions**,” Proc. 2nd UN International Conference on Peaceful Uses of Atomic Energy, Geneva, 1958, 1827, United Nations, New York, 27 (1958).
  - 166 R. Eliassen and M.I. Goldman, “**Disposal of High-Level Wastes by Fixation in Fused Ceramics**,” in *Hearings on Industrial Radioactive Waste Disposal*, Vol. 3, Ed. R.L. Doan, US Govt Printing Office, Washington, DC, 1966-1979, (1959).
  - 167 C.A. Mawson, **Management of Radioactive Wastes**, D. VanNostrand Co., Inc., New Jersey, 196 pp (1965).

- 
- 168 J.L. McElroy, W.J. Bjorklund, and W.F. Bonner, “**Waste Vitrification, A Historical Perspective,**” in *The Treatment and Handling of Radioactive Wastes*, Eds. A.G. Blasewitz, J.M. Davis, and M.R. Smith, Springer, New York, 171-177 (1982).
- 169 J. R. Grover and B. E. Chidley, “**Glasses Suitable for the Long Term Storage of Fission Products,**” British Rept. No. AERE-R 3178, Atomic Energy Research Establishment, Harwell, England, 1960.
- 170 W. Bocola, A. Donato, G. Sgalambro, “**Survey of the Present State of Studies on the Solidification of Fission Product Solutions in Italy**”; p. 449 in *Symposium on the Management of Radioactive Wastes from Fuel Reprocessing*, International Atomic Energy Agency, Vienna , Austria (1972)
- 171 J.L. McElroy, K.J. Schneider, J.N. Hartley, J.E. Mendel, G.L. Richardson, R.W. McKee and A.G. Blasewitz, “**Evaluation of WSEP (Waste Solidification Engineering Prototypes) High Level Waste Solidification Processes,**” Waste Solidification Program Summary Report Vol. 11, U.S. DOE Report BNWL-1667 529pp. (July 1972).
- 172 J.A. Kelley, “**Evaluation of Glass as a Matrix for Solidification of Savannah River Plant Waste,**” U.S. DOE Report DP-1382, E.I. DuPont deNemours and Co., Savannah River Laboratory, Aiken, SC 28pp. (May 1975).
- 173 J.M. White and G. Hahaie, “**Ultimate Fission Product Disposal; The Disposal of Curie Quantities of Fission Products in Siliceous Materials,**” AECL-391, 18pp (March 1955).
- 174 K.B. Harvey, “**The Development of Borosilicate Glasses as Media for the Immobilization of High-Level Recycle Wastes, 1. Literature Survey,**” AECL Technical Record TR-239, 73pp. (January 1984).
- 175 R.W. Durham, “**Disposal of Fission Products in Glass,**” Second Nuclear Engineering and Scientific Conference AECL #476, 354-358 (1957).
- 176 W.F. Merritt, “**The Leaching of Radioactivity from Highly Radioactive Glass Blocks Buried Below the Water Table: Fifteen Years of Results,**” Atomic Energy of Canada Ltd Report No. AECL-5317, Ontario, Canada (1976).
- 177 A.R. Bancroft and J.D. Gamble, “**Initiation of a Field Burial Test of the Disposal of Fission Products Incorporated into Glass,**” Atomic Energy of Canada Ltd. Report No. AECL-718, Ontario, Canada (1978).

- 
- 178 T.W. Melnyk, F.B. Walton, and L.H. Johnson, “**High Level Waste Glass Field Burial Test: Leaching and Migration of Fission Products,**” Nuclear & Chem. Waste Management, 5, 49-62 (1984).
- 179 J.C. Tait, W.H. Hocking, J.S. Betteridge, and G. Bart, “**Field Burial Results and SIMS Analysis of the Chalk River Glass Blocks,**” Advances in Ceramics, V.20: “Nuclear Waste Management II, Eds. D.E. Clark, W.B. White, and A.J. Machiels, American Ceramic Society, Columbus, OH, 559-565 (1986).
- 180 C.M. Jantzen, “**Systems Approach to Nuclear Waste Glass Development,**” J. Non-Cryst Solids ,84 [1-3], 215-225 (1986).
- 181 J. Boulton, “**Management of Radioactive Fuel Wastes: The Canadian Disposal Program,**” Report No. AECL-6314 (1978)
- 182 F.P. Sargent, R.B. Lyon and L.H. Johnson, “**Status of the Canadian Nuclear Fuel Waste Management Program,**” WM86, Vol 1, 73-83 (1986)
- 183 W. Lutze and R.C. Ewing, “**Radioactive Waste Forms for the Future,**” North-Holland Publishers, Amsterdam, 778pp. (1988).
- 184 E.J. Tuthill, G.G. Weth, L.C. Emma, G. Strickland and L.P. Hatch, “**Phosphate Glass Process for Disposal of High Level Radioactive Wastes,**” Ind. Eng. Chem. Proc. Des. Dev, 6[3], 314-321 (1967).
- 185 W. Lutze, J. Borchardt, and A.K. De, “**Characterization of Glass and Glass Ceramic Nuclear Waste Forms,**” Sci. Basis for Nuclear Waste Mgt. I, G.J. McCarthy, Plenum Press, New York, 69-81 (1979).
- 186 W. Heimerl, “**Solidification of HLW Solutions with the PAMELA Process,**” Proceedings International Symposium on Ceramics in Nuclear Waste Management; CONF-790420, U.S. DOE, Cincinnati, Ohio, 97-101 (1979).
- 187 B.C. Sales and L.A. Boatner, “**Lead-Iron-Phosphate Glass: A Stable Storage Medium for High-Level Nuclear Waste,**” Science 226, 45-48 (1984).
- 188 B.C. Sales and L.A. Boatner, “**Physical and Chemical Characteristics of Lead-Iron-Phosphate Nuclear Waste Glasses,**” J. Non-Cryst. Solids, 79, 83-116 (1986).
- 189 B.C. Sales and L.A. Boatner, “**Lead Phosphate Glass as a Stable Medium for the Immobilization and Disposal of High-Level Nuclear Waste,**” Materials Letters, 2 [4B]301-304 (1984).

- 
- 190 B.C. Sales and L.A. Boatner, “**Physical and Chemical Characteristics of Lead-Iron-Phosphate Nuclear Waste Glasses,**” US DOE Report ORNL-6168, Martin Marietta Energy Systems, Inc., Oak Ridge, TN (May 1985).
  - 191 B.C. Sales and L.A. Boatner, “**Structural Properties of Lead-Iron-Phosphate Glasses,**” J. Non-Cryst. Solids, 71, 103-112 (1985).
  - 192 C.M. Jantzen, “**Investigation of Lead-Iron-Phosphate Glass for SRP Waste,**” Advances in Ceramics, 20, D.E. Clark, W.B. White and A.J. Machiels (Eds.), American Ceramic Society, Westerville, OH, 157-165 (1986).
  - 193 L. Kahl, “**Hydrolytic Durability of Lead-Iron-Phosphate Glasses,**” Advances in Ceramics, 20, D.E. Clark, W.B. White and A.J. Machiels (Eds.), American Ceramic Society, Westerville, OH, 141-148 (1986).
  - 194 L.A. Chick, L.R. Bunnell, D.M. Strachan, H.E. Kissinger, and F.N. Hodges, “**Evaluation of Lead-Iron-Phosphate Glass as a High Level Waste Form,**” Advances in Ceramics, 20, D.E. Clark, W.B. White and A.J. Machiels (Eds.), American Ceramic Society, Westerville, OH, 149-156(1986).
  195. D.E. Day, X. Yu, G.J. Long, and R.K. Brow, “**Properties and Structure of Sodium-Iron Phosphate Glasses,**” J.Non-Crystalline Solids, 215(1): 21-31 (1997)
  196. M. Mesko, D.E. Day, and B.C. Bunker, “**Immobilization of CsCl and SrF<sub>2</sub> in Iron Phosphate Glass,**” Waste Management, 20(4): 271-278 (2000).
  197. G.K. Marasinghe, M. Karabulut, X. Fang, C.S. Ray, D.E. Day, “**Vitrified Iron Phosphate Nuclear Waste Forms Containing Multiple Waste Components,**” Ceramic Transactions, Vol. 107, pp.115-122. American Ceramic Society, Westerville, Ohio (2000).
  198. M. Karabulut, G.K. Marasinghe, C.S. Ray, D.E. Day, O. Ozturk, and G.D. Waddill, “**X-ray Photoelectron and Mossbauer Spectroscopic Studies of Iron Phosphate Glasses Containing U, Cs, and Bi,**” J. Non-Crystalline Solids, 249(2-3): 106-116 (1999).
  199. F. Chen and D.E. Day, “**Corrosion of Selected Refractories by Iron Phosphate Melts**” Ceramic Transactions, Vol. 93, pp. 213-220. The American Ceramic Society, Westerville, Ohio (1999).
  200. D.E. Day and C.W. Kim, “**Reaction of Inconel 690 and 693 in Iron Phosphate Melts: Alternative Glasses for Waste Vitrification,**” Final Report for Contract DE-FG02-04ER63831 Project 0010255 (2005).
  - 201 D.J. Bradley, “**Behind the Nuclear Curtain: Radioactive Waste management in the Former Soviet Union,**” Battelle Press, Columbus, OH, 716pp. (1997).

- 
- 202 N.E. Brezneva, A.A. Minaev, and S.N. Oziraner, “**Vitrification of High Sodium-Aluminum Wastes: Composition Ranges and Properties,**” Sci. Basis for Nuclear Waste Mgt. I, G.J. McCarthy, Plenum Press, New York, 43-50 (1979).
- 203 G.J. McCarthy, “**Quartz-Matrix Isolation of Radioactive Wastes,**” J. Mat. Sci. 8, 1358-59 (1973).
- 204 G.J. McCarthy and M.T. Davidson, “**Ceramic Nuclear Waste Forms: I. Crystal Chemistry and Phase Formation**” Bull. Am. Ceram. Soc. 54 782-786 (1975).
- 205 R.O. Schoebel, “**Stabilization of High Level Waste in Ceramic Form,**” Bull. Am. Ceram. Soc, 54 [4], 459 (1975).
- 206 A.E. Ringwood, V.M. Oversby and S.E. Kesson, “**SYNROC: Leaching Performance and Process Technology,**” in “Proc. Seminar on Chemistry and Process Engineering for High-Level Liquid Waste Solidification, R.Odoj and E. Merz (Eds), Julich Conference 42, vol 1, 495-506 (1981).
- 207 P.E.D. Morgan, D.R. Clarke, C.M. Jantzen and A.B. Harker, “**High-Alumina Tailored Nuclear Waste Ceramics,**” J. Am. Ceram. Soc., 64 [5] 249–58 (1981).
- 208 J.B. Dunson Jr., A.M. Eisenberg, R.L. Schuyler III, H.G. Haight Jr., V.E. Mello, T.H. Gould Jr., J.L. Butler, and J.B. Pickett, “**Assessment of Processes, Facilities, and Costs for Alternative Solid Forms for Immobilization of SRP Defense Wastes,**” U.S. DOE Report DP-1625, E.I. DuPont deNemours & Co, Savannah River Laboratory, Aiken, SC (March 1982).
- 209 A.K. De, B. Luckscheiter, W. Lutze, G. Malow, and E. Schiewer, “**Development of Glass Ceramics for the Incorporation of Fission Products,**” Ceramic Bulletin, 55, 500-503 (1976).
- 210 D. R. Clarke, “**Preferential Dissolution of an Intergranular Amorphous Phase in a Nuclear Waste Ceramic,**” J. Am. Ceram. Soc., 64 [6] C–89–C–90 (1981).
- 211 Z. Zhang and M.L. Carter, “**An X-Ray Photoelectron Spectroscopy Investigation of Highly Soluble Grain-Boundary Impurity Films in Hollandite,**” J. Am. Ceram. Soc., 93[3] 894-899 (2010).
- 212 W. J. Buykx, K. Hawkins, D. M. Levins, H. Mitamura, R. St. C. Smart, G. T. Stevens, K. G. Watson, D. Weedon, and T. J. White, “**Titanate Ceramics for the Immobilization of Sodium-Bearing High-Level Nuclear Waste,**” J. Am. Ceram. Soc., 71 [8] 678–88 (1988).

- 
- 213 J. A. Cooper, D. R. Cousens, J. A. Hanna, R. A. Lewis, S. Myhra, R. L. Segall, R. St. C. Smart, P. S. Turner, and T. J. White, “**Intergranular Films and Pore Surfaces in Synroc C: Structure, Composition, and Dissolution Characteristics,**” J. Am. Ceram. Soc., 69 [4] 347–52 (1986).
- 214 L. P. Hatch, “**Ultimate Disposal of Radioactive Wastes,**” Am. Sci., 41, 410–21 (1953).
- 215 R. Roy, “**Ceramic Science of Nuclear Waste Fixation,**” Bull. Am. Ceram. Soc. 54, 459 (1975).
- 216 R. Roy, “**Rationale Molecular Engineering of Ceramic Materials,**” J. Am. Ceram. Soc. 60, 350-363 (1977).
- 217 A.E. Ringwood, “**Safe Disposal of High Level Nuclear Reactor Wastes: A New Strategy,**” Australian Nuclear Univeristy Presss, Canberra, Ausatralia, 1-64 (1978).
- 218 A.E. Ringwood, S.E. Kesson, N.G. Ware, W.O. Hibberson, and A. Major, “**The SYNROC Process:A Geochemical Approach to Nuclear Waste Immobilization,**” Geochemical Journal, 13, 141-165 (1979).
- 219 G.J. McCarthy, J.G. Pepin, D.E. Pfoertsch, and D.R. Clarke, “**Crystal Chemistry of the Synthetic Minerals in Current Supercalcine-Ceramics,**” U.S. DOE Report CONF-790420, 315-320 (1979).
- 220 C.M. Jantzen, J. Flintoff, P.E.D. Morgan, A.B. Harker, and D.R. Clarke, “**Ceramic Nuclear Waste Forms,**” in “Proc. Seminar on Chemistry and Process Engineering for High-Level Liquid Waste Solidification, R.Odoj and E. Merz (Eds), Julich Conference 42, vol 2, 693-706 (1981).
- 221 P. E. Raison, R. G. Haire, T. Sato and T. Ogawa, “**Fundamental and Technological Aspects of Actinide Oxide Pyrochlores: Relevance for Immobilization Matrices,**” Sci. Basis for Nuclear Waste Mgt. XXII, Symp. Proc. Vol. 556, Materials Research Society, Warrendale, PA, 3-10 (1999).
- 222 A.A. Minaev, S.N. Oziraner, and N.P. Prrokorova, “**The Use of Glass-Ceramic Materials for the Fixation of Radioactive Wastes,**” U.S. DOE Report CONF-790420, 229-232 (1979).
- 223 N. Ninomiya, T. Yamanaka, T. Sakane, M. Hora, S. Nakamura, and S. Kawamura, “**Diopside Glass-Ceramic Material for the Immobilization of Radioactive Wastes,**” in “Proc. Seminar on Chemistry and Process Engineering for High-Level Liquid Waste Solidification, R.Odoj and E. Merz (Eds), Julich Conference 42, vol 2, 675-693 (1981).

- 224 R.A. Speranzini and P.J. Hayward, “Development of Sphene-Based Ceramics for Disposal of Some Canadian Wastes,” Adv. Ceram. V. 8, 273-281 (1984).
- 225 W. E. Lee, M. I. Ojovan, M. C. Stennett, and N. C. Hyatt, “Immobilisation of Radioactive Waste in Glasses, Glass Composite Materials and Ceramics,” Advances in Applied Ceramics, 105[1], 3-12 (2006).
- 226 M. T. Peters, R. C. Ewing, C. I. Steefel, “GNEP Waste Form Campaign Science & Technology and Modeling & Simulation Program: Roadmap With Rationale & Recommendations,” GNEP-M50-3040-303 (March 2008).

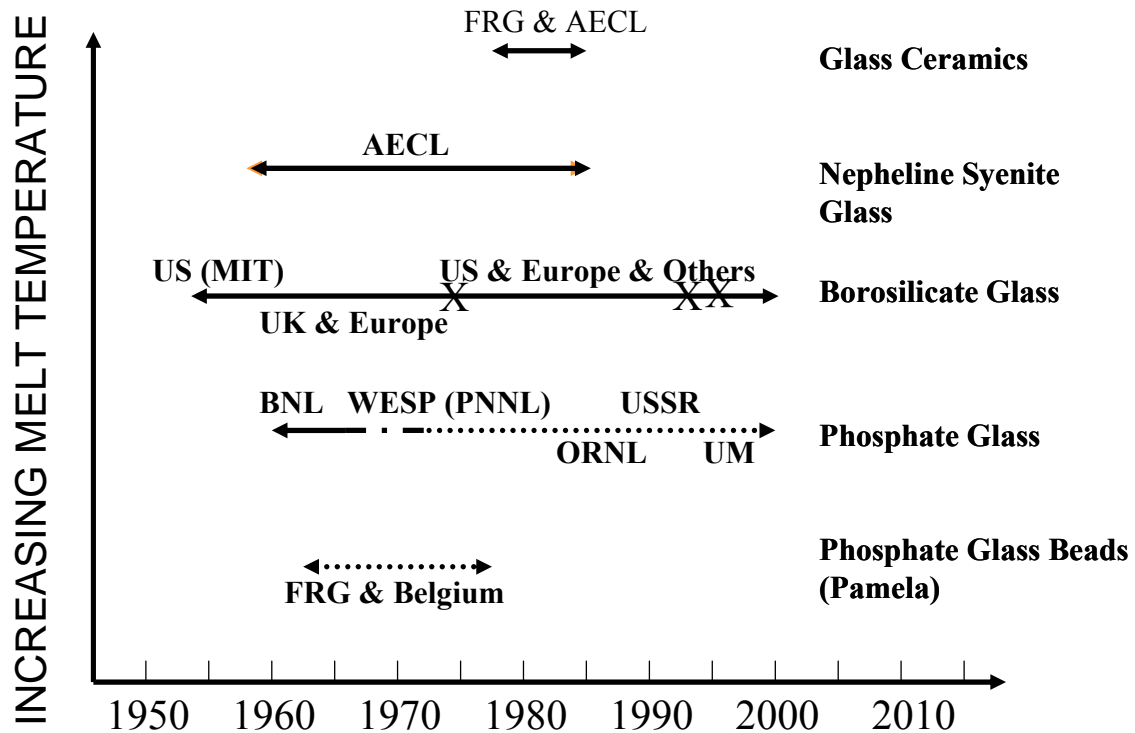


Figure A1. Waste form development time line. The X at 1975 is when the Savannah River Site (SRS) decided to use a borosilicate waste form. The X at 1994 is the non-radioactive startup of the DWPF at SRS and the X at 1996 is the radioactive startup of the DWPF at SRS.

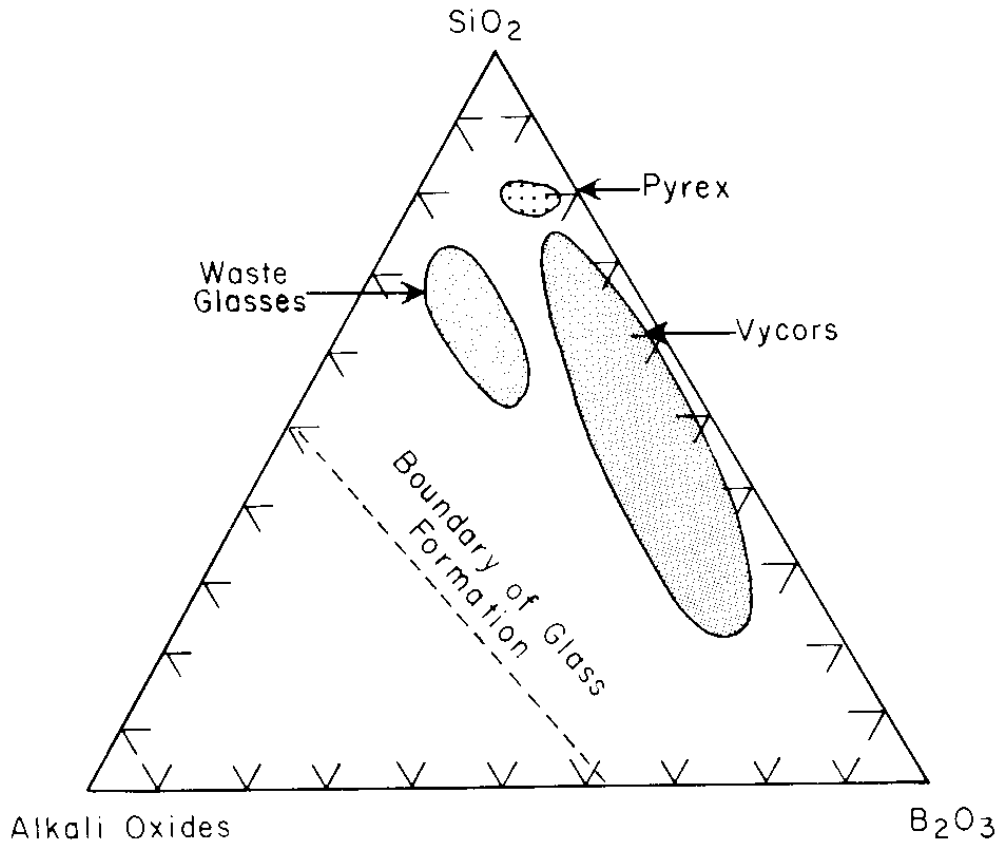


Figure A2. Pseudoternary phase diagram of the alkali oxide-silica-boron oxide system. Compositional ranges of borosilicates glasses including Pyrex, Vycor and borosilicate nuclear waste glasses are superimposed (after reference 180).